Peptide Thiolate Fe_2S_2 Complexes as Model of Plant-Type Ferredoxins.

A Doctoral Thesis

by

Satoru Ueno

Submitted to the Faculty

of Science, Osaka University

1988

Peptide Thiolate Fe_2S_2 Complexes as Model of Plant-Type Ferredoxins.

A Doctoral Thesis

by

Satoru Ueno

Submitted to the Faculty

of Science, Osaka University

1988

Approvals

November, 1988

This thesis is approved as to

style and content by

牛村 圭

Member-in-chief

勝部幸輝

Member

蒲池幹治

Member

Acknowledgments

This research work has been performed under the direction of Professor Akira Nakamura, Department of Macromolecular Science, Faculty of Science, Osaka University. I would like to express my sincere gratitude to Professor Akira Nakamura for his continuing guidance and encouragement.

I wish to express my thanks to Associate Professor Tomitake Tukihara, Tottori University, for his generous gift of Spinach ferredoxin and for his discussion on molecular design and conformational calculation of Plant-type ferredoxin model peptides. I also express my thanks to Dr. Shumpei Sakakibara, peptide institute, protein research foundation, helpful advices on synthesis methods of the 20-peptide plant-type ferredoxin model. I express my thanks to Professor Hiroshi Matsubara , Department of Biology in this Faculty, for helpful advices on the properties of native ferredoxin and its model peptides. I am indebted to Professor Mikiharu Kamachi, in this Department, for his measurements of EPR spectra.

I thank sincerely to Dr. Norikazu Ueyama for his valuable suggestion and discussion, and Mr. Takasi Sugawara for his collaboration, and to other members of Nakamura Laboratory for their helpful discussion.

November, 1988

S. Ueno

Satoru Ueno

Contents

Chapter 1.

Approach of This Thesis.

General introduction.

Enzymes are indispensable to all living organisms. Beside this fundamental importance, enzymes are finding increasing use in the wide industrial fields (e.g. food stuffs, pharmaceuticals, cosmetics etc.).

Metalloenzymes which contain metal ions or metal clusters other than alkali metal are an important class of enzymes. Metalloenzymes perform unique reactions (e.g. nitrogen fixation etc.) at ordinary temperature and pressure under aqueous environments by utilizing various metal ions in their active centers. There are a number of proteins containing metals which are named metalloproteins. The characteristic properties of metalloproteins are derived from the interaction between the metal ions and the peptide part of the whole biopolymers. However, details of the mechanisms of the interaction are not clear. It has great significance to clarify the mechanisms of the function of metalloproteins as an example of functional macromolecular metal complexes.

Metalloproteins are distinguishable by the presence or absence of heme (e.g. hemeproteins or non-hemeproteins). Metal porphyrinate moiety is characteristic of hemeproteins. The non-hemeproteins are classified by the metal ions in the active center. Thus, non-heme iron

proteins contain active center(s) formed by macromolecular protein ligand coordinated to iron or other ions.

Non-heme iron-sulfur proteins include rubredoxin, plant-type ferredoxin, and bacterial-type ferredoxin, etc. In their active centers, the iron-sulfur core(s) (see Fig. 1) is connected to cysteine thiolates (Cys residues of the peptide chains). These iron-sulfur proteins are widely distributed from bacteria to higher plants and animals. And their functions are mostly the electron mediators in the biological electron transfer systems.

Plant-type ferredoxins are typical 2Fe-2S ferredoxins and exist in the photosystem I (PS I) of the higher plants or algae, and are efficient electron mediators. These metalloproteins show the redox potential at ca. -640 mV (vs. SCE).[1] The position of the redox potential of an electron mediator protein is very important for its function. Generally, an electron transport system consists of the sequence of the electron-mediated components of metalloproteins, each of which has a distinctive redox potential. Thus, the electron mediator proteins must have a redox potential which is in the fixed range, and stable oxidation and reduction states.

Various model complexes of plant-type ferredoxin have been synthesized as shown in Fig. 2. These 2Fe-2S model complexes with simple thiolate ligands have the redox potentials at -1490, -1090, -1310 mV (vs. SCE) for **1**, **2**, and **3**, respectively.[2] These values are quite different from the value of plant-type ferredoxin (-640 mV (vs.

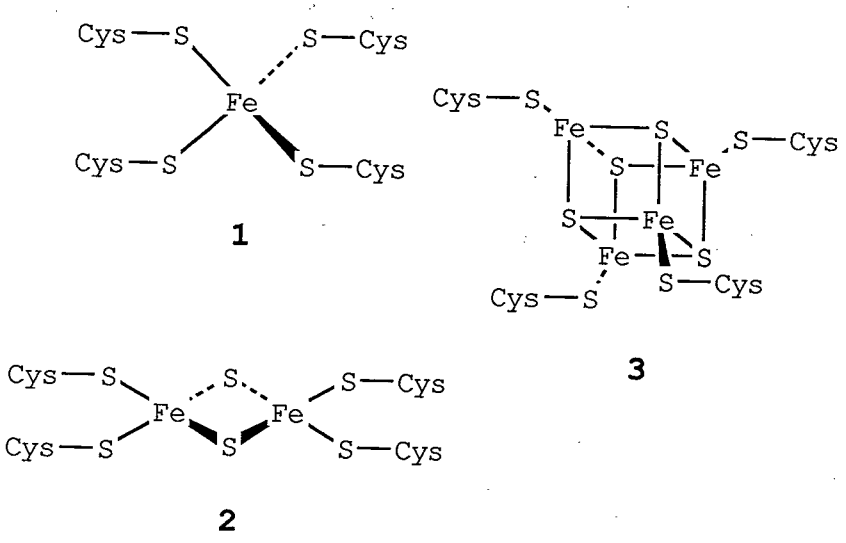

Figure 1. Schematic structure of the active site structures of (1)rubredoxin, (2)plant-type ferredoxin, and (3)bacteria-type ferredoxin.

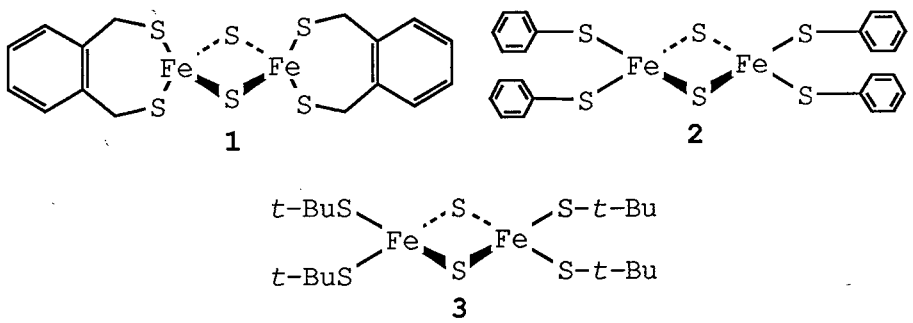

Figure 2. The structures of plant-type ferredoxin model complexes, (1) $[Fe_2S_2(S_2\text{-}o\text{-xyl})_2]^{2-}$ (S_2-*o*-xyl = *o*-xylene-α,α'-dithiolate), (2) $[Fe_2S_2(S\text{-Ph})_4]^{2-}$, and (3) $[Fe_2S_2(S\text{-}t\text{-Bu})_4]^{2-}$.

SCE)). The difference in the redox potentials indicates that these simple thiolate ligands are not good enough to realize the characteristic functions. Finer adjustment of the micro environment created by the surrounding polypeptide chains must be done for an understanding of plant-type ferredoxins and simulating of the electron transport by any model complexes.

Approach.

It has long been discussed whether the whole protein sequence or the partial sequence (around the active center) is really needed to realize the characteristic functions of metalloproteins.

Recently, Orme-Johnson et al. has shown that the bacterial-type ferredoxin which has a 8Fe-8S structure was enzymatically digested to two half molecules (see Fig. 3) and the half ferredoxin has the full functions in the electron transfer system.[3] This result shows the partial sequence around the active site is important to their functions.

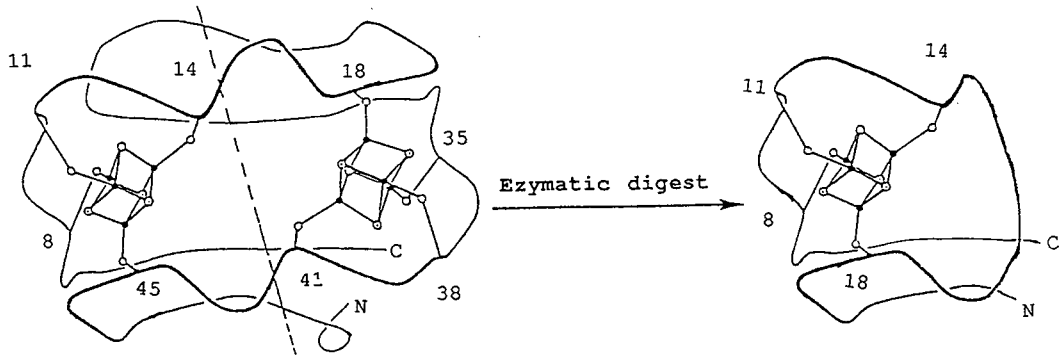

Figure 3. The half bacteria-type ferredoxin molecule.

To answer the question whether only the amino acid sequence around active site is necessary to realize the metalloprotein functions or not, a model peptide (a 20-peptide) which contains all the amino acid residues around the active site of the plant-type ferredoxin was designed.[4]

From the X-ray structure analysis, the plant-type ferredoxin active site exists at the top of the protein molecule and separated from the β-turn rich part as shown in Fig.4[5]. The 20-peptide is expected to realize the functions of plant-type ferredoxin when combined with a 2Fe-2S core.

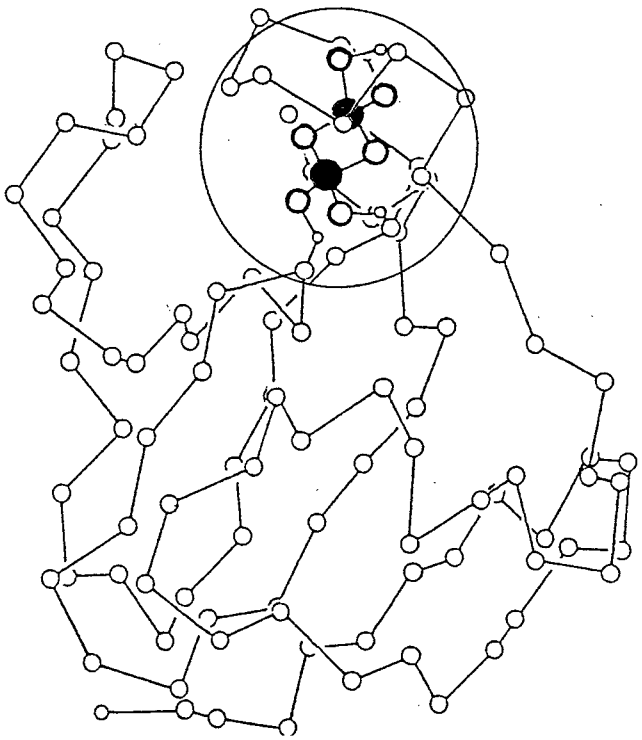

Figure 4. The polypeptide Chain of *S. platensis* ferredoxin. The circle part shows the active center of the ferredoxin.

Thus, we synthesized the model peptide (20-peptide) and its 2Fe-2S complex [Fe_2S_2(20-peptide)] and compared the properties with those of native plant-type ferredoxin.

Synthesis of the 20-peptide and [Fe_2S_2(20-peptide)].

The structure of 20-peptide shown in Figure 5[4] was synthesized by the liquid phase method, and incorporation of a 2Fe-2S core to the 20-peptide was performed under anaerobic condition. Due to extreme sensitivity of the complex to air and water, the peptide complex, [Fe_2S_2(20-peptide)]$^{2-}$, was not isolated, but the absorption, CD spectrum and redox potential were carefully measured in DMF under Ar.

The 20-peptide complex shows the two absorption maxima at 424 nm and 460 nm at 400 ~ 500 nm region. These two absorption maxima are characteristic of the native plant-type ferredoxin.

The redox potential of native plant-type ferredoxin was found at -0.64 V vs. SCE. This redox potential value is very important for the electron carrier in the photo system I. The peptide complex shows two redox potentials at -0.64 and -0.96 V vs. SCE in DMF solution by differential pulse polarography. The value (-0.64 V vs. SCE) is equal to the value of native plant-type ferredoxin. However, two other independent redox waves indicate two kinds of isomeric 2Fe-2S complexes are included in the complex. The electric current ratio of the

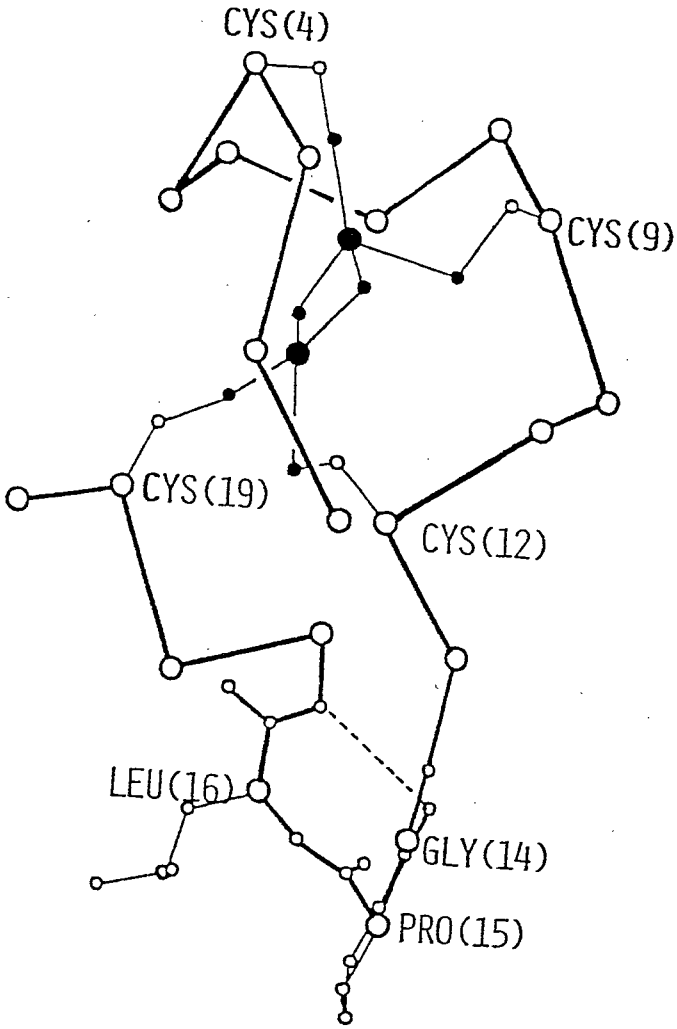

Figure 5. proposed structure of [Fe_2S_2(20-peptide)].

two redox waves is $i_{-0.64}/i_{-0.96}=0.43$. This ratio may indicate the molar ratio of two isomers. One isomer which has a redox couple at -0.64 V vs. SCE may have analogous structure of the native ferredoxin active center (Fig. 6-I), and the other one may involve the part of the tetrapeptide sequence chelating to one Fe^{III} ion of 2Fe-2S core (Fig. 6-II).

The one isomer of the peptide complex shows almost the same redox potential of native plant-type ferredoxin in DMF. The other isomer probably has a different coordination mode to a Fe_2S_2 core and show different redox potentials. The interaction between the conformation of the peptide chains around the active center and the Fe_2S_2 core is thus found so complicated in the 20-peptide complex. Therefore, oligopeptides which have partial amino acid sequences of the plant-type ferredoxin active site (e.g.:Cys-X-Y-Cys; tetrapeptide, Cys-A-B-C-D-Cys; hexapeptide, and Cys-A-B-C-D-Cys-X-Y-Cys; nonapeptide) are synthesized to study the essential part of the oligopeptide - 2Fe-2S core interactions.

Synthesis of 2Fe-2S complexes of smaller peptides.

Characteristic tetrapeptide sequences (Cys-X-Y-Cys) have been discerned in the various types of iron-sulfur protein sequences (e.g. rubredoxin, bacteria-type ferredoxin, and plant-type ferredoxin etc.). In the rubredoxin sequence, two tetrapeptide sequences are chelating a Fe ion. But, in bacteria-type ferredoxin and plant-type ferredoxin, the tetrapeptide sequence bridges

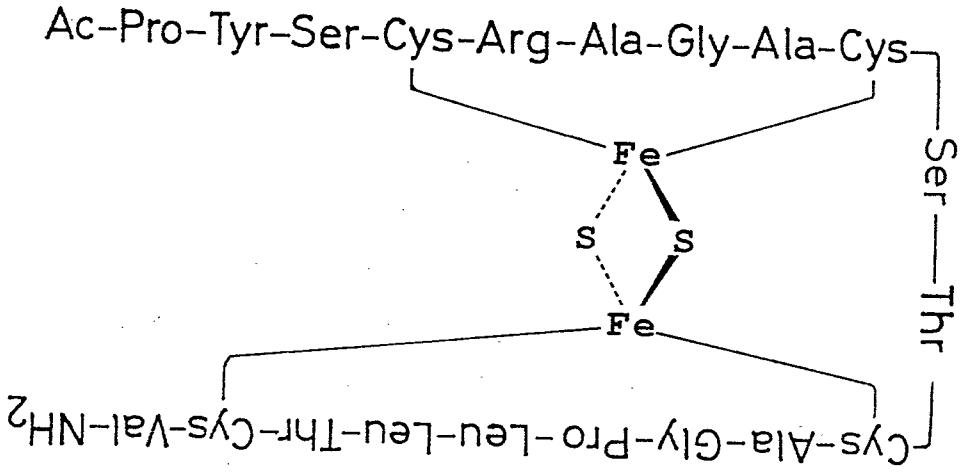

I

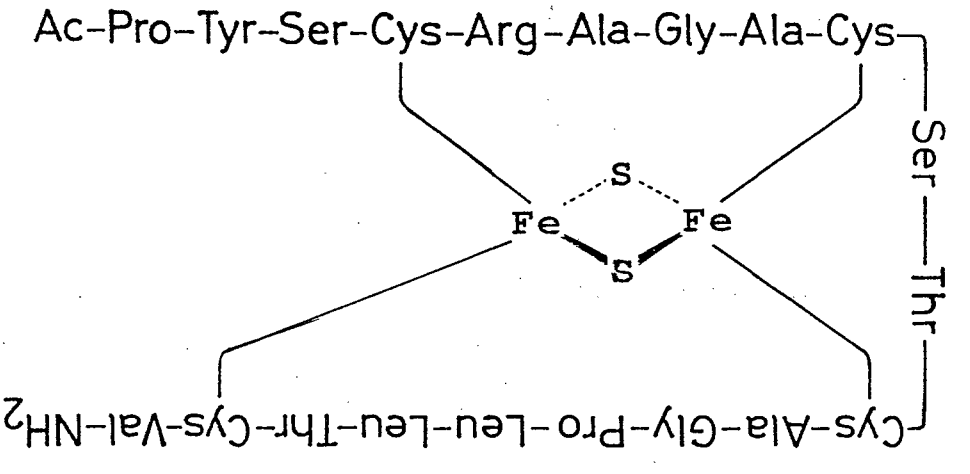

II

Figure 6. Possible two structures of the 20-peptide 2Fe-2S complexes.

two Fe ions of a iron-sulfur core. I was interested in the sequence of the X-Y part of the tetrapeptide which influences coordination mode and chemical properties of the peptide complexes.

Further interest in other peptide sequences led to two points in hexapeptide sequence. One is the chelating structure and the other is the conformation of the amino acid sequence (e.g. native ferredoxin hexapeptide sequence ($-Cys^{41}-Arg^{42}-Ala^{43}-Gly^{44}-Ala^{45}-Cys^{46}-$) is unfavorable to form NH---S hydrogen bond, cause to the β-C atom of Arg^{42} amino acid residues).

To study the coordination structure of the nonapeptide sequence, Z-Cys-Gly-Ala-Gly-Ala-Cys-Ala-Ala-Cys-OMe and its 2Fe-2S complexes were synthesized. This nonapeptide ligand has three amino acid residues changed from native plant-type ferredoxin sequence (e.g. Arg^{42} to Gly and Ser^{47} and Thr^{48} to Ala and Ala).

Effect of Bulky Thiolate Ligand.

Efficient control of Fe-S bond character with variation of S*-Fe-S-Cβ torsion angles have been proposed for the model complexes of high potential iron-sulfur protein[6-8] and rubredoxin.[9]

Effect of variation of S*-Fe-S-Cβ torsion angle on the redox property was examined using $[Fe_2S_2(2,4,6\text{-trimethylbenzenethiolato})_4]^{2-}$ which exhibits an unusual positive shift of redox potential. The X-ray analysis revealed that the complex has two eclipsed torsion angles and

two staggered angles for the four Fe-S bonds. In native ferredoxin, one eclipsed torsion angle has been found by the X-ray analysis as shown in Figure 7.[10] Extended Hückel calculations were performed to get information for the bond characters of Fe-S.

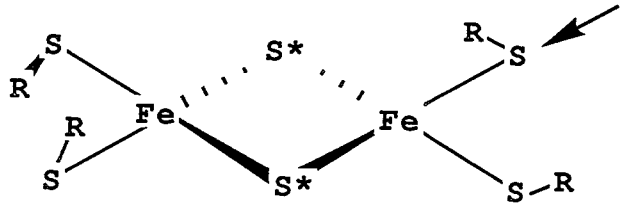

a

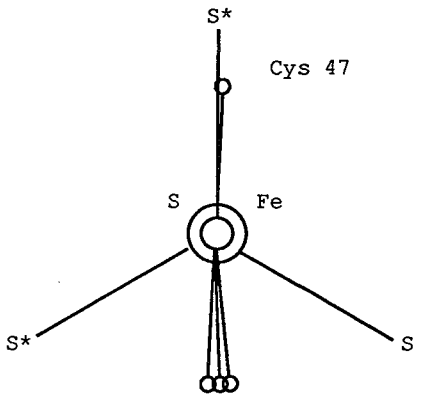

Cys 39 Cys 77 Cys 44

b

Figure 7. (a) Illustration of S*-Fe-S_γ-Cβ torsion angle in $[Fe_2S_2(SR)_4]^{2-}$. (b) S*-Fe-S_γ-Cβ torsion angle of *S. platensis* ferredoxin.

Outline of each chapter.

Chapter 2. describes the synthesis of the 20-peptide (molecular designed by Tsukihara et al.) and its 2Fe-2S complex and the properties. The complex shows the same redox potential of the native ferredoxin in N,N-dimethylformamide solution. But the 20-peptide complex contains two isomers about 1:1 mol ratio.

In Chapter 3., synthesis of tetrapeptide ligand (e.g. Z-Cys-Ala-Ala-Cys-OMe, Z-Cys-Pro-Leu-Cys-OMe, Z-Cys-Thr-Val-Cys-OMe, Z-Cys-Val-Val-Cys-OMe) 2Fe-2S complexes. In native ferredoxin, tetrapeptide sequence is bridged to two Fe^{3+} ions in 2Fe-2S core. But, I have found that the tetrapeptide ligand other than Z-Cys-Val-Val-OMe , had chelating the one Fe^{3+} ion of 2Fe-2S core.

Chapter 4. describes the properties of the hexapeptide (Z-Cys-Gly-Ala-Gly-Ala-Cys-OMe, Z-Cys-Ala-Ala-Gly-Ala-Cys-OMe) 2Fe-2S complexes. Both hexapeptide complexes are chelating one Fe^{3+} ion of the 2Fe-2S core similar chelate structure than the hexapeptide sequence in the native ferredoxin, and only $[Fe_2S_2(Z\text{-cys-Gly-Ala-Gly-Ala-cys-OMe})_2]^{2-}$ shows the solvent effect between in N,N-dimethylformamide and in acetonitrile.

Chapter 6. describes synthesis and crystal structure of bulky trimethylbenezenethiolate (tmbt) 2Fe-2S complex. I found that the unique characters (absorption spectra,redox potential) are found to be due to the abnormal torsion angle of Fe-S-C bond.

References

(1) Tagawa, K.; Arnon, D.I. *Biochem. Biophys. Acta* **1968**, 153, 166.

(2) a) Mayerle, J.J.; Frankel, R.B.; Holm, R.H.; Ibers, J.A.;Phillips, W.D.; Weiher, J.F. *Proc. Nat. Acad. Sci. U.S.A.* **1973**, 70, 2429.

b) Mayerle, J.J.; Denmark, B.V.; DePamphilis, B.V.; Ibers, J.A.; Holm, R.H. *J. Am. Chem. Soc.* **1975**, 97, 1032.

c)Ueno, S.; Ueyama, N.; Nakamura, A.; Tsukihara, T. *Inorg. Chem.* **1986**, 25, 1000.

(3) Orme-Johnson, W. H.; Beinert, H. *Biochem. Biophys. Res. Commun.* **1969**, 36, 337.

(4) Tsukihara, T.; Kobayashi, M.; Nakamura, M.; Katsube, Y.; Fukuyama, K.; Hase, T.; Wada, K.; Matsubara, H. *BioSystems* **1982**, 15, 243.

(5) Fukuyama, K.; Hase, T.; Matsumoto, S.; Tsukihara, T.; Katsube, Y.; Tanaka, N.; Kakudo, M.; Wada, K.; Matsubara, H. *Nature* **1980**, 286, 552.

(6) Ueyama, N.; Terakawa, T.; Sugawara, T.; Fuji, M.; Nakamura, A. *Chem. Lett.* **1984**, 1287.

(7) Ueyama, N.; Sugawara, T.; Fuji, M.; Nakamura, A.; Yasuoka, N., *Chem. Lett.* **1985**, 175.

(8) Beardwood, P.; Gibson, J. F. *J. Chem. Soc. Dalton Trans.* **1983**, 737.

(9) Ueyama, N.; Sugawara, T.; Tatsumi, K.; Nakamura, A. *Inorg. Chem.* **1987**, 26, 1978.

(10) Tsukihara, T., private communication.

Chapter 2.

The Synthetic Analogue of the Plant-Type Ferredoxin Active Site.

2-1. Introduction

Plant-type ferredoxins widespread in algae and higher plants have approximate one hundred amino acid residues and one $Fe_2S_2^{2+}$ core. These ferredoxins play important roles for reduction of $NADP^+$ in cooperation with ferredoxin-$NADP^+$ oxidoreductase.[1] Native spinach ferredoxin has a redox potential at -0.42 V (vs. Normal Hydrogen Electrode (NHE)), which is converted to approximate value, -0.67 V (vs. Saturated Calomel Electrode (SCE)).[2] This value is important for one of the components which exists in the electron transfer chains in biological photosystem I.

Many synthetic model complexes of plant-type ferredoxin e.g. $[Fe_2S_2(S_2\text{-}o\text{-xyl})_2]^{2-}$ (S_2-*o*-xyl = *o*-xylyl-α,α'-dithiolene) have been synthesized by Holm's group.[3,4] These complexes exhibit two characteristic absorption maxima due to a ligand-metal charge transfer absorption, for example, at 414 and 453 nm for $[Fe_2S_2(S_2\text{-}o\text{-xyl})_2]^{2-}$ in N,N-dimethylformamide (DMF). These maxima are different from the native ones at 423 and 466 nm in *S. platensis* ferredoxin. Simple peptide model complexes have two absorptions at 423 and 453 nm (sh) for $[Fe_2S_2\{Ac\text{-}Gly_2\text{-}(cys\text{-}Gly_2)_2\text{-}NH_2\}]^{2-}$,[5] in Me_2SO or at 417 and 450 nm for

$[Fe_2S_2(Z\text{-cys-Ala-Ala-cys-OMe})_2]^{2-}$ (Z = benzyloxycarbonyl) in DMF.[6]

The CD spectra of $[Fe_2S_2(Z\text{-cys-Ala-Ala-cys-OMe})_2]^{2-}$ and $[Fe_2S_2(Z\text{-Ala-cys-OMe})_4]^{2-}$ were found to be different from that of the native *Spirulina maxima* ferredoxin.[7]

The synthetic model complexes exhibit extremely negative redox potentials, for examples, -1.50 V (vs. SCE) for $[Fe_2S_2(S_2\text{-}o\text{-xyl})_2]^{2-}$. In Chapter 3, we will describe the positive shift of redox potential (-1.06 V vs. SCE) of $[Fe_2S_2(Z\text{-cys-Ala-Ala-cys-OMe})_2]^{2-}$ in DMF which has two bidentate chelating peptide ligands coordinating to one Fe^{III} ion of $[Fe_2S_2]^{2+}$ core.[6,8] However, still large difference in redox potential was observed between the tetrapeptide complex and native plant-type ferredoxin.

Such spectral and electrochemical differences between the synthetic analogue and native plant-type ferredoxins are caused by unique environment of a peptide chain surrounding an $Fe_2S_2^{2+}$ core. The spectral and electrochemical properties thus depend on the amino acid residues in the vicinity of the $Fe_2S_2^{2+}$ core. Therefore, a peptide with a sequence of amino acid residues which is invariant in all plant-type ferredoxins (invariant amino acid sequence) is important in this respect. Fortunately, four Cys residues ligating $Fe_2S_2^{2+}$ core in *Spirulina platensis* are located in a small domain separated from a large domain, illustrated as shown in Figure 1. A 20-peptide containing four Cys residues as shown in Figure 2 was designed in consideration of the preferable

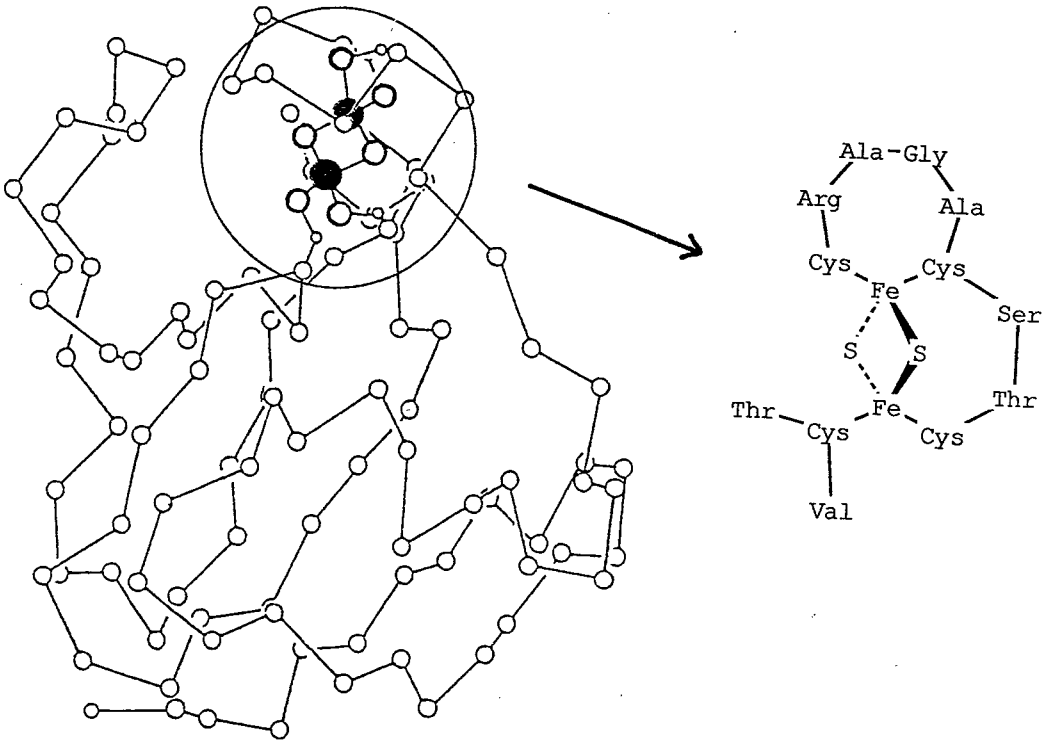

Figure 1. The polypeptide Chain of *S. platensis* ferredoxin. The circle part shows the active center of the Ferredoxin.

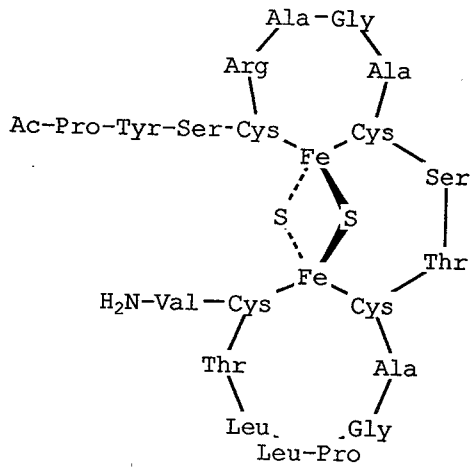

Figure 2. Schematic structure of [Fe_2S_2(20-peptide)].

conformation.[9]

In this chapter we present the synthesis and the spectral, and electrochemical properties of a 20-peptide/$Fe_2S_2^{2+}$ complex designed on the basis of the conformational energy calculation and the X-ray structure analysis.[10]

2-2. Experimental section.

Materials.

Boc-Ala-OH (Boc = *t*-butyloxycarbonyl), Boc-Arg(Tos)-OH, Boc-Leu-OH•H_2O, Boc-Pro-OH, Boc-Ser(Bzl)-OH, Boc-Thr(Bzl)-OH, Boc-Leu-ONSu, Boc-Pro-ONSu, Boc-Ser(Bzl)-ONSu, Boc-Tyr[Bz(Cl)$_2$]-ONSu, Boc-Thr(Bzl)-ONSu, Boc-Ala-Gly-OBzl, trifluoroacetic acid (TFA), anhydrous hydrogen chloride in dioxane (4.5 and 4.8 N), N,N'-dicyclohexylcarbodiimide (DCC), N-hydroxybenzotriazole (HOBt), acetic acid N-hydroxysuccinimide ester (AcONSu), and 1-ethyl-3-(3-diethylaminopropyl) carbodiimide (WSCI) were obtained from Protein Research Foundation, Osaka. All solvents were purified by distillation before use. All other reagents were use of commercial grade.

Native spinach ferredoxin was gifted by Dr. T. Tsukihara.

Peptide Synthesis

General procedures.

WSCI condensation method.

A HCl salt of amine component (7 mmol) was dissolved in DMF (150 ml) and HOBt (7 mmol) and Boc-amino acid (7 mmol) was added to the solution. WSCI (7 mmol) was added to the stirring solution at -20 °C, pH of reaction mixture was adjusted at about 6 by using N-methylmorpholine.and

stirred for 3 h at room temperature. The solution was concentrated under reduced pressure. The purify method of the oligopeptides were described below.

Active ester condensation method

A trifluoroacetic acid salt of amine component (3.1 mmol) was dissolved in DMF (60 ml) solution of Et_3N (3.1 mmol) and Boc- amino acid succinimide ester(3.1 mmol) at -6 °C. After stirring for 2 h at -6 °C, the reaction mixture was allowed to stand at room temperature. The solution was concentrated under reduced pressure, and oligopeptides purified by the method described below.

Purification method

Unless otherwise mentioned condensation reaction products were purified by one of the following procedures.

procedure A.

For purification of protected peptide ester soluble in ethyl acetate (AcOEt) or $CHCl_3$ the extract was washed with H_2O, 1 N HCl aq., H_2O, 5 % $NaHCO_3$ aq., and H_2O dried over Na_2SO_4 and concentrated. The crude product was recrystallized or precipitated by addition of appropriate solvent.

procedure B.

For purification of protected peptide ester less soluble in AcOEt or $CHCl_3$, the crude product was triturated with H_2O, 1/3 N HCl aq., H_2O, 5 % $NaHCO_3$ aq., and H_2O, and recrystallized or precipitated from appropriate solvents.

Deprotection of Boc-group.

The N^{α}-protecting group was cleaved by the following procedures.

For active ester condensation.

Boc peptide was dissolved in trifluoroacetic acid (TFA) (20 mol eq.) at -6°C. After stirring for 20 min with cooling, the reaction mixture then stirred at room temperature. The reaction mixture was concentrated under reduced pressure. The residue was washed with ether, dried over NaOH pellets in vacuo.

For WSCI condensation.

Boc peptide was dissolved in TFA (20 mol eq.) at -6 °C. The reaction mixture was concentrated to about a half volume under reduced pressure, 4.8 N or 4.5 N HCl/dioxan (1.5 mol eq.) was added to the solution. All solvents were evaporated in vacuo. The residue was washed with ether, dried over NaOH pellets in vacuo.

Deprotection of OPac group.

A solution of peptide phenacyl ester(0.43 mmol) in AcOH (30 ml) containing Zn powder (8.6 mmol) was stirred for 2.5 h at 40 °C. After the reaction, the reaction mixture was filtered. The filtrate was concentrated and added ether ant dried over NaOH pellets in vacuo.

The peptide synthesis were undergoes the following schemes 1-4 by the liquid phase condensation method.

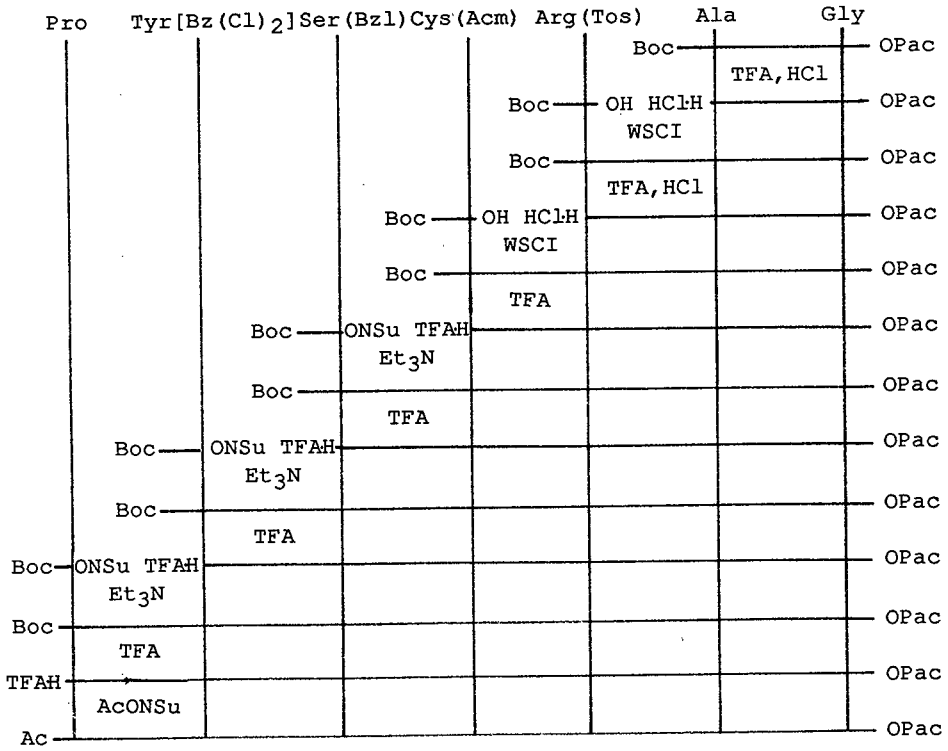

Scheme 1. Synthesis route of I-7 fragment.

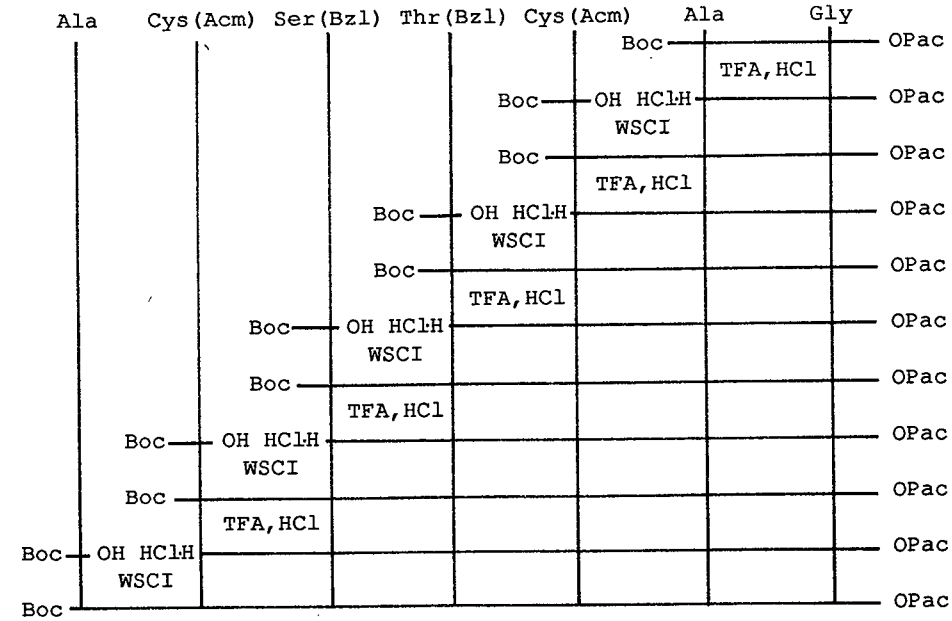

Scheme 2. Synthesis route of II-7 fragment.

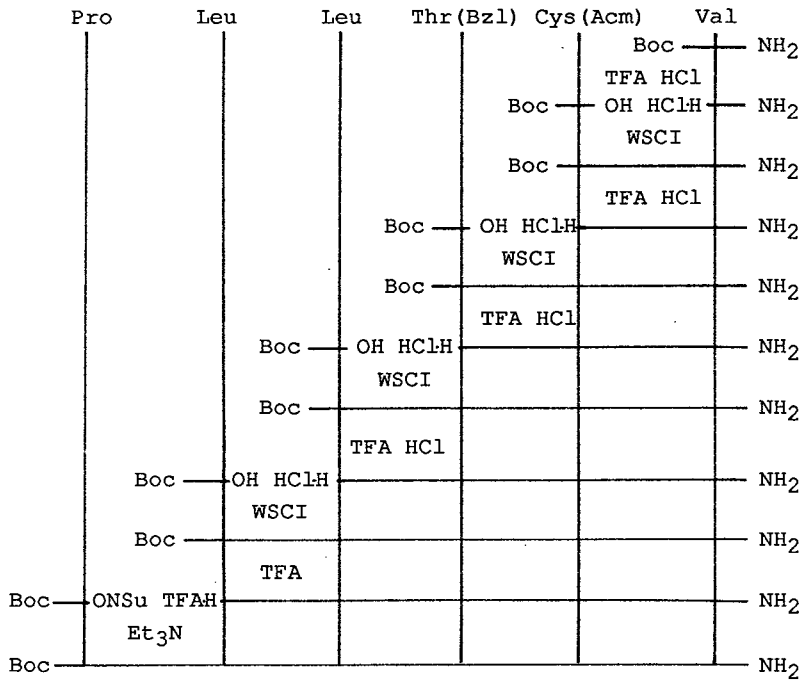

Scheme 3. Synthesis route of III-6 fragment.

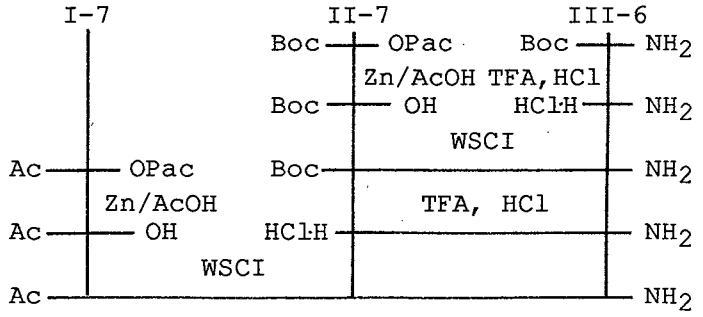

Scheme 4. Fragment Condensation route of 20-peptide (blocked).

Table. Analytical data for the 20-Peptide(Blocked)

Peptide	$[\alpha]_D$,°	Anal.,	C	H	N
Boc-Ala-Gly-OPac	-30.6 (c=0.66)[a]	Calcd.	59.33	6.63	7.69
		Found.	59.31	6.63	7.68
Boc-Arg(Tos)-Ala-Gly-OPac +0.8 H_2O	-21.4 (c=0.827)[a]	Calcd.	54.03	6.38	12.19
		Found.	53.99	6.35	12.26
Boc-Cys(Acm)-Arg(Tos)-Ala-Gly-OPac +0.7 H_2O	-26.6 (c=1.047)[a]	Calcd.	51.58	6.25	13.01
		Found.	51.55	6.21	12.91
Boc-Ser(Bzl)-Cys(Acm)-Arg(Tos)-Ala-Gly-OPac +0.8 H_2O	-10.6 (c=0.462)[b]	Calcd.	55.14	6.19	12.28
		Found.	54.26	6.19	12.18
Boc-Tyr[Bz(Cl)$_2$]-Ser(Bzl)-Cys(Acm)-Arg(Tos)-Ala-Gly-OPac	-8.0 (c=1.061)[b]	Calcd.	56.12	5.68	10.39
		Found.	54.08	5.81	10.95
Ac-Pro-Tyr[Bz(Cl)$_2$]-Ser(Bzl)-Cys(Acm)-Arg(Tos)-Ala-Gly-OPac +2.3 H_2O[c]	-25 (c=0.359)[b]	Calcd.	54.64	5.76	10.78
		Found.	54.67	5.58	10.70

Table (continude)

Boc-Cys(Acm)-Ala-Gly-OPac +0.15 H_2O	-30.0 (c=0.983)[a]	Calcd.	53.25	6.39	10.35
		Found.	53.25	6.49	10.35
Boc-Thr(Bzl)-Cys(Acm)-Ala-Gly-OPac +0.5 H_2O	-29.3 (c=0.996)[a]	Calcd.	56.90	6.55	9.48
		Found.	56.89	6.49	9.41
Boc-Ser(Bzl)-Thr(Bzl)-Cys(Acm)-Ala-Gly-OPac +0.5 H_2O	-6.0 (c=0.745)[b]	Calcd.	59.00	6.49	9.17
		Found.	58.95	6.42	9.08
Boc-Cys(Acm)-Ser(Bzl)-Thr(Bzl)-Cys(Acm)-Ala -Gly-OPac +0.6 H_2O	-0.3 (c=0.819)[b]	Calcd.	56.09	6.39	10.26
		Found.	56.13	6.29	10.07
Boc-Ala-Cys(Acm)-Ser(Bzl)-Thr(Bzl)-Cys(Acm) -Ala-Gly-OPac + H_2O[d]	-6.1 (c=1.60)[b]	Calcd.	55.42	6.46	10.77
		Found.	55.37	6.51	10.87
Boc-Val-NH_2	-2.0 (c=0.928)[a]	Calcd.	55.54	9.27	12.95
		Found.	55.62	9.27	12.95
Boc-Cys(Acm)-Val-NH_2	-27.0 (c=0.875)[a]	Calcd.	49.21	7.74	14.35
		Found.	45.37	7.29	13.23

Table (continued)

Boc-Cys(Acm)-Val-NH_2	-27.0 (c=0.875)[a]	Calcd.	49.21	7.74	14.35
		Found.	45.37	7.29	13.23
Boc-Thr(Bzl)-Cys(Acm)-Val-NH_2 +2 H_2O	-15.6 (c=1.182)[a]	Calcd.	52.49	7.67	11.34
		Found.	52.25	7.61	11.14
Boc-Leu-Thr(Bzl)-Cys(Acm)-Val-NH_2 +0.5 H_2O	-40.0 (c=0.422)[a]	Calcd.	56.31	7.88	11.94
		Found.	56.37	7.80	11.91
Boc-Leu-Leu-Thr(Bzl)-Cys(Acm)-Val-NH_2 +0.2 H_2O	-5.3 (c=0.260)[b]	Calcd.	57.71	8.12	12.08
		Found.	57.66	8.10	12.00
Boc-Pro-Leu-Leu-Thr(Bzl)-Cys(Acm)-Val-NH_2[e] +0.7 H_2O	-25.6 (c=1.081)[b]	Calcd.	57.59	8.03	12.15
		Found.	57.58	8.06	12.21

(a) In methanol. (b) In N,N-dimethylformamide. (c) Scheme 1. (d) Scheme 2. (e) Scheme 3.

Ac-Pro-Tyr-Ser-Cys(Acm)-Arg-Ala-Gly-Ala-Cys(Acm)-Ser-Thr-Cys(Acm)-Ala-Gly-Pro-Leu-Leu-Thr-Cys(Acm)-Val-NH_2 (20-peptide(S-Acm)).

20-peptide(blocked) (230 mg, 0.08 mmol) was treated with HF and anisole (0.5 ml, 4.6 mmol) by literature method.[11] The product was purified by CM sephadex (pH 5 AcOH-$AcONH_4$ buffer solution, A linear gradient from 0.02 M to 0.1 M, The product was recollected from fraction No. 44-50.), sephadex G-25 (pH 5 AcOH-AcONH4 buffer solution, A linear gradient from 0.02 M to 0.1 M, The product was recollected from fraction No. 17-22.), and LH-20 (AcOH-H_2O 0.1 % solution. The product was recollected from fraction No. 15-18) to give the title compound (34 mg, 6.7 %). The elusion pattern of each steppes were shown in Fig. 3.

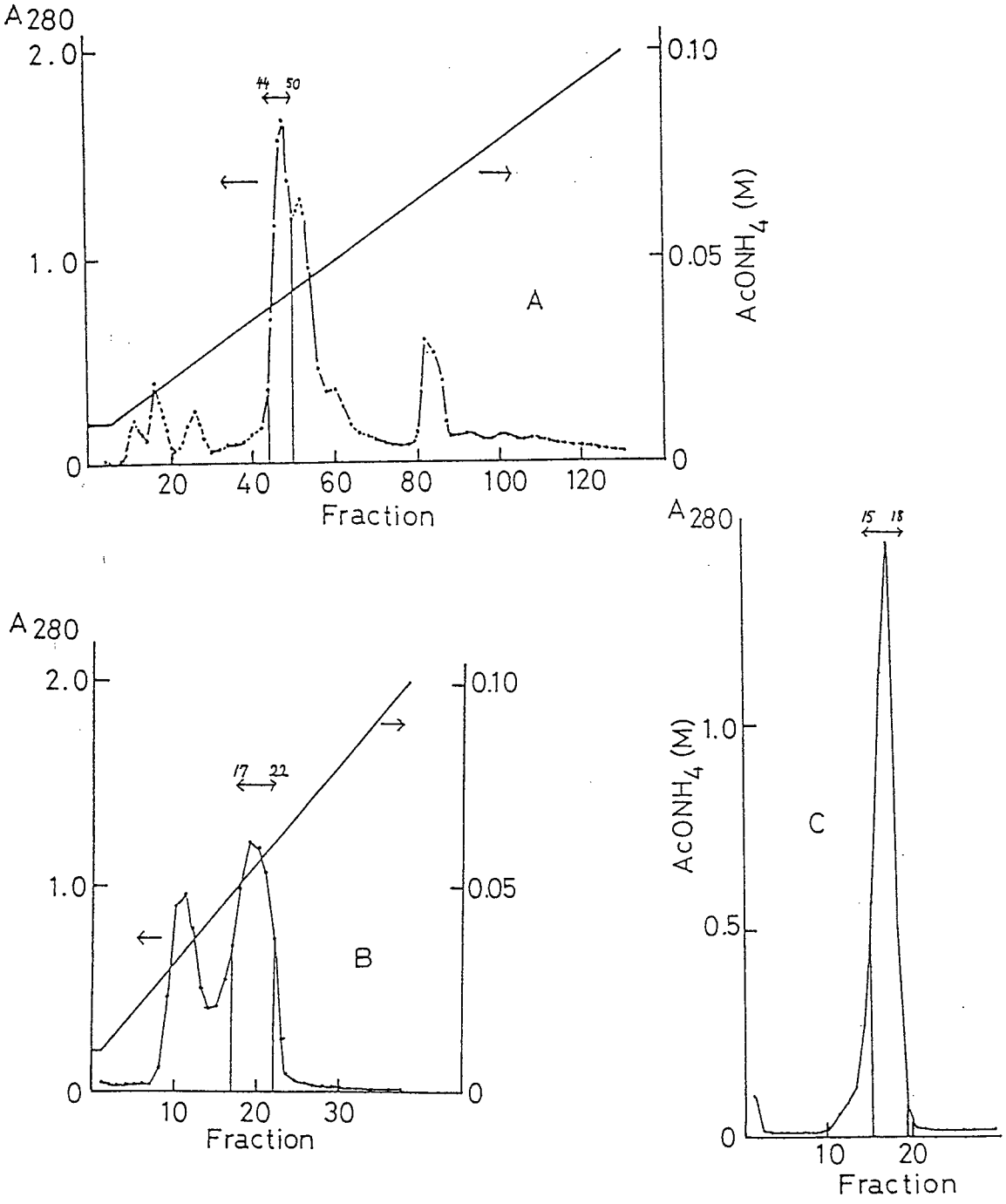

Figure 3. The purification scheme of 20-peptide(S-Acm). (a) CM Sephadex, (b) Sephadex G-25, and (c) Sephadex LH-20.

20-peptide

To an aqueous solution (5 ml) of 20-peptide(S-Acm) (10 mg, 4.4×10^{-6} mol) was added $HgCl_2$ (7.2 mg, 2.5×10^{-5} mol) at room temperature. The solution was stirred vigorously for 4 hr and washed three times with 6 ml of ether. The solution was flushed with argon gas, followed by blowing hydrogen sulfide through for 3 hr at room temperature. Black precipitate was removed by filtration. The filtrate was lyophilized and white solid contained was stocked under argon atmosphere.

Synthesis of [Fe_2S_2(20-peptide)]

all manipulations were carried out under argon atmosphere. Two methods were used for the synthesis of [Fe_2S_2(20-peptide)].

Method (a) is from the 20-peptide and $[Fe_2S_2Cl_4]^{2-}$ with the addition of triethylamine in DMF.[5,12]

Method (b) is by a ligand exchange method between the 20-peptide and $[Fe_2S_2(S\text{-}t\text{-}Bu)_4]^{2-}$ in DMF. The ligand exchange method is more suitable for the quantitative formation of 20-peptide/$Fe_2S_2^{2+}$ complex in DMF solution because *t*-butylthiol liberated was easily removed in vacuo.[6]

A DMF solution of 20-peptide (4.4 mg, 2.2×10^{-6} mol)was mixed with a DMF solution (3 ml) of $[NEt_4]_2[Fe_2S_2(S\text{-}t\text{-}Bu)_4]$ (1.5 mg, 2.2×10^{-6} mol) at room temperature. The solution was concentrated under reduced pressure at room temperature. The residue was washed with acetonitrile and

dried in vacuo.

Physical measurement.

Absorption spectra were measured on a JASCO UVIDEC-5A spectrophotometer in visible region. CD spectra were recorded on a JASCO J-40 spectropolarimeter, using a cell of 1 mm path length. Sample concentrations were 3.7 $\times 10^{-4}$ M in DMF. ε and $\Delta\varepsilon$ values were calculated in units of $mol^{-1}cm^{-1}$. 400 MHz ^{1}H-NMR spectra were recorded on a JEOL GSX-400 spectrometers at 30°C for GSX-400. Spinach ferredoxin (10 mg) in 5 ml of 3 M NaCl soln. were dialyzed five times with D_2O for desalting and finally 0.5 ml of the solution was taken. To the solution was added to 0.5 ml Me_2SO-d_6 to measure the ^{1}H-NMR spectrum of denatured ferredoxin at room temperature. ESR spectra were recorded at 77 K on a Jeol JESFEIX instrument with 100 kHz magnetic field modulation. The g value was standardized using the 7,7,8,8,-tetracyanoquinodimethane (TCNQ) radical (g = 2.0025) and Mn(II) (g = 1.981). The ESR sample was prepared by the following method. One ml solution (8.7×10^{-4} M) of $[NEt_4]_2[Fe_2S_2$(20-peptide)] was mixed with 0.2 ml of DMF solution (3.7×10^{-4} M) of $Na_2S_2O_4$ at room temperature. Differential pulse polarograms were performed under Ar with a Yanaco-P-1100 polarographic analyzer. Sample solutions were 2×10^{-4} $mol\cdot dm^{-3}$. [N(*n*-Bu)$_4$][ClO_4] and KCl was used as a supporting electrolyte. The voltamograms were recorded at room temperature with a saturated calomel electrode (SCE) as the reference.

2-3. Results and Discussion

Synthesis

Two underscored sequences in Fig. 2 correspond to the Pro(38)---Gly(51) and Leu(77)---Val(80) around the active site of the ferredoxin. The remaining fragment, Pro-Leu, which was employed instead of Thr(52)---Val(76) in the native ferredoxin, was expected to form a preferable β-turn structure. 20-peptide(S-Acm) was synthesized by the sequential condensation in solution of Pro---Gly, Ala---Gly, and Pro---Val fragments. The 20-peptide(blocked) was isolated by chromatographical purification with Sephadex G-25. The purity of the 20-peptide(S-Acm) was established by observation of four sets of ^{1}H-NMR signals of Cys(Acm) methyl groups at 1.84, 1.85, 1.86, and 1.88 ppm in D_2O. Direct synthesis of the complex **1** was attempted from reaction of $FeCl_3$, S^{2-}, and the 20-peptide in aqueous solution. The reaction mixture gave an absorption maximum at 400 nm due to $Fe_4S_4^{2+}$-type complex was decomposed by hydrolysis and the solution decolorized concomitantly.

[Fe_2S_2(20-peptide)] (**1**) was synthesized by the method (a) and (b). Unavoidable contamination of Cl derivatives $[Fe_2S_2Cl_4]^{2-}$ was encountered in the method (a). Successfully we synthesized **1** by the method (b). **1** is sensitive against air or water, and soluble in DMF or dimethylsulfoxide and insoluble in acetonitrile and dichloromethane.

Visible and CD spectra of [Fe_2S_2(20-peptide)]

The solution of [Fe_2S_2(20-peptide)] (**1**) exhibits S-Fe ligand-metal charge transfer absorption in DMF at 423 nm (ε:6580) and 461 nm (ε:5000) which are to be compared with the maxima at 423 nm (ε:9700) and 466 nm (ε:8520) for native oxidized 2Fe-2S ferredoxin.[8] The addition of water to the DMF solution of **1** resulted in decomposition with disappearance of the absorption maxima at 423 and 461 nm. This is consistent with failure of the direct synthesis of **1** from $FeCl_3$, S^{2-}, and 20-peptide in aqueous solution. The peptide chain, therefore, does not form the favorable conformation to keep an $Fe_2S_2^{2+}$ core in water.

The CD extrema of **1** in DMF were observed at 380 nm (Δε:-0.3), 396 nm (Δε: +0.65), 413 nm (Δε:-1.1), 458nm (Δε: +2.15), 490 nm (Δε: +0.65), and 592 nm (Δε: -1.5). The results indicate that **1** has a very similar conformation with that of the active site of the denatured form of plant-type ferredoxin.[13]

In an aqueous Triton X-100 solution, plant-type ferredoxin has been reported to give a denatured form.[12] Two characteristic absorptions of **1** in 10 % aqueous Triton X-100 solution were observed at the same wavelength at 420 and 450 nm as those of plant-type ferredoxin in DMF. The present results suggest the presence of stable 2Fe-2S complex in hydrophobic micelles just like Triton X-100 (10 %) aqueous solution. If **1** has the expected structure as shown in Fig 2-b, hydrophobic amino acid side chains are exposed to solution and protects **1** from solvent.

Therefore, use of nonpolar solvent is crucial for construction of the suitable structure, otherwise water solvent induces aggregation of the hydrophobic amino acid side chains and probably decomposes $Fe_2S_2^{2+}$ core by hydrolysis.

^{1}H-NMR spectra of [Fe_2S_2(20-peptide)] and denatured plant-type ferredoxin

The results of the CD spectra of **1** indicate that the environment around $[Fe_2S_2]^{2+}$ core is similar to that of denatured plant-type ferredoxin.

^{1}H-NMR spectra of [Fe_2S_2(20-peptide)] in Me_2SO-d_6 and denatured spinach ferredoxin in D_2O-Me_2SO-d_6 mixed solvent (v/v = 1/1)[14] at Cys CH_2 region are shown in Fig.4. Denatured Fd shows two broad signals at 39.0 and 32.3 ppm, although the native plant-type ferredoxin has been reported to give one broad peak around 35 ppm.[15] This peak separation may be due to the conformational difference around $[Fe_2S_2]^{2+}$ core between native Fd and denatured Fd.

1 shows three peaks at 39.7, 33.9, and 24.5 ppm. The two peaks (39.7 and 33.9 ppm) at low fields were observed at the normal position of Cys CH_2 signal in the plant type Fd, similar to those of denatured spinach ferredoxin. The results show that the four Cys residues of **1** are present with almost the same environment as those of the denatured spinach ferredoxin.

Previously, we have reported that [Fe_2S_2(Z-cys-Ala-Ala-cys-OMe)$_2$]$^{2-}$ having a chelating peptide ligand exhibits

one of the Cys CH_2 signals at 22.4 ppm due to the difference between two Fe-S bond characters of Cys^1 and Cys^2 in Cys^1-X-Y-Cys^2.[6] Therefore, the presence of this low field peak at 24.5 ppm indicates that the isomeric 2Fe-2S complex having structure A of scheme 1 is contaminated in the sample solution.

A single peak at 18.1 ppm or at 15.8 ppm appears in both samples. This peak at 10~20 ppm region was similar to the signal (around 17 ppm) reported for the native plant-type ferredoxin. In this region (10~20 ppm), both of the [4Fe-4S] type ferredoxin and [4Fe-4S] peptide model complex also provide the Cys CH_2 proton signals at around 17 ppm.[5]

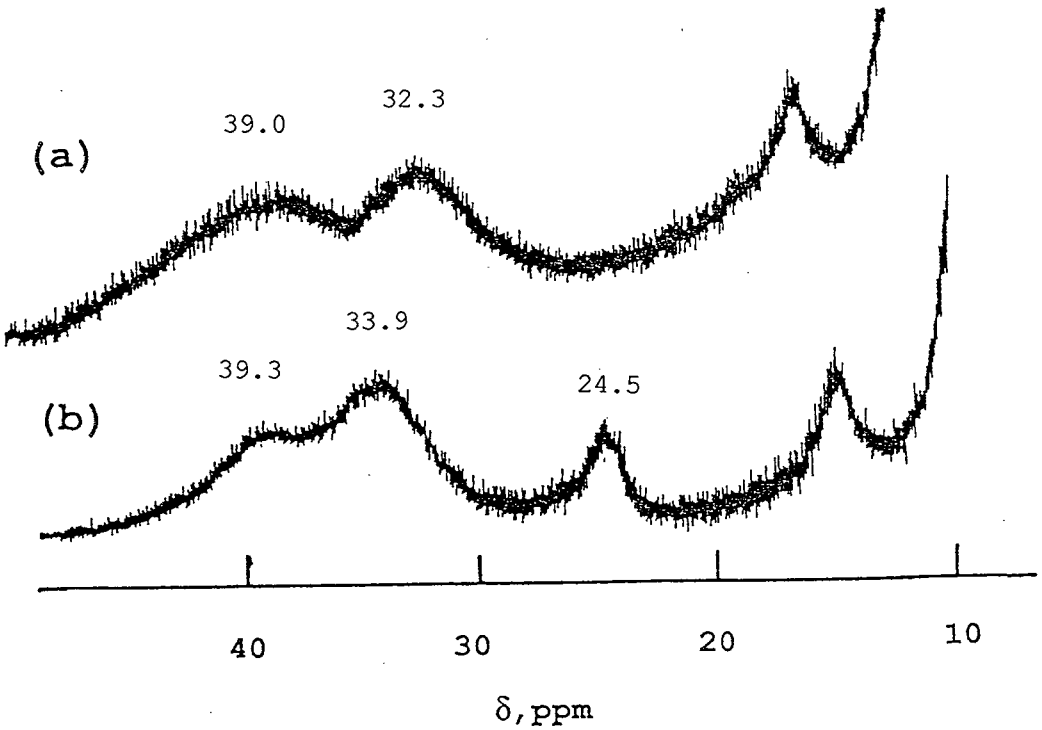

Figure 4. 400 MHz ^{1}H-NMR spectra in Cys $C\beta H_2$ region of (a) denatured Spinach ferredoxin in D_2O/Me_2SO-d_6 (v/v = 1/1) solution and (b) [Fe_2S_2(20-peptide)] in Me_2SO-d_6.

Electrochemical properties

The redox potential of **1** was obtained using pulse polarography or cyclic voltammography. A DMF solution of **1** exhibited two redox couples and the major one was at -0.64 V vs. SCE (i_{pc}/i_{pa} = 0.94) at room temperature. We have studied the electrochemical properties of a peptide model complex, $[Fe_2S_2$(Z-cys-Gly-Ala-Gly-Ala-cys-Ala-Ala-cys-OMe)(S-*t*-Bu)$]^{2-}$ (**2**) which exhibited also two redox couples at -0.81 V (i_{pc}/i_{pa} = 0.73) and -0.91 V vs. SCE (i_{pc}/i_{pa} = 0.73) due to the presence at least of two isomers as shown in Figure 5. In complex **1**, the peptide fragment (Cys-Arg-Ala-Gly-Ala-Cys-Ser-Thr-Cys) is also considered to chelate to $Fe_2S_2^{2+}$ core with two different coordination types as those of **2**. The Cys-X-Y-Cys fragment of isomer A bridges between the two Fe(III) ions of $[Fe_2S_2]^{2+}$ core and the Cys-A-B-C-D-Cys fragment chelates one of the two Fe(III) ions. Another structure B has a bridging fragment of Cys-A-B-C-D-Cys and then Cys-X-Y-Cys chelates one Fe(III) ion. The presence of the two isomers is due to trivial difference in bridging or chelation ability between both peptide fragments.

The redox potential of the main couple at -0.64 V vs. SCE in DMF is almost the same as that of spinach ferredoxin in aqueous solution corrected in the unit of SCE. The electrochemical results suggest that isomer A of $[Fe_2S_2$(20-peptide)$]^{2-}$ has a similar circumstance to the active site of the native one. Although experiment is impossible in nonpolar solvent such as dichloromethane can be done

because of its insolubility. Realization of the same redox potential by **1** suggests that solvent has almost no influence on the electrochemical properties of $Fe_2S_2^{2+}$ core since the 20-peptide ligand covers over the $Fe_2S_2^{2+}$ core and shield the core from solvent.

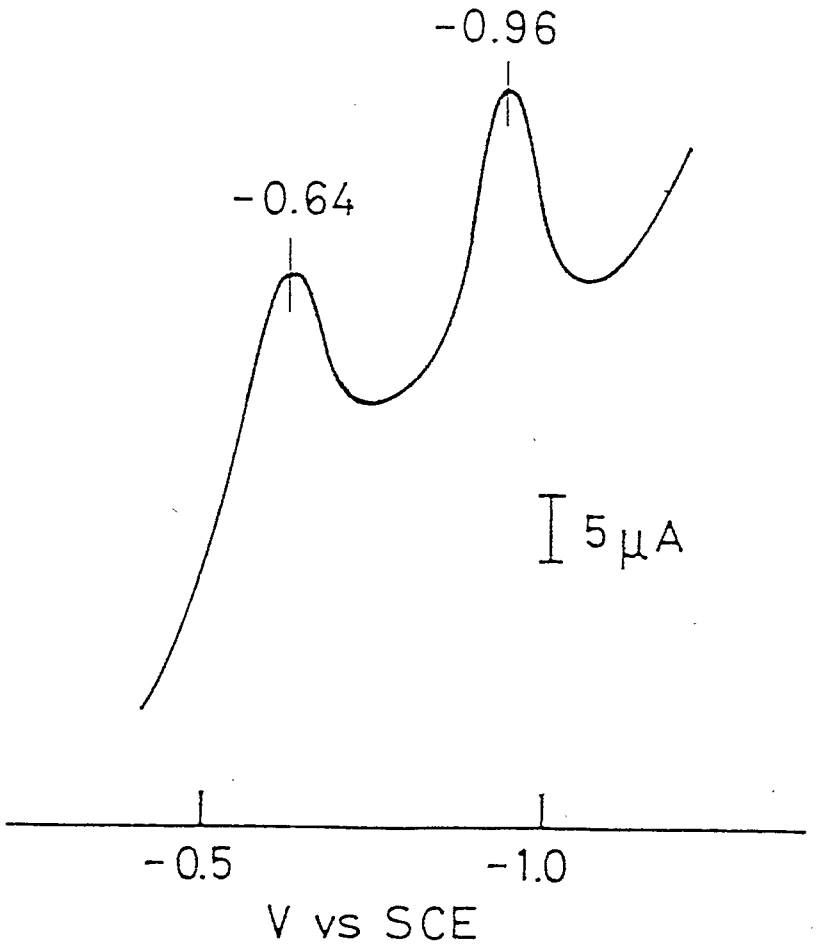

Figure 5. Differential pulse polarogram of [Fe_2S_2(20-peptide)] in DMF.

ESR spectra of the reduced model complex.

The presence of a characteristic 2Fe-2S core is also confirmed by the ESR spectrum of the reduced **1**. The (3-) species of the simple Fd analogues as reduced by addition of an aqueous solution of 18-crown-6 $Na_2S_2O_4$ exhibits an ESR signal at g = 2.014, 2.000,and 1.963 for $[Fe_2S_2(S\text{-}t\text{-}Bu)_4]^{2-}$ or at g = 2.014, 1.982 and 1.959 for $[Fe_2S_2(Z\text{-cys-Ala-Ala-cys-OMe})_2]^{2-}$ in DMF at 77 K, respectively. These signals were assigned to those of the $[Fe_2S_2(L)_4]^{3-}$(L = S-*t*-Bu, cys-peptide) because of absence of high-spin signal in the region of g = 4. The addition of an excess of the reducing reagent resulted in decomposition of the (3-) species exhibiting a signal at g_{av} = 4.26 ~ 4.55. The formation of the (3-) species of **1** is evidenced by an ESR spectrum with g = 2.014, 1.973, and 1.399 at 77 K. The spectrum is quite similar to the denatured ferredoxins reported for *H· halobium* ferredoxin[16] and for *Spirurina maxima* ferredoxin. The 2Fe-2S core in denatured ferredoxins was reported not to be destroyed but relaxed from the peptide constraint. Therefore, the rhombic ESR signals in the native ferredoxins are considered to arise from the restricted orientation of cysteinyl thiolato ligand against the 2Fe-2S core by folding the peptide chains.

Conclusions

The artificial construction of the chemical environments of the active site of 2Fe ferredoxin by using the model peptide fragment realized a positive shift of redox potential (-0.64 V vs. SCE in DMF) from the simple model complexes. The peptide circumstance of the model complex is thus similar to that of the denatured form of the ferredoxin. Therefore, upon incorporation of $[Fe_2S_2]^{2+}$ core into the 20-peptide, the Fe-S(cys) bond formation occurs randomly to give at least two isomers. In the case of the denatured form of plant-type ferredoxins, the original Fe-S(cys) bonds are maintained even with random conformations of the surrounding protein. Our results strongly suggest importance of a specific conformation around from Cys residues for the specific $[Fe_2S_2]^{2+}$ core incorporation. The sensitivity of **1** against air or water is presumably associated with the conformational rigidity of the peptide chain. The model complex is still quite sensitive as compared with the native protein with rigid conformation around the active site. The peptide sequences around the active site are now found to control the redox potential of the plant-type ferredoxin. The 2Fe-2S core incorporation, however, was not controlled under the flexible conformation environment of the 20-peptide (like as denatured state of the native ferredoxin).

References

(1) Masaki, R.; Yoshikawa, S.; Matsubara, H. *Biochem. Biophys. Acta* **1982**, 700, 101.

(2) Tagawa, K.; Arnon, D.I. *Biochem. Biophys. Acta* **1968**, 153, 166.

(3) Mayerle,J. J. ; Frankel, R. B.; Holm, R. H.; Ibers, J. A.; Phillips, W. D.; Weiher, J. F. *Proc. Natl. Acad. Sci. U.S.A.* **1973**, 70, 249.

(4) Mayerle, J.J.; Denmark, B.V.; DePamphilis, B.V.; Ibers, J.A.; Holm, R.H. *J. Am. Chem. Soc.* **1975**, 97, 1032.

(5) Balasubramaniam, A.; Coucouvanis, D. *Inorg. Chim.Acta*, **1983**, 78, L35.

(6) Ueno, S.; Ueyama, N.; Nakamura, A.; Tsukihara, T. *Inorg. Chem.* **1986**, 25, 1000.

(7) Stephens, P. J.; Thomson, A. J.; Dunn, J. B. R.; Keiderling, T. A.; Rawlings, J.; Rao, K K.; Hall, D. O. *Biochemistry* **1978**, 17, 4770.

(8) Ueyama, N.; Ueno, S.; Nakamura, A. *Bull. Chem. Soc. Jpn.* **1987**, 60, 283.

(9) Tsukihara, T.; Kobayashi, M.; Nakamura, M.; Katsube, Y.; Fukuyama, K.; Hase, T.; Wada, K.; Matsubara, H. *BioSystems* **1982**, 15, 243.

(10) Fukuyama, K.; Hase, T.; Matsumoto, S.; Tsukihara, T.; Katsube, Y.; Tanaka, N.; Kakudo, M.; Wada, K.; Matsubara, H. *Nature* **1980**, 286, 552.

(11) Sakakibara, S.; Shimonisi, Y.; Okada, M.; Sugihara, H.

Bull. Chem. Soc. Jpn. **1967**, 40, 2164.

(12) Do, Y.; Simhon, E.D.; Holm, R. H. *Inorg. Chem.***1983**, 22, 3809.

(13) Bonomi, F.; Kurtz, P. M., Jr. *Biochemistry* **1982**, 21, 6838.

(14) Ueyama, N.; Terakawa, T.; Nakata, M.; Nakamura, A. *J. Am. Chem. Soc.* **1983**, 105, 7098.

(15) Nagayama, K.; Ozaki, Y.; Kyogoku, Y.; Hase, T.; Matsubara, H. *J. Biochem.* **1983**, 94, 893 .

(16) Bertrand, P.; Gayda, J. P. *Biochim. Biophys. Acta* **1979**, 579, 107.

Chapter 3.

Chelating Tetrapeptide 2Fe-2S Complexes. Synthesis and Physicochemical Properties

3-1. Introduction.

A effect of amino acid residues in the protein is suspected to be responsible for the positive shift of redox potentials of the native 2Fe-2S ferredoxin. In fact, we have found the positive shift in an electrochemical study of the 4Fe-4S complexes of Z-Cys-Gly-Ala-OMe at low temperature in CH_2Cl_2.[1] The synthesis of 2Fe-2S complexes of oligopeptides, $[Fe_2S_2\{Ac\text{-}Gly_2\text{-}(cys\text{-}Gly_2)_2\text{-}NH_2\}_2]^{2-}$, $[Fe_2S_2(Z\text{-}cys\text{-}Ala\text{-}Ala\text{-}cys\text{-}OMe)_2]^{2-}$ and $[Fe_2S_2(Z\text{-}Ala\text{-}cys\text{-}OMe)_4]^{2-}$ which were used by the reaction of $[Fe_2S_2Cl_4]^{2-}$ with the corresponding oligopeptides has been reported.[2,3] In this chapter we report the synthesis, structure, the electrochemical properties of 2Fe-2S complexes of tetrapeptides by the ligand exchange reaction from $[Fe_2S_2(S\text{-}t\text{-}Bu)_4]^{2-}$.

We have chosen the four tetrapeptide segments i) Cys-Thr-Val-Cys and Cys-Pro-Leu-Cys which exist in rubredoxin active site and chelate an Fe^{3+} ion with their Cys thiolato side chains,[4] ii) Cys-Val-Val-Cys, which is unable to chelate the Pd^{2+} ion[5] and iii) Cys-Ala-Ala-Cys, an analogous segment of Cys-Ser-Thr-Cys which exists in 2Fe-2S ferredoxin. This Cys-Ser-Thr-Cys segment was reported to bridge between two Fe ions of $[Fe_2S_2]^{2+}$ core. From the X-ray analysis data, the

side chains of Ser-Thr segment is far from the 2Fe-2S core and have no interactions with it. The Cys-Ala-Ala-Cys segment has steric properties similar to the Cys-Ser-Thr-Cys segment and can be used for the present purpose. This chapter also describes a novel method for determination of a chelation mode of Cys-X-Y-Cys to $[Fe_2S_2]^{2+}$ core, utilizing the ligand-exchange reaction with 3,4-toluenedithiol.

3-2. Experimental Section

All procedures were carried out under argon atmosphere.

Materials.

All solvents were purified by distillation under argon atmosphere before use. The synthesis of Z-Ala-Cys-OMe, Z-Cys-Ala-Ala-Cys-OMe, and Z-Cys-Val-Val-Cys-OMe were performed by the literature method.[5] Z-Cys-Thr-Val-Cys-OMe and Z-Cys-Pro-Leu-Cys-OMe were synthesized as described elsewhere.[6] $[Et_4N]_2[Fe_2S_2Cl_4]$ was prepared according to the procedure reported by Simhon et al.[7] 3,4-Toluenedithiol (tdt-H_2) was obtained from Nakarai Chemical Co. and used without purification.

Synthesis of $[Et_4N]_2[Fe_2S_2(S\text{-}t\text{-}Bu)_4]$. (1)

$[Et_4N]_2[Fe_2S_2(S\text{-}t\text{-}Bu)_4]$ was synthesized from $[Et_4N]_2[Fe_2S_2Cl_4]$ (1 g, 2×10^{-3} mol) and *t*-BuSNa (976 mg, 8×10^{-3} mol) in THF (100 cm^3). The product was isolated by precipitation and recrystallized twice from THF-ether, yield 40 %. Absorption maximum ($c=1.28\times10^{-3}$ mol·dm^{-3} (DMF)) 334 (ε 13800), 433 (ε 8700), and 460 (sh, ε 8000); ^1H NMR (acetonitrile-d_3) δ 1.19 (24H $N(CH_2CH_3)_4$), 3.12 (16H $N(CH_2CH_3)_4$), and 4.72 (36H $SC(CH_3)_3$); Anal. Calcd for $C_{32}H_{76}N_2S_6Fe_2$: C, 48.46; H, 9.66; N, 3.53. Found: C, 47.36; H, 9.57; N, 3.49.

Determination of the cluster types of this complex by core extrusion reaction with benzenethiol was performed as previously reported.[8] Addition of an excess of benzenethiol

to the complex solution gives a benzenethiolato complex. The ratio of absorbance at 458 nm to that at 550 nm of this complex indicates a molar ratio of the $[Fe_2S_2]^{2+}$ core to the $[Fe_4S_4]^{2+}$ core. The absorbance ratios of pure $[Fe_2S_2(SPh)_4]^{2-}$ and $[Fe_4S_4(SPh)_4]^{2-}$ were 1.12 and 1.92.[8] The absorbance ratio of at 458 nm to at 550 nm of $[Et_4N]_2[Fe_2S_2(S\text{-}t\text{-}Bu)_4]$ in the reaction with 10 equiv. of benzenethiol in DMF was 1.08. From NMR spectrum, contaminating $[Fe_4S_4(S\text{-}t\text{-}Bu)_4]^{2-}$ was below 0.3 % of the 2Fe-2S complex.

Synthesis of $[Et_4N]_2[Fe_2S_2(Z\text{-cys-Ala-Ala-cys-OMe})_2]$ (2)

2 was synthesized by the ligand exchange reaction of $[Et_4N]_2[Fe_2S_2(S\text{-}t\text{-}Bu)_4]$ (10.15 mg, 1.41×10^{-5} mol) with Z-Cys-Ala-Ala-Cys-OMe (16.60 mg, 3.24×10^{-5} mol) in DMF (2 cm^3). After 5 min of mixing the reactants, the solution was concentrated in vacuo to give a brown semisolid which was washed with degassed DME and dried in vacuo. ^1H NMR (Me_2SO-d_6) δ 1.3 (24H $N(CH_2CH_3)_4$), 3.3 (16H $N(CH_2CH_3)_4$), 5.1 (4H Ph-CH_2), and 22.9, 30.7 (8H Cys C*H*). Cys CH peaks at 22.9 and 30.7 ppm and absence of a peak due to methyl protons of *t*-Bu at 4.72 ppm indicate a complete exchange of S-*t*-Bu ligand with peptide ligand. Core extrusion reaction was performed with benzenethiol (10 equiv.) in DMF to give A_{458}/A_{550}=1.12.

Synthesis of $[Et_4N]_2[Fe_2S_2(Z\text{-cys-Pro-Leu-cys-OMe})_2]$

(3)

3 was synthesized by the reaction of $[Et_4N]_2[Fe_2S_2(S\text{-}t\text{-}Bu)_4]$ (12.35 mg, 1.71×10^{-5} mol) with Z-Cys-Pro-Leu-Cys-OMe (23.1 mg, 4.0×10^{-5} mol) in 2 cm^3 of DMF as mentioned above. Core extrusion reaction by benzenethiol (10 equiv.) in DMF gave A_{458}/A_{550}=1.10.

Synthesis of $[Et_4N]_2[Fe_2S_2(Z\text{-cys-Thr-Val-cys-OMe})_2]$ (4)

4 was synthesized by the reaction of $[Et_4N]_2[Fe_2S_2(S\text{-}t\text{-}Bu)_4]$ (13.0 mg, 1.8×10^{-5} mol) with Z-Cys-Thr-Val-Cys-OMe (24.0 mg, 4.2×10^{-5} mol) in DMF (2 cm^3) as mentioned above. Core extrusion reaction by benzenethiol (10 equiv.) in DMF gave A_{458}/A_{550}=1.14

Synthesis of $[Et_4N]_{2n}[Fe_2S_2(Z\text{-cys-Val-Val-cys-OMe})_2]_n$ (5)

This was synthesized at two different concentrations to give isomeric products **5A** and **5B**. **5A** was obtained by the reaction of $[Et_4N]_2[Fe_2S_2(S\text{-}t\text{-Bu})_4]$ (10.6 mg, 1.47×10^{-5} mol) with Z-Cys-Val-Val-Cys-OMe (17.15 g, 3.0×10^{-5} mol) in DMF (2 cm^3) as mentioned above. ^1H NMR (Me2SO-d_6) δ 1.3 (24H $N(CH_2CH_3)_4$), 3.3 (16H $N(CH_2CH_3)_4$), 5.1 (4H Ph-CH_2), and 22.6, 30.3 (8.4H Cys CH); Core extrusion reaction by benzenethiol (10 equiv.) in DMF gave A_{458}/A_{550}=1.14. **5B** was synthesized by the reaction of $[Et_4N]_2[Fe_2S_2(S\text{-}t\text{-Bu})_4]$ (15.40 mg, 1.9×10^{-5} mol) with Z-Cys-Val-Val-Cys-OMe (24.40 mg, 4.2×10^{-5} mol) in DMF (15 cm^3) as mentioned above. Core extrusion reaction by benzenethiol (10 equiv.) in DMF gave A_{458}/A_{550}=1.16.

Synthesis of $[Et_4N]_2[Fe_2S_2(Z\text{-}Ala\text{-}cys\text{-}OMe)_4]$ (6).

6 was prepared by the reaction of $[Et_4N]_2[Fe_2S_2(S\text{-}t\text{-}Bu)_4]$ (8.2 mg, 1.1×10^{-5} mol) and Z-Ala-Cys-OMe (16.6 mg, 4.8×10^{-5} mol) in DMF (1 cm^3) and washed with ether as mentioned above. ^1H NMR (Me2SO-d_6) δ 1.3 (24H $N(CH_2CH_3)_4$), 3.3 (16H $N(CH_2CH_3)_4$), 5.1 (4H Ph-CH_2), and 31.3(3H Cys CH); Core extrusion reaction by benzenethiol (10 equiv.) in DMF gave A_{458}/A_{550}=1.20.

Synthesis of $[Et_4N]_2[Fe_2S_2(S_2\text{-}o\text{-}xyl)_2]$ (7)

7 was prepared according to the reported procedure.[9]

Synthesis of $[Et_4N]_2[Fe_2S_2(tdt)_2]$ (tdt = 3,4-toluenedithiolate).

To a solution of **1** (200 mg. 2.5×10^{-4} mol) in acetonitrile (20 cm^3) was added 3,4-toluenedithiol (35 mg, 2.3×10^{-4} mol) with stirring at room temperature. The solution was concentrated under reduced pressure and the residue was washed with fresh THF. The powder obtained was recrystallized with acetonitrile and ether and gave black microcrystals. Found: C, 46.73; H, 7.39; N, 3.33. Calcd for $C_{30}H_{62}N_2S_6Fe_2$: C, 48.38; H, 7.39; N, 3.76. Absorption maxima (DMF); 550 nm (ε 4000), 496 nm (ε 5260), 475 nm (sh. ε 4800), 383 nm (ε 9100), and 320 nm (ε 9700). ^1H NMR spectrum:o-CH_3,δ 4.5;Ph-H_2, 10.2 and 10.5 (Me_2SO-d_6).

Detection of H_2S.

Argon gas was bubbled into a DMF solution (2 cm^3) of **2** (30.3 mg 2.1×10^{-5} mol) and the gas was vented through an 8 mM aqueous silver nitrate solution. After addition of tdt-H_2(6.4 mg, 4×10^{-5} mol) into the DMF solution, the silver nitrate solution gave a black precipitate upon bubbling argon gas at room temperature. The black precipitate was collected with filtration. Yield 7 mg of silver sulfide (68 %).

Physical measurement

Absorption spectra were measured on a JASCO UVIDEC-5A spectrophotometer in visible region. CD spectra were recorded on a JASCO J-40 spectropolarimeter. The calibration of the spectropolarimeter was carried out with *epi*-androsterone in dioxane.[10] The values of ε and $\Delta\varepsilon$ were given in the unit of $M^{-1}cm^{-1}$. 90 MHz and 400 MHz ^{1}H-NMR spectra were recorded on a JEOL FX-90Q and GX-400 spectrometers at 31°C for FX-90Q and 23 °C for GX-400. ESR spectra were obtained at 77 K on a JEOL JESFEIX with 100 kHz magnetic field modulation. The g-value was standardized by using 7,7,8,8 - tetracyanoquinodimethane (TCNQ) radical (g=2.0025) and Mn(II) (g=1.981). The reduction of 2Fe-2S peptide complexes was carried out by the addition of 1/4 equiv. of 18-crown-6/$Na_2S_2O_4$ to the complex solution. Cyclic voltammetries were performed under Ar with a Yanaco-P8-CV equipped with a function generator Yanaco model FG- 1218. Sample solutions were 5 - 8×10^{-3} mol·dm^{-3}. [N(*n*-Bu)$_4$][ClO_4] was used as a supporting electrolyte. The voltamograms were recorded at room temperature with a saturated calomel

electrode (SCE) as the reference.

Calculation method

Calculations of the idealized structure were carried out according to the Hendrickson and Konnert procedure,[11] using a HITAC M-150 at the computer center of Tottori university. A three-dimensional molecular model of $[Fe_2S_2(cys\text{-}Val\text{-}Val\text{-}cys)_2]^{2-}$ was deduced from the chelating structure of Cys-Thr-Val-Cys segment in a *C. pasteurianum* rubredoxin, which was used as an initial model; the molecular model was generated by replacing Thr with Val.

The difference visible spectra of the above systems were obtained by subtracting (a) from (b) to give a spectrum corresponding to the spectrum of a DMF solution of authentic $[Et_4N]_2[Fe_2S_2(tdt)_2]$.

3-3. Results and Discussion

New synthetic method of 2Fe-2S peptide complexes derived from $[Et_4N]_2[Fe_2S_2(S\text{-}t\text{-}Bu)_4]$.

Synthesis of peptide complexes.

Previously, the synthesis of peptide 2Fe-2S complexes from $[Fe_2S_2Cl_4]^{2-}$ was reported.[3] The 2Fe-2S complex synthesized from Z-Cys-Ala-Ala-Cys-OMe and $[Fe_2S_2Cl_4]^{2-}$ with addition of NEt_3 shows a similar absorption spectrum to **1** synthesized from $[Fe_2S_2(S\text{-}t\text{-}Bu)_4]^{2-}$. The former complex, however, shows weaker CD extrema in DMF and less stable redox couples of 3-/2-. The substitution of Cl^- with RS^- described in the previous chapter was now found to be not proceeding completely. Difficulty in complete Cl^-/RS^- exchange has also been found by Wong et al.[12] The ligand exchange reaction from $[Fe_2S_2(S\text{-}t\text{-}Bu)_4]^{2-}$ with the addition of 4 equiv. of Cl^- and of peptides was carried out to examine the effect of co-existence of Cl^- ion. The product was found to be mostly $[Fe_2S_2Cl_4]^{2-}$ by the ligand exchange reaction. Thus, competition between Cl^- and RS^- is favorable to Cl^- for binding with $[Fe_2S_2]^{2+}$ core.

The ^1H NMR spectra of the model complexes are to be compared with the native ones. Thus Cys CH_2 signals of 4Fe-4S ferredoxins and their model complexes were reported to be observed at 10-20 ppm region[13,14] and the signals of 2Fe-2S ferredoxins were observed at 32-37 ppm.[13] The results of ^1H NMR Cys CH_2 signals of the complexes at 20-35 ppm and core

extrusion reaction by benzenethiol in DMF confirm the presence of a 2Fe-2S core in all tetrapeptide complexes. Thus, 2Fe-2S core was conserved during a ligand exchange reaction.

t-Bu-S$^-$ ligand in $[Fe_2S_2(S\text{-}t\text{-}Bu)_4]^{2-}$ can be easily expelled by Cys-containing peptides such as Z-Ala-Cys-OMe and Z-Cys-Ala-Ala-Cys-OMe. This ligand-exchange reaction in the following equation was utilized for the synthesis of [2Fe-2S]/Cys-containing peptide complexes[15] as well as the synthesis of [4Fe-4S] peptide complexes.[16-18] The authentic $[Et_4N]_2[Fe_2S_2(tdt)_2]$ was synthesized by the same method.

$$[Fe_2S_2(S\text{-}t\text{-}Bu)_4]^{2-} \xrightarrow{RS^-} [Fe_2S_2(SR)_4]^{2-} + t\text{-BuSH}$$

(SR^- = Z-Ala-Cys-OMe, Z-Cys-Ala-Ala-Cys-OMe/2)

Examination of Chelation of Peptide Ligands on $[Fe_2S_2]^{2+}$ Core by Ligand-Exchange Reaction with 3,4-Toluenedithiol (tdt-H_2).

tdt-H_2 readily exchanges with the monodentate ligand of [2Fe-2S] complexes of **1** and **5**. Figure 1-i or ii shows the visible spectra of **1** or **5** in DMF and the spectral change by the addition of various molar equivs of tdt-H_2 to **1**. The addition resulted in formation of a new species give an isosbestic point at 465 nm. The visible spectrum of the new species obtained by the addition of one equiv of tdt-H_2 is shown in Fig. 1-i-b. Fig. 1-ii-b shows a difference spectrum between **1** and the reaction mixture. The new species exhibits absorption maxima at 566, 495, 470, 375(sh), and 336 nm for **1** or 566, 493, 470, 373(sh), and 335 nm for **5** in DMF. The absorption maximum at 566 nm is assignable to a characteristic ligand-metal charge-transfer (LMCT) band for $[Fe_2S_2(S\text{-}R)_4]^{2-}$ complex. The species having these absorption maxima (550, 496, 470, 370, 320 nm) was thus identified as the authentic $[Fe_2S_2(tdt)_2]^{2-}$ complex. The formation of $[Fe_2S_2(tdt)_2]^{2-}$ was observed by ^1H NMR spectrum of a reaction mixture of $[Fe_2S_2(Z\text{-}Ala\text{-}cys\text{-}OMe)_4]^{2-}$ with tdt-H_2 in Me_2SO-d_6. Two broad peaks at δ 10.2 and 10.8 were found and assignable to the phenyl protons of tdt ligand, since the authentic tdt complex exhibited two Ph-*H* signals at δ 10.2 and 10.5 in Me_2SO-d_6. The methyl proton peaks of the ligand were overlapped with *t*-Bu peaks at δ 4.7.The addition of tdt-H_2 to **6** results in formation of $[Fe_2S_2(tdt)_2]^{2-}$ with a smooth substitution reaction of Z-Ala-Cys-OMe with the tdt ligand.

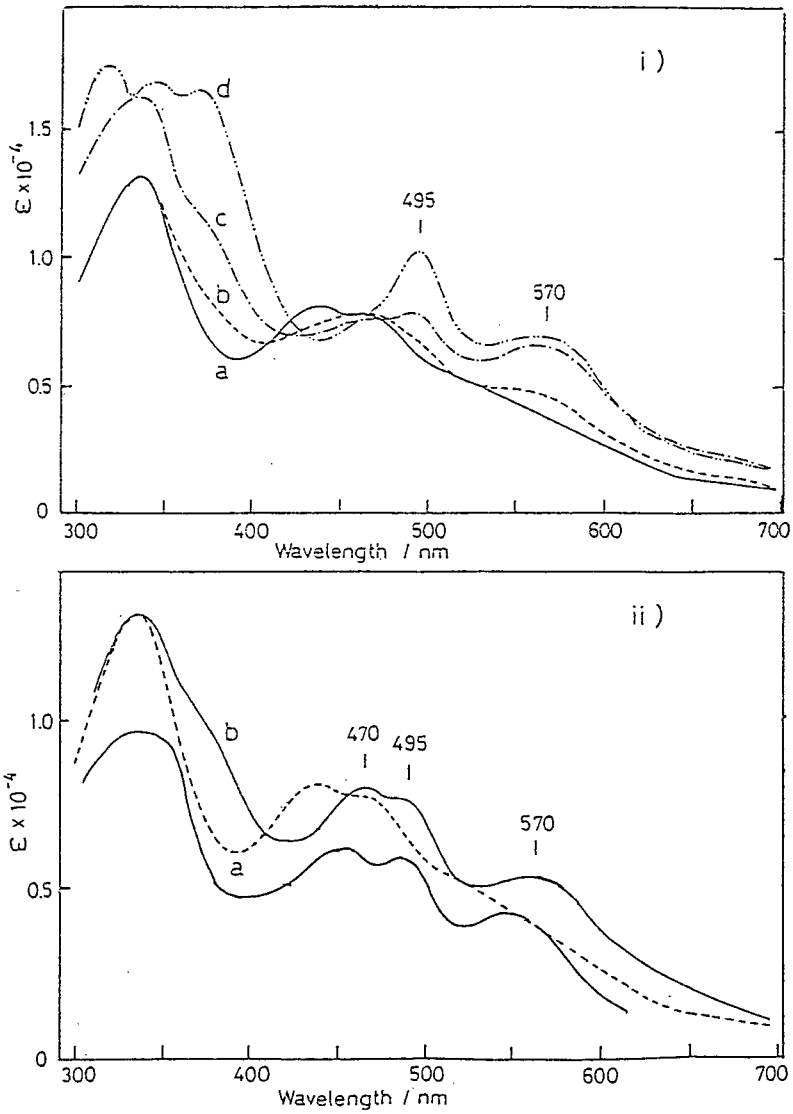

Figure 1. Visible spectra of i) (a) a DMF solution of $[NEt_4]_2[Fe_2S_2(S\text{-}t\text{-}Bu)_4]$ at room temperature, (b) solution-(a) + tdt-H_2(1 equiv.), (c) solution-(a) + tdt-H_2(2 equiv.) and (c) solution-(a) + tdt-H_2(4 equiv.) and ii) (a) a DMF solution of $[NEt_4]_2[Fe_2S_2(S\text{-}t\text{-}Bu)_4]$, (b) the difference visible spectrum of the reaction mixture of $[NEt_4]_2[Fe_2S_2(S\text{-}t\text{-}Bu)_4]$ and tdt-H_2 (1:1), and (c) the visible spectrum of a DMF solution of $[NEt_4]_2[Fe_2S_2(tdt)_2]$ at room temperature.

In this case, the $[Fe_2S_2]^{2+}$ core remains until the addition of over 5 equivs of tdt-H_2.

The addition of over 3 equivs of tdt-H_2 to **1** resulted in formation of another new species having absorption maxima at 495 nm (ε 14500), 375 nm (ε 27400), and 313 nm (ε 19500) (Fig. 2). The addition of tdt-H_2 to a DMF solution of $[Fe_2S_2(S_2\text{-}o\text{-}xyl)_2]^{2-}$ (**7**) (Fig. 3) or $[Fe_2S_2(Z\text{-}cys\text{-}Ala\text{-}Ala\text{-}cys\text{-}OMe)_2]^{2-}$ (**2**) (Fig.4) at (1:1) molar ratio gave another species which exhibits absorption maxima at 492 nm (ε 9700), 370 nm (sh. ε 13000),and 339 nm (ε 16000). The difference spectrum of the species is shown in Fig. 4-b. The chelation of two tdt ligands is expected for Fe(III).

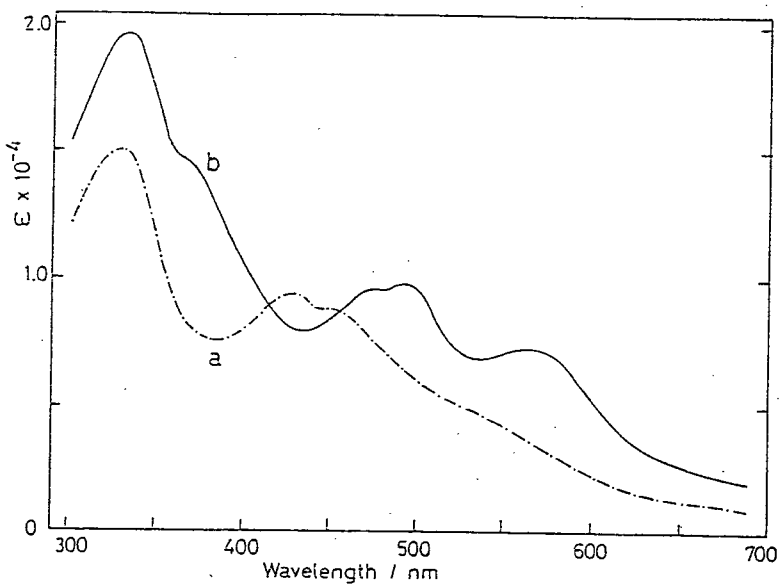

Figure 2. Visible spectra of (a) $[NEt_4]_2[Fe_2S_2(Z\text{-}Ala\text{-}cys\text{-}OMe)_4]$ and (b) the difference visible spectrum of the species obtained from the ligand-exchange reaction (solution-(a) + tdt-H_2 (1:1)) in DMF at room temperature.

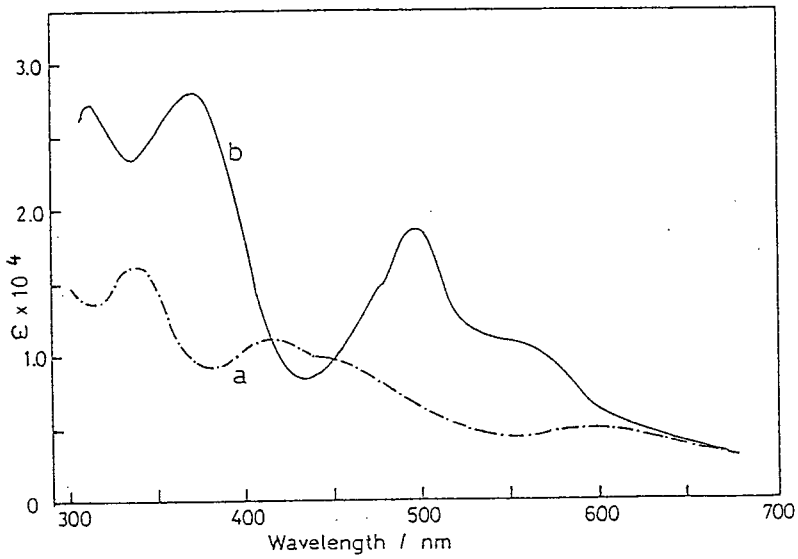

Figure 3. Visible spectra of (a) $[NEt_4]_2[Fe_2S_2(S_2\text{-}o\text{-}xyl)_2]$ and (b) the difference visible spectrum of the species obtained from the ligand-exchange reaction (solution-(a) + tdt-H_2 (1:1)) in DMF at room temperature.

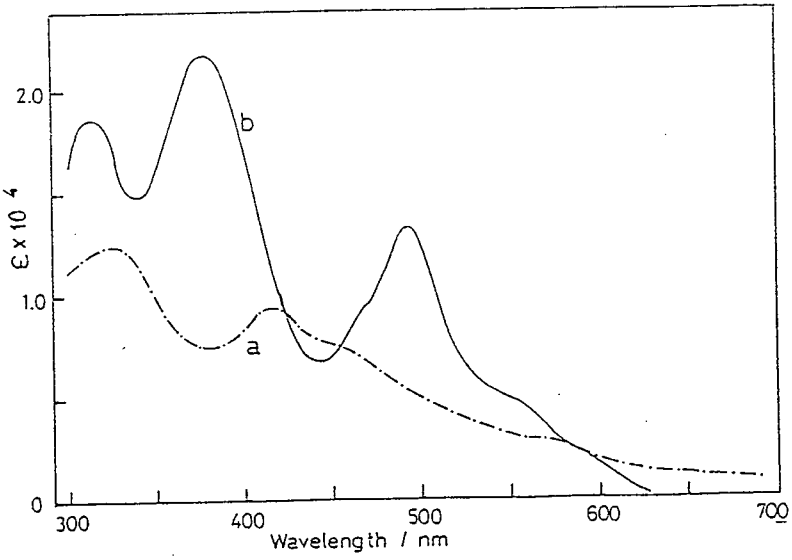

Figure 4. Visible spectra of (a) $[NEt_4]_2[Fe_2S_2(Z\text{-}cys\text{-}Ala\text{-}Ala\text{-}cys\text{-}OMe)_2]$ and (b) the difference visible spectrum of the species obtained from the ligand-exchange reaction (solution-(a) + tdt-H_2 (1:1)) in DMF at room temperature.

The absorption maxima of $[Fe(tdt)_2]^{1-}$ in DMF were reported to be observed at 645 nm (ε 100), 503 nm (ε 10000), and 386 nm (ε 17000).[19] The bis(peptide)Fe(III) complex ($[Fe(Z\text{-}cys\text{-}Ala\text{-}Ala\text{-}cys\text{-}OMe)_2]^-$) has been found to have absorption maxima at 495 nm (ε 3400) and 353 nm (ε 5500).[20] Therefore, these two bis-chelated species are not present at (1:1) ratio. Then, the new species suggests the formation of $[Fe(tdt)(Z\text{-}cys\text{-}Ala\text{-}Ala\text{-}cys\text{-}OMe)]^{1-}$. This ligand-exchange reaction gave hydrogen sulfide which was detected as silver sulfide in 68% yield. The addition of tdt-H_2 to a DMF solution of **2** results in preferential cleavage of Fe-S* at (1:1) molar ratio.

Addition of *o*-xylene-α,α'-dithiol (*o*-xyl-$(SH)_2$) to a Solution of 2Fe-2S Peptide Complex.

o-xyl-$(SH)_2$ is also one of effective chelating reagents for Fe(III) ion. The successive addition of 1-5 equiv. of *o*-xyl-$(SH)_2$ to a DMF solution of **6** and **2** shows a visible maximum at 588 nm with high molar absorption coefficient which is assignable to a LMCT absorption maximum (ε 4800) of $[Fe_2S_2(S_2\text{-}o\text{-}xyl)_2)]^{2-}$ (Fig. 5). The formation of the 2Fe-2S complex was monitored by the CD spectral method and resulted in observation of 20 % of Δε value at 580 nm (Fig. 6). Clear isosbestic points in the CD spectra were observed at 350, 395 and 437 nm. The results indicate a substitution of Z-Cys-Ala-Ala-Cys-OMe with *o*-xyl-$(SH)_2$ giving mixed ligand [2Fe-2S] complexes as shown in the following scheme. The K value (K_1,K_2) obtained by the CD method is 0.4 (K_1=0.2,

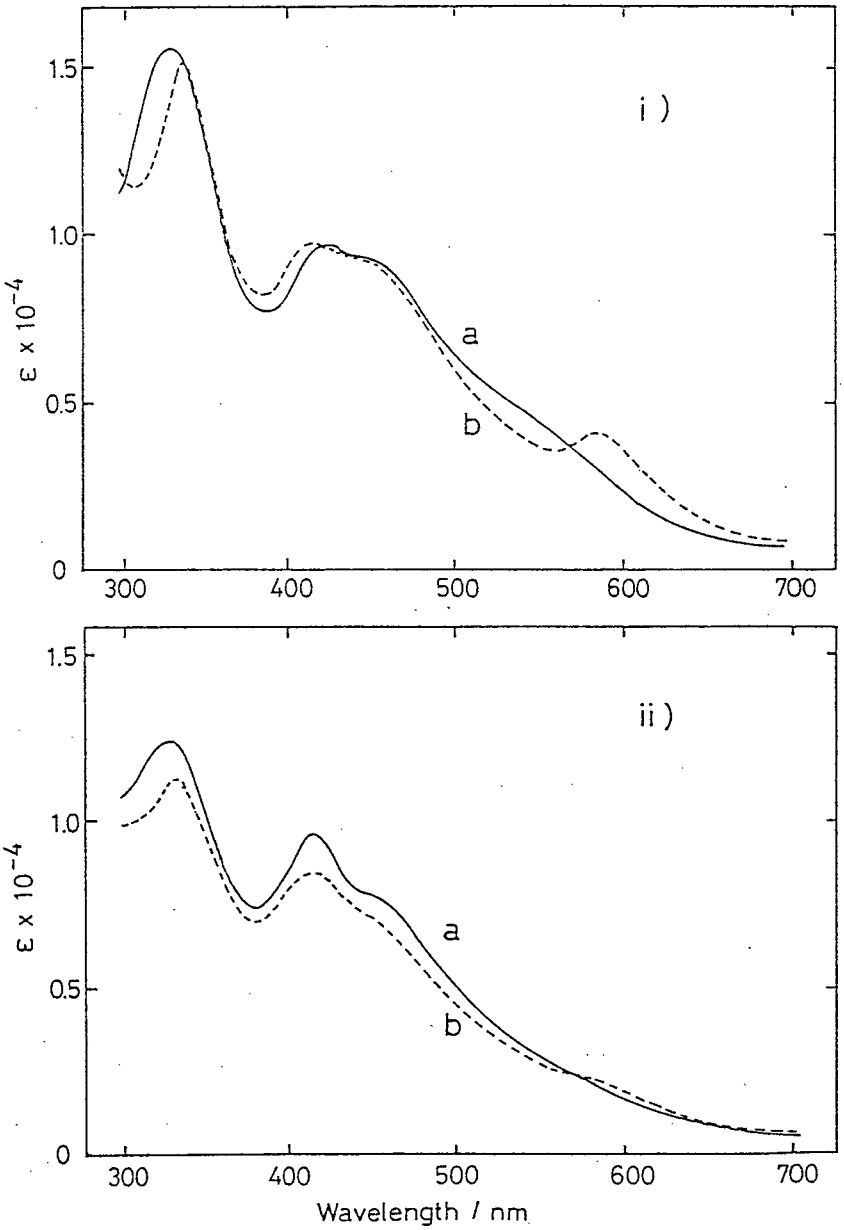

Figure 5. Visible spectral change of the ligand-exchange reaction of i) (a) $[NEt_4]_2[Fe_2S_2(Z\text{-Ala-cys-OMe})_4]$ and (b) solution-(a) + *o*-xyl-$(SH)_2$ (1:2) and ii) (a) $[NEt_4]_2[Fe_2S_2(Z\text{-cys-Ala-Ala-cys-OMe})_2]$ and (b) solution-(a) + *o*-xyl-$(SH)_2$ (1:2) in DMF at room temperature.

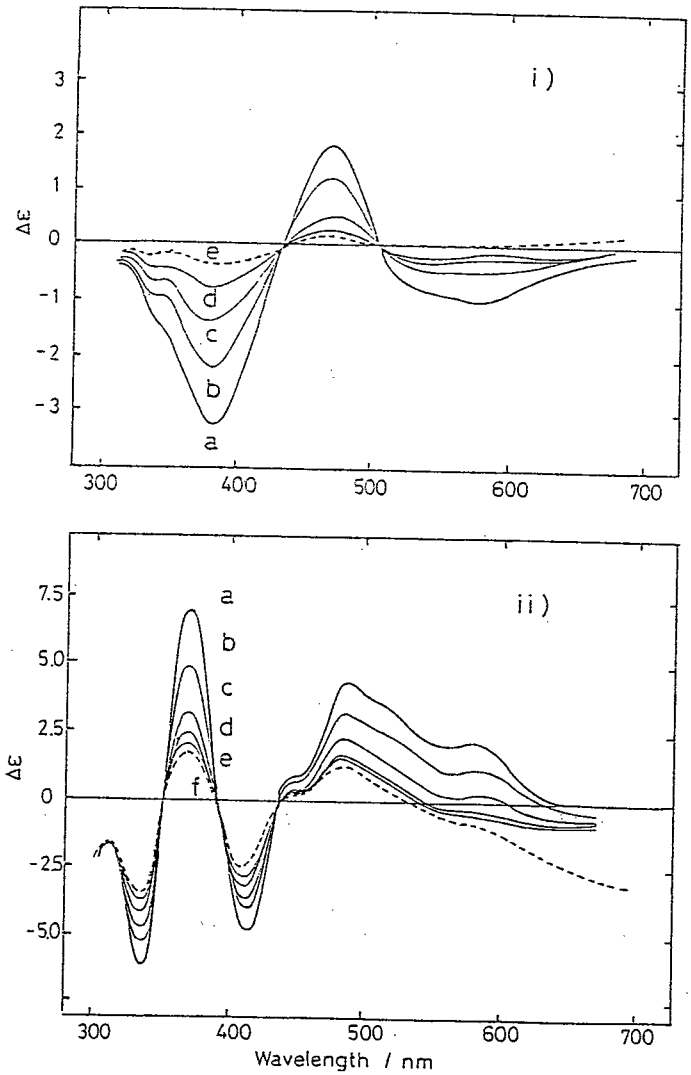

Figure 6. CD spectral change of the ligand-exchange reaction of i) (a) $[NEt_4]_2[Fe_2S_2(Z\text{-Ala-cys-OMe})_4]$, (b) solution-(a) + *o*-xyl-$(SH)_2$ (1:1), (c) (1:2), (d) (1:3), and (e) (1:4) and ii) (a) $[NEt_4]_2[Fe_2S_2(Z\text{-cys-Ala-Ala-cys-OMe})_2]$ and (b) solution-(a) + *o*-xyl-$(SH)_2$ (1:1), (c) (1:2), (d) (1:3), (e) (1:4), and (f) (1:5) in DMF at room temperature.

K_2=2.0) in DMF. On the contrary, the successive addition of *o*-xyl-$(SH)_2$ to **6** results in gradual appearance of an absorption maximum at 592 nm. K value for the ligand-exchange reaction of **6** is 0.0007 mol^2 in DMF (by the CD method).

Chelating Ability of Z-Cys-Ala-Ala-Cys-OMe.

The ligand displacement reaction by tdt-H_2 was found to be different from that by *o*-xyl-$(SH)_2$. The addition of *o*-xyl-$(SH)_2$ to **1** and **6** results in formation of $[Fe_2S_2(S_2$-*o*-$xyl)_2]^{2-}$ with a characteristic absorption maximum at 592 nm, which corresponds to the reported maximum at 590 nm (ε 4800) in DMF.[9] The difference between the K values (0.0007 for **6** and 0.4 mol^2 for **2**) is ascribed to the chelation effect of Z-Cys-Ala-Ala-Cys-OMe in **2**. The presence of the clear isosbestic point of CD spectra with addition of *o*-xyl-$(SH)_2$ to **7** indicates monodentate ligand must be substituted first with tdt ligand. The successful employment of *o*-xyl-$(SH)_2$ for the core extrusion of [2Fe-2S] adrenal ferredoxin has already been reported.[21,22]

The addition of tdt-H_2 to a DMF solution of **6** and **7** results in the cleavage of Fe-S* bond in the $Fe_2S_2^{2+}$ core, giving $[Fe(tdt)(S_2$-*o*-$xyl)]^{1-}$ or $[Fe(tdt)$(Z-cys-Ala-Al-cys-OMe)$]^{1-}$ with the following reaction scheme.

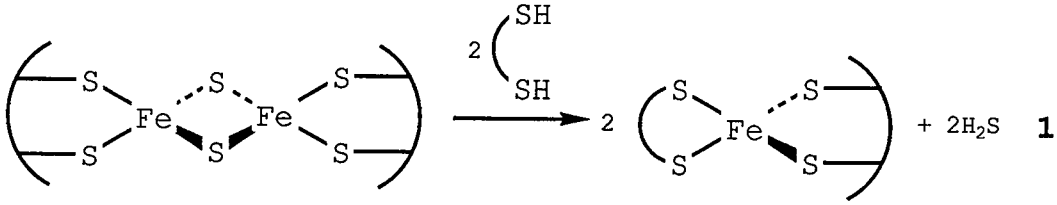

1

Previously, Ueyama et al.[23] reported that $[Fe(Z\text{-}cys\text{-}Ala\text{-}Ala\text{-}cys\text{-}OMe)_2]^{1-}$ exhibits CD extrema at 560 nm ($\Delta\varepsilon$ +1.3) and 500 nm ($\Delta\varepsilon$ -1.6) in DMF. The (1:1) species, $[Fe(tdt)(Z\text{-}cys\text{-}Ala\text{-}Al\text{-}cys\text{-}OMe)]^{1-}$, exhibits an absorption maximum at 494 nm (ε 12000) and CD extrema at 550 nm ($\Delta\varepsilon$ -0.6), 495 nm ($\Delta\varepsilon$ -1.0), and 335 nm ($\Delta\varepsilon$ -13.0). Formation of hydrogen sulfide was confirmed by precipitation of silver sulfide from silver nitrate. The satisfactory yield (68 %) of silver sulfide indicates that the addition of tdt-H_2 to **7** preferentially cleaves the Fe-S* bonds according to the eq.1. Averill et al. have reported the core extrusion of [2Fe-2S] adrenodoxin with tdt-H_2.[22] They speculated the formation of $[Fe(tdt)_2]^{2-}$ with addition of 19 equivs of tdt-H_2 to adrenodoxin. The reduction of $[Fe(tdt)_2]^{1-}$ should be involved in this case because the mononuclear bis(1,2-dithiolene) Fe(III) complex has a relatively positive redox potential and is easily reduced by the dithiol giving (2-) species ($[Fe^{II}(tdt)_2]^{2-}$). Our results suggest that, upon the core extrusion from iron-sulfur proteins, some of the dithiols destroy a native core itself.

Thus, we found that the addition of one equiv of tdt-H_2 to $[Fe_2S_2(SR)_4]^{2-}$ complex results in the formation of either $[Fe(tdt)(SR)_2)]^{1-}$ or $[Fe_2S_2(tdt)_2]^{2-}$. The former complex is formed by cleavage of Fe-S* and the latter product is obtained by the substitution of SR with tdt ligand. Although we have examined only a few cases of the ligand exchange reactions for Cys-containing peptide complexes, the chelation of the peptide thiolate ligand to $[Fe_2S_2]^{2+}$ core can be

conveniently determined by using tdt-H_2.

The Nature of the Tetrapeptide 2Fe-2S Complexes and the effect of the Tetrapeptide-Ligand sequences.

^1H NMR spectra of 2Fe-2S peptide complexes.

Due to the paramagnetic property of 2Fe-2S complexes, ^1H NMR peaks of Cys CH_2 were found at the lower field side. Figure 7 shows the ^1H NMR spectra of $[Fe_2S_2(Z\text{-cys-Ala-Ala-cys-OMe})_2]^{2-}$ (**2**), $[Fe_2S_2(Z\text{-cys-Val-Val-cys-OMe})_2]^{2-}$ (**5A**), $[Fe_2S_2(Z\text{-Ala-cys-OMe})_4]^{2-}$(**6**), and $[Fe_2S_2(Z\text{-cys-Gly-Val-OMe})_4]^{2-}$ in Me_2SO-d_6. **2** exhibited very broad Cys CH_2 signals at 30.7 ppm (line width 800 Hz) and 22.9 ppm (line width 720 Hz) due to the contact shift through Cys thiolate from $[Fe_2S_2]^{2+}$ core. The Cys CH_2 peaks of **2** and **5A** show the presence of two non-equivalent Cys residues of the tetrapeptide ligand. **6** shows one Cys CH_2 peak at 31.3 ppm (760Hz).

Oxidized native 2Fe-2S ferredoxin was reported to show Cys CH_2 signals at 34-37 ppm[13,23] and oxidized 2Fe-2S model complexes show peaks at 32 ppm e.g. for $[Fe_2S_2(S\text{-Et})_4]^{2-}$.[24] Two peaks were found at 30.3, and 22.6 ppm for **5A** and one peak at 35 ppm for $[Fe_2S_2(S_2\text{-}o\text{-xyl})_2]^{2-}$.[25] **6** and $[Fe_2S_2(Z\text{-cys-Gly-Val-OMe})_4]^{2-}$ show that the chemical shift values the Cys CH_2 peak were almost the same when the Cys residue is at the N or C terminal.

Nagayama et.al.[13] suggested an intrinsic linewidth of Cys CH_2 resonance was about 1000 Hz in native 2Fe-2S

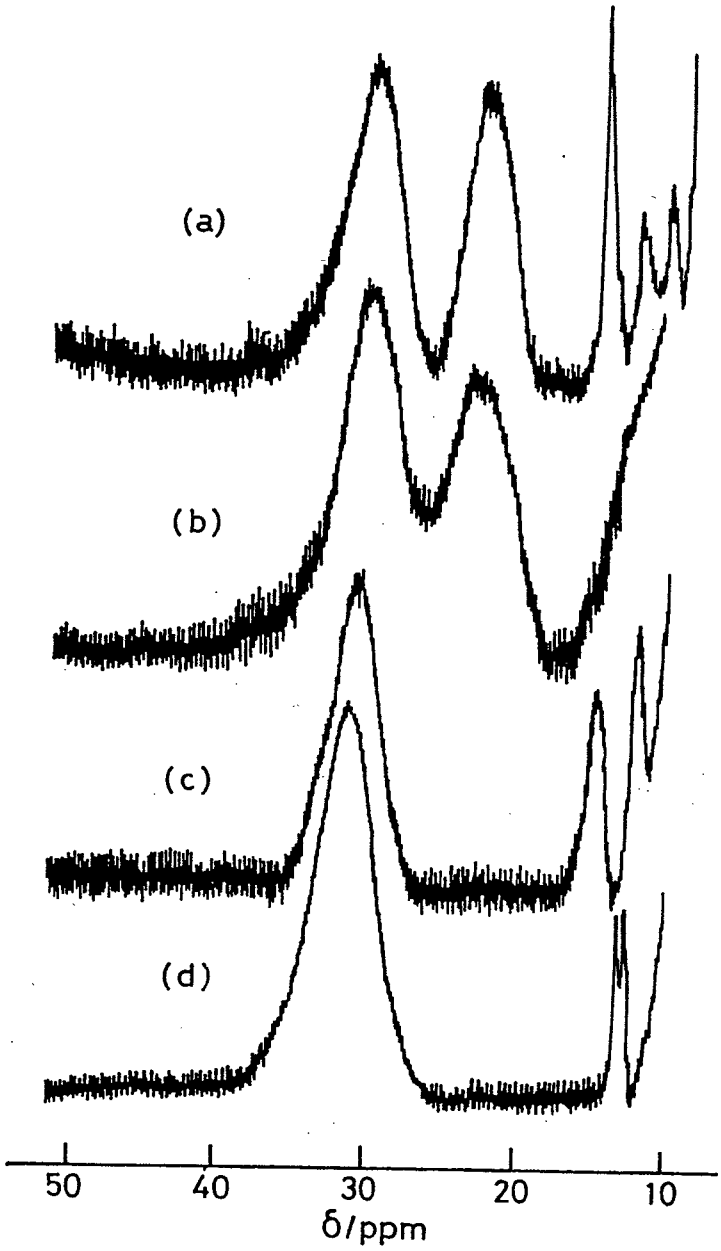

Figure 7. 400 MHz ^{1}H-NMR spectrum of (a) $[NEt_4]_2[Fe_2S_2(Z\text{-cys-Ala-Ala-cys-OMe})_2]$, (b) $[NEt_4]_2[Fe_2S_2(Z\text{-cys-Val-Val-cys-OMe})_2]$ **5A**, (c) $[NEt_4]_2[Fe_2S_2(Z\text{-Ala-cys-OMe})_4]$, and $[NEt_4]_2[Fe_2S_2(Z\text{-cys-Gly-Val-OMe})_2]$ in Me_2SO-d_6 at the Cys $C\beta H_2$ region.

ferredoxins from the linewidth data of $[Fe_2S_2(S_2\text{-}o\text{-}xyl)_2]^{2-}$. Our ^1H NMR linewidth data of Cys CH_2 region of **2**, **5A**, and **6** were 720 - 800 Hz which indicate the intrinsic linewidth of Cys CH_2 in 2Fe-2S complexes. The linewidth of $[Fe_2S_2(S_2\text{-}o\text{-}xyl)_2]^{2-}$ **4** is now (1830 Hz) explicable by an overlap of two slightly different methylene peaks at around 35 ppm. From the X-ray analysis of plant type ferredoxin and *C. pasteurianum* native rubredoxin, the torsion angle of S-Fe-Sγ-Cβ were illustrated in Fig. 8. In plant type ferredoxin (Fig. 8-a), three S*-Fe-Sγ-Cβ torsion angles are 180° and in rubredoxin (Fig. 8-b) N-terminal Cys (6,39) were in a plane, but C-terminal Cys (9,42) were not. In the chelating tetrapeptide 2Fe-2S complexes (**2-4**), the conformation of the tetrapeptide were the same as the native rubredoxin. The N-terminal Cys CβH_2 were in the same environment as native plant type ferredoxin (ca. 32 ppm). The C-terminal cysteinyl CβH_2 of the tetrapeptide ligand (Z-Cys-X-Y-Cys-OMe) has

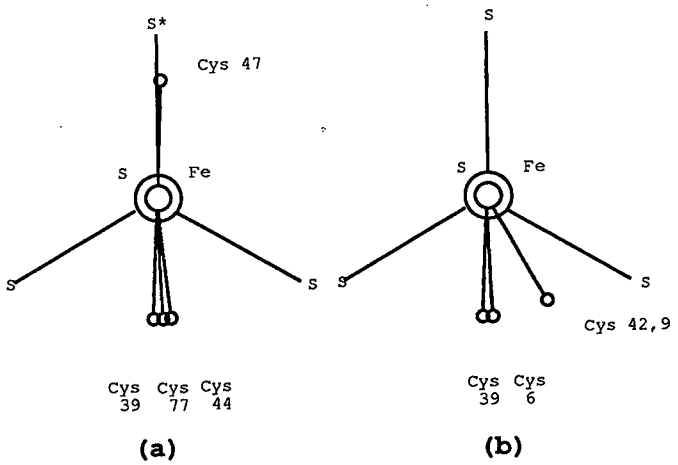

Figure 8. The torsion angles of Fe-S bonds for (a) plant-type ferredoxin and (b) rubredoxin.

special torsion angle almost same as rubredoxin C-terminal one were shown 22.9 ppm high field sifted ^1H NMR peak.

Structure of the Tetrapeptide Complexes.

2 and **5** exhibit two Cys $C_\beta H_2$ peaks at 30.7 and 22.9 ppm for **2** and 30.3 and 22.6 ppm for **5**. These 22.9 and 22.6 ppm signals of **2** and **5**, respectively, are at higher field than that of native ferredoxins and simple model complexes. These signals show that the tetrapeptide segments, Cys-Ala-Ala-Cys and Cys-Val-Val-Cys have different structure from native ferredoxin segments; i.e., the Cys-X-Y-Cys segment bridges two Fe ions but **2** and **5** have chelating coordination to one Fe ion. The partial peptide sequences, Cys-Thr-Val-Cys and Cys-Pro-Leu-Cys, in the active site of *C. pasteurianum* rubredoxin.[4] Z-Cys-Ala-Ala-Cys-OMe was found to form a stable chelate ring for a square planar Pd^{II} ion, but Z-Cys-Val-Val-Cys-OMe was not.[3] The present study on rubredoxin model complexes indicated that Z-Cys-Ala-Ala-Cys-OMe, Z-Cys-Thr-Val-Cys-OMe and Z-Cys-Pro-Leu-Cys-OMe can form chelates with $Fe^{II,III}$ ions.[26,27] The difficulty in chelation of Cys-Val-Val-Cys to Fe is due to the sterically hindered Val-Val sequence.

Absorption spectra of 2Fe-2S peptide complexes.

Figure 9 shows the absorption spectra of **2** - **4**, **5A**, and **6** in DMF and Table 1 lists their absorption maxima in the region of 300 - 700 nm. **2**,- **4**, and **6** exhibited three characteristic absorptions due to the ligand-metal charge

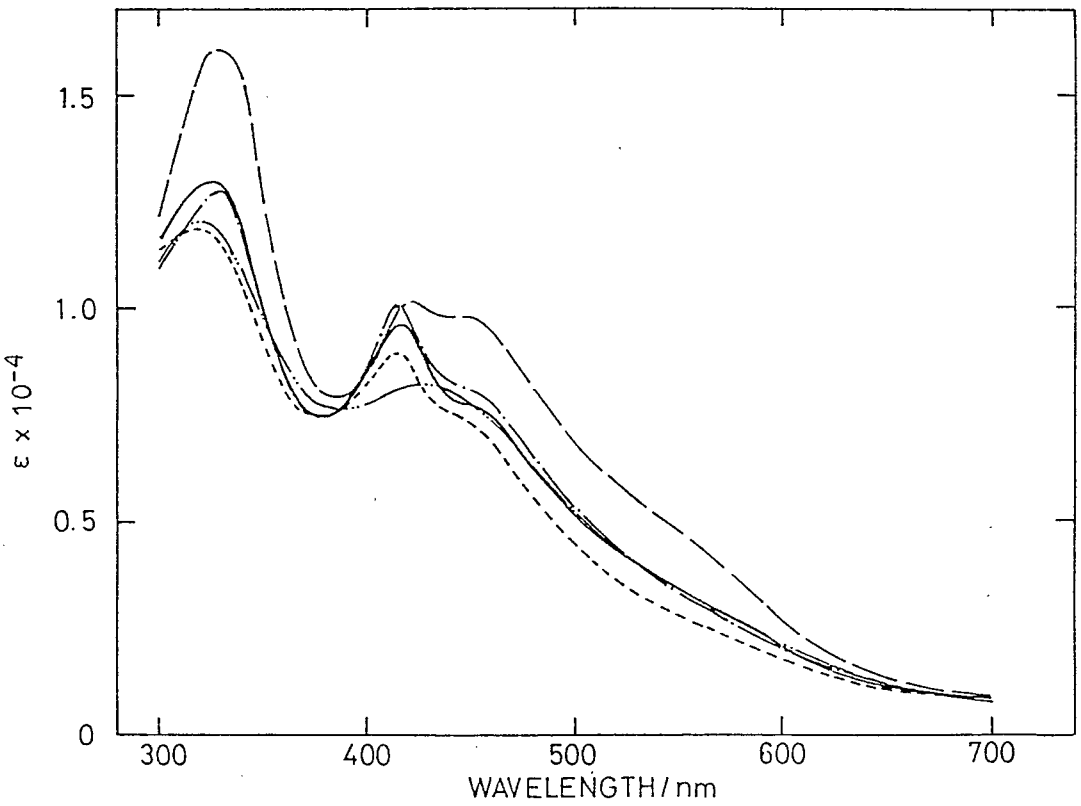

Figure 9. Absorption spectra of (——) $[NEt_4]_2[Fe_2S_2(Z\text{-cys-Ala-Ala-cys-OMe})_2]$, (– – –) $[NEt_4]_2[Fe_2S_2(Z\text{-cys-Pro-Leu-cys-OMe})_2]$, (—·—) $[NEt_4]_2[Fe_2S_2(Z\text{-cys-Thr-Val-cys-OMe})_2]$, (— – — –) $[NEt_4]_2[Fe_2S_2(Z\text{-cys-Val-Val-cys-OMe})_2]$ **5A**, and (——) $[NEt_4]_2[Fe_2S_2(Z\text{-Ala-cys-OMe})_4]$ in DMF.

Table 1. Absorption Maxima of 2Fe-2S Complexes in DMF

complex	absorption max λ/nm (ε/$M^{-1}cm^{-1}$)		
$[Fe_2S_2(Z\text{-cys-Ala-Ala-cys-OMe})_2]^{2-}$	326.9(14300)	417.0(10000)	450 sh (8900)
$[Fe_2S_2(Z\text{-cys-Pro-Leu-cys-OMe})_2]^{2-}$	322.5(10000)	415.9(7500)	450 sh (6100)
$[Fe_2S_2(Z\text{-cys-Thr-Val-cys-OMe})_2]^{2-}$	330.2(12900)	416.4(10200)	450 sh (7700)
$[Fe_2S_2(Z\text{-cys-Val-Val-cys-OMe})_2]^{2-}$	327.3(12200)	426.3(8300)	
$[Fe_2S_2(Z\text{-Ala-cys-OMe})_4]^{2-}$	331.6(16200)	424.2(10100)	450 sh (9800)
$[Fe_2S_2(S\text{-}t\text{-Bu})_4]^{2-}$	334.0(13800)	433.4(8600)	460 sh (8100)
native 2Fe-2S ferredoxin[a,b]	325(12000)	423(9700)	466(8500)

a) Refference 28, b) In aqueous solution.

transfer at 323 - 332 nm (ε: 10000 - 16000 $M^{-1}cm^{-1}$), 416 - 424 nm (ε 10000 - 10200), and 450 nm (sh, ε 6100 - 9800). Complex **5A** exhibited only two absorptions at 327 nm (ε: 12200) and at 400 - 460 nm (ε 8300).

CD spectra of 2Fe-2S peptide complexes.

Figure 10 shows the CD spectra of **2** - **6** in DMF solution. Table 2 lists the CD extrema of **2**, **3**, and **4**. These complexes show three well-defined troughs and three peaks. **5A** and **6** have one trough and two peaks. From the CD spectral data, the tetrapeptide complexes can be classified into two groups. Complex **5** appears to be different from the other three tetrapeptide complexes (**2**, **3**, and **4**). These CD spectral results correspond to the classification based on the absorption maxima. The CD spectra of these five complexes are quite different from that of native 2Fe-2S ferredoxin as listed in Table 2.

The concentration effect on formation of the complexes was examined to infer the structure of tetrapeptide ligands in the 2Fe-2S complexes, e.g. intermolecular crosslinked structure or intramolecular chelating or bridging structure. Table 3 shows a CD spectral change with variation of the concentrations in formation of the complexes by the ligand exchange reactions. The CD spectra of **2** and **6** showed no change in 1×10^{-3} - 1×10^{-2} $mol\cdot dm^{-3}$ range but complex **5** has a remarkable spectral change between the concentrations 9.7×10^{-3} $mol\cdot dm^{-3}$ and 4.8×10^{-3} $mol\cdot dm^{-3}$. The CD spectra of **5A** has one trough and two peaks while **5B** has two troughs and three

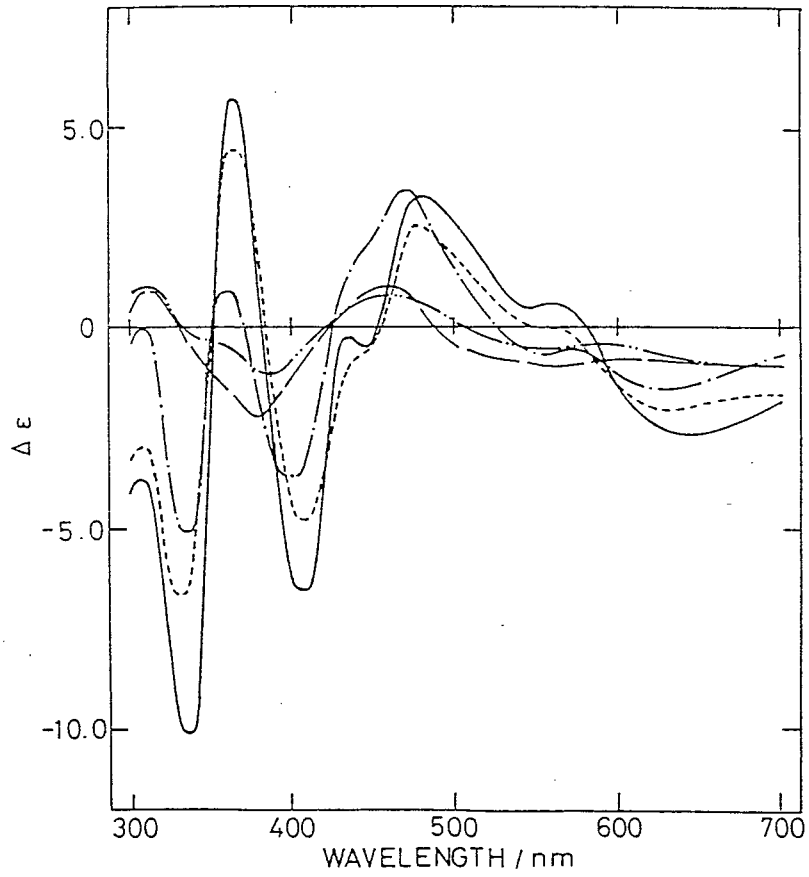

Figure 10. CD spectra of (——) $[NEt_4]_2[Fe_2S_2(Z\text{-cys-Ala-Ala-cys-OMe})_2]$, (– – –) $[NEt_4]_2[Fe_2S_2(Z\text{-cys-Pro-Leu-cys-OMe})_2]$, (—·—) $[NEt_4]_2[Fe_2S_2(Z\text{-cys-Thr-Val-cys-OMe})_2]$, (—– – –) $[NEt_4]_2[Fe_2S_2(Z\text{-cys-Val-Val-cys-OMe})_2]$ **5A**, and (——) $[NEt_4]_2[Fe_2S_2(Z\text{-Ala-cys-OMe})_4]$ in DMF.

Table 2. CD Spectral Data of 2Fe-2S Complex in DMF

complex	CD extrema λ/nm ($\Delta\varepsilon/M^{-1}cm^{-1}$)			
$[Fe_2S_2(Z\text{-cys-Ala-Ala-cys-OMe})_2]^{2-}$	311(-3.63)	334(-10.12)	365(+5.67)	407(-6.6)
	436(-0.22)	445(-0.44)	476(+3.3)	545(+0.44)
	564(+0.61)	640(-2.53)		
$[Fe_2S_2(Z\text{-cys-Pro-Leu-cys-OMe})_2]^{2-}$	310(-2.90)	331(-6.69)	362(+4.44)	408(-4.75)
	440sh(-0.7)	477(+2.55)	560sh(-0.09)	630(-1.92)
$[Fe_2S_2(Z\text{-cys-Thr-Val-cys-OMe})_2]^{2-}$	307(0)	333(-5.04)	360(+0.99)	400(-3.70)
	440sh(+1.76)	468(+3.48)	545(-1.41)	570(-0.53)
	620(-1.54)			
$[Fe_2S_2(Z\text{-cys-Val-Val-cys-OMe})_2]^{2-}$ **5A**	310(+1.05)	345(-0.33)	385(-1.10)	455(+0.72)
	554(-0.55)	586(-0.39)	670(-0.94)	
$[Fe_2S_2(Z\text{-Ala-cys-OMe})_4]^{2-}$	312(+0.91)	377(-1.19)	450(+0.98)	
native ferredoxin (spinach)[a,b]	356(+1.81)	378(-2.85)	433(+20.0)	512(-1.81)
	521(-1.73)	549(-3.38)		
denatured ferredoxin (spinach)[a,c]	366(-2.3)	381(-4.55)	396(-4.1)	409(-4.5)
	474(+3.95)	559(-2.0)	588(-1.7)	

a) Referrence 29. b) Inaqueous solution. c) In DMF-H_2O solution.

Table 3. CD spectral Data of 2Fe-2S Complexes under Different Synthetic Conditions.[a]

synth condition /moldm^{-3}		CD extrema λ/nm($\Delta\varepsilon$)[b]		
$[Fe_2S_2(Z\text{-cys-Ala-Ala-cys-OMe})_2]^{2-}$				
9.3×10^{-3}		311(-3.63)	334(-10.12)	365(+5.65)
		407(-6.6)	436(-0.22)	445(-0.44)
		476(+3.3)		
1.5×10^{-3}		314(-4.07)	335(-10.14)	369(+6.03)
		409(+7.44)	438(-0.96)	446(-1.09)
		480(+3.25)		
$[Fe_2S_2(Z\text{-cys-Val-Val-cys-OMe})_2]^{2-}$				
9.7×10^{-3}	**5A**	312(+1.32)	382(-1.41)	454(+1.05)
4.8×10^{-3}	**5B**	308(+0.8)	338(-0.4)	352(-0.06)
		390(-1.26)	460(+0.35)	
$[Fe_2S_2(Z\text{-Ala-cys-OMe})_4]^{2-}$				
1.1×10^{-2}		312(+0.91)	377(-1.19)	450(+0.86)
1.3×10^{-3}		312(+0.96)	377(-1.30)	451(+0.92)

a) $[Fe_2S_2(S\text{-}t\text{-Bu})_4]^{2-}$/peptide = 0.44 for $[Fe_2S_2(Z\text{-cys-Ala-Ala-cys-OMe})_2]^{2-}$, 0.45 for $[Fe_2S_2(Z\text{-cys-Val-Val-cys-OMe})_2]^{2-}$, and 0.23 for $[Fe_2S_2(Z\text{-Ala-cys-OMe})_4]^{2-}$. b) In DMF.

peaks. These data show that complex **5** has two isomeric structures depending on the conditions of complexation.

Electrochemical Properties of 2Fe-2S Peptide Complexes.

The redox behavior of the 2Fe-2S peptide complexes in DMF was examined by cyclic voltammetry. Redox potentials ($(E_{pc}+E_{pa})/2$, vs. SCE) of **2** - **6** are listed in Table 4. The redox potential of spinach 2Fe-2S ferredoxin has been reported at -0.65 V (vs. SCE).[30] Those of alkanethiolato 2Fe-2S complexes in DMF were reported to be at -1.31 V for $[Fe_2S_2(S\text{-}Et)_4]^{2-}$ [24] and -1.49 V for $[Fe_2S_2(S_2\text{-}o\text{-}xyl)_2]^{2-}$.[25] The 2Fe-2S model complexes are also classified into two groups from the redox potentials as well as from the absorption and the CD spectral results. One group which contains $[Fe_2S_2(S\text{-}t\text{-}Bu)_4]^{2-}$, $[Fe_2S_2(S\text{-}Et)_4]^{2-}$, $[Fe_2S_2(S_2\text{-}o\text{-}xyl)_2]^{2-}$, and complex **5** has more negative redox potentials than -1.30 V (vs SCE). The other group containing **2**, **3**, **4**, and **6** has more positive redox potentials than -1.20 V (vs.SCE). The i_{ox}/i_{red} values summarized in Table 4 indicate that the tetrapeptide complexes have more stable 3-/2- redox couples than complex **6** or other known alkanethiolato complexes. Thus, the chelating structure was found to play a significant role for stabilization of the 3-/2- redox couples.

Positive shift of redox potentials in tetrapeptide complexes. The close location of the amide group of the peptide ligands to 2Fe-2S core contributes to an increase in

Table 4. Electrochemical Data of 2Fe-2S Complexes in DMF

complex	$((E_{pc} + E_{pa})/2)/V^a$ $(E_{pa}/V, E_{pc}/V)$	i_{pc}/i_{pa}
$[Fe_2S_2(Z\text{-cys-Ala-Ala-cys-OMe})_2]^{2-}$	-1.06(-0.96,-1.15)	0.8
$[Fe_2S_2(Z\text{-cys-Pro-Leu-cys-OMe})_2]^{2-}$	-1.18(-1.11,-1.25)	0.7
$[Fe_2S_2(Z\text{-cys-Thr-Val-cys-OMe})_2]^{2-}$	-1.09(-1.01,-1.16)	0.9
$[Fe_2S_2(Z\text{-cys-Val-Val-cys-OMe})_2]^{2-}$	-1.41(-1.36,-1.45)	0.8
$[Fe_2S_2(Z\text{-Ala-cys-OMe})_4]^{2-}$	-1.04(-0.94,-1.14)	0.3
$[Fe_2S_2(S\text{-}t\text{-Bu})_4]^{2-}$	-1.46(-1.32,-1.41)	0.8

a) Obtained vs. SCE; scan rate was 100 mV/s.

the dielectric constant around the electron-transfer-related region. In the case of 4Fe-4S ferredoxin model complexes, it is known that the increase in solvent dielectric constant results in a positive shift of 3-/2- redox potential, experimentally[31] and theoretically.[32]

The formation of NH-S hydrogen bond is proposed to be another important factor to control the redox potential. Of course, a part of the protic solvent molecules used e.g. water, contributes to the formation of the hydrogen bond. In the case of the 4Fe-4S ferredoxin model complex, $[Fe_4S_4(Z\text{-}cys\text{-}Gly\text{-}Ala\text{-}OMe)_4]^{2-}$ has been found to possess a positive-shifted redox potential due to NH-S hydrogen bond formation with a specific peptide conformation.[33] At present, we have less information about the NH-S hydrogen bond formation between Cys thiolate sulfur and the amide NH group in the chelating peptides of **2-4**.

The redox potentials of **2-4** negatively shifted in the order **2≤3<4**. This order corresponds to the steric hindrance of the X-Y part in the Cys-X-Y-Cys tetrapeptide segments. This negative shift can be explained by the decrease in strength of the NH-S hydrogen bond due to the steric hindrance of the X-Y part. Results of the calculation for idealized peptide conformations show the chelating Cys-Val-Val-Cys complex has weaker NH-S hydrogen bonds than those of the Cys-Ala-Ala-Cys complex. The calculated trend in the NH-S hydrogen bonds is in agreement with the order of the redox potentials described above.

The tetrapeptides **2** (Z-Cys-Ala-Ala-Cys-OMe) and **5A** (Z-

Cys-Val-Val-Cys-OMe) contain the same number of amide NH groups, which induces the positive shift of the redox potentials. Actually, the redox potential of **5A** is more negative than that of **1**. A negative redox potential of **5A**, even with the same number of amide groups, suggests the importance of the peptide conformation. The hydrophobic side chains of the Val-Val fragment in the oligomeric structure induce the low dielectric environment around the 2Fe-2S core. Then the amide groups probably locate conformationally far from the core. Such a heterogeneity in one molecule, namely a coexistence of the hydrophobic and the polar region, can be introduced by an oligopeptide chain with a relatively rigid structure. This is considered to be one of the crucial factors to control the redox potential in native protein.

In the native ferredoxin, the tetrapeptide sequence Cys-X-Y-Cys have one NH-S hydrogen bond with a bridging structure but the chelating sequence (Cys-A-B-C-D-Cys) have four NH-S hydrogen bonds. These NH-S hydrogen bonds serve to control the redox potential of native ferredoxin.

Calculation of idealized structures of 2Fe-2S peptide complexes on basis of X-ray analysis of the native *C. pasteurianum* rubredoxin show a difference in the idealized structures between Cys-Ala-Ala-Cys complex and Cys-Val-Val-Cys complex. The former complex shows only a small structural deviation from the native rubredoxin structure but the latter has a 3_{10}-turn like structure.[34] The structural difference between Cys-Ala-Ala-Cys complex and Cys-Val-Val-Cys complex is due to the difference in steric crowding in

the Ala-Ala from the Val-Val segment

The side chain of Val(3) position in Cys(1)-Val(2)-Val(3)-Cys(4) segment is located closely at the inorganic sulfur atom. The distances between the center of the inorganic sulfur atom and that of carbon atom of two CH_3 and a CH groups in Val(3) side chain are 0.380 nm, 0.395 nm and 0.388 nm, respectively. These distances are almost equal to 0.385 nm which is sum of the van der Waals contact between a sulfur atom and a methyl group. These close contacts between the inorganic sulfur atom and the side chain atoms of Val(3) may prevent the tetrapeptide of Cys-Val-Val-Cys from chelating an Fe^{III} ion of 2Fe-2S cluster.

The X-ray analysis of *S. maxima* ferredoxin indicates that the tetrapeptide segment (Cys-Ser-Thr-Cys) bridges between two Fe ions of a 2Fe-2S core.[35] However, the tetrapeptide segment of the present model complexes chelate one Fe ion of 2Fe-2S core. The tetrapeptides bridging of the two different Fe ions of 2Fe-2S core are not preferred, but the bridging structure is realized by the stability of the chelating ring of Cys-A-B-C-D-Cys sequence is the native plant type ferredoxin.

ESR spectra of reduced species of 2Fe-2S peptide complexes.

Figure 4 shows the ESR spectra of **2**, **5A**, and **6** after reduction by $Na_2S_2O_4$ in DMF at 77 K. The presence of $[Fe_2S_2(\text{tetrapeptide})_2]^{3-}$ species is clearly shown. The spectra show less rhombic pattern to that of native ferredoxin. Reduced **5A** shows narrower signals than the

signals of reduced **2** and **6**. The ESR spectra of **2** and **5A** in reduced state indicated different structure of reduced **2** from the reduced **5A**. Reduced **2**, **5A**, and **6** have no signals at g= 4 region to indicate absence of decomposed species. The 2Fe-2S complexes exhibit ESR signals when one-electron reduced at liq. N_2 temperature (See Fig.11). Spinach ferredoxin has a rhombic spectrum (g= 2.046, 1.957, 1.887)[36] and adrenodoxin (adrenal ferredoxin) has a nearly axial spectrum (g= 2.02, 1.935, 1.93).[37] Among model complexes of 2Fe-2S ferredoxin, $[Fe_2S_2(S_2\text{-}o\text{-}xyl)_2]^{3-}$ and $[Fe_2S_2$(2,2' biphenyldithiolato$)_2]^{3-}$ show axial spectra (g=2.01, 1.94, 1.93 and 2.025, 1.914, 1.914)[38,37] respectively, but arylthiolato complexes $[Fe_2S_2(S\text{-}Ph(p\text{-}X))_4]^{3-}$ exhibit rhombic spectra.[36] The reduced species of present peptide complexes **2**, **5A**, and **6** also exhibit rhombic spectra, see Fig. 5.[37] From a theoretical study of reduced 2Fe-2S ferredoxin, Gayda et al. reported that the difference between g_x and g_y values (g_x-g_y) could be expressed by a linear function of the d orbital mixing.[39] Thus, the g_x-g_y value is important in the understanding of electronic structure of reduced 2Fe-2S complex. The g_x-g_y values of **2** and **6** are similar, but different from native plant-type ferredoxins. Large g_x-g_y values show the weak $d_x{}^2$-$d_y{}^2$ and $d_z{}^2$ orbital mixing and small values indicate the strong mixing.[39] The orbital mixing is related to the distortion of the coordination geometry of Fe ions. For example, $[Fe_2S_2(S_2\text{-}o\text{-}xyl)_2]^{2-}$ which has very small g_x-g_y value has narrow S-Fe-S angles (106.4°) due to the S_2-*o*-xyl chelating ligands.[21] The g_x-g_y values of **2** and **5A** indicate

that these peptide ligands exert different distortion to the 2Fe-2S core. The difference in structure of the complexes **2** and **5A** is thus revealed.

In conclusion, the chelation of Z-Cys-Ala-Ala-Cys-OMe to each Fe(III) ion in the [2Fe-2S] complex is confirmed. The bridging coordination of this sequence in native [2Fe-2S]-ferredoxins is thus enforced by the peptide sequence of the other parts.

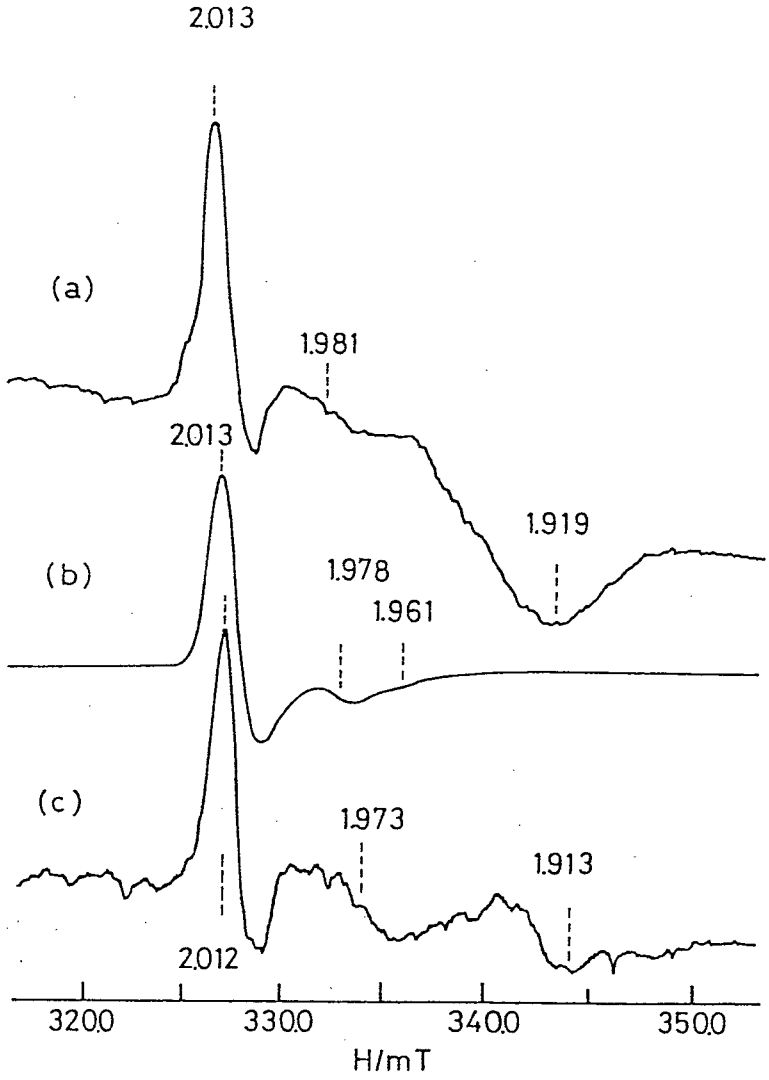

Figure 11. ESR spectra of 2Fe-2S peptide complexes in DMF at liquid-N_2 temperature: (a) $[NEt_4]_2[Fe_2S_2(Z\text{-cys-Ala-Ala-cys-OMe})_2]$, (b) $[NEt_4]_2[Fe_2S_2(Z\text{-cys-Val-Val-cys-OMe})_2]$ **5A**, and (c) $[NEt_4]_2[Fe_2S_2(Z\text{-Ala-cys-OMe})_4]$

References

(1) Ueyama, N.; Terakawa, T.; Nakata, M.; Nakamura, A. *J. Am. Chem. Soc.* **1983**, 105, 7098.

(2) Balasubramaniam, A.; Coucouvanis, D. *Inorg. Chim.Acta*, **1983**, 78, L35.

(3) Ueyama, N.; Ueno, S.; Nakata, M.; Nakamura, A. *Bull. Chem. Soc. Jpn.* **1984**, 57, 984 .

(4) Herrio, J. R. Jr.; Sieker, L. C.; Jensen, L. H.; Lovenberg, W. *J. Mol. Biol.* **1970**, 50, 391.

(5) Ueyama, N.; Nakata, M.; Nakamura, A. In "Peptide Chemistry 1979"; Yonehara, H., Ed.; Protein Research Foundation: Osaka, Japan, 1980; p 145.

(6) Ueyama, N.; Nakata, M.; Nakamura, A. *Bull. Chem. Soc. Jpn.* **1985**, 58, 464 .

(7) Do, Y.; Simhon, E. D.; Holm, R. H. *Inorg. Chem.* **1983**, 22, 3809.

(8) Gillum, W. O.; Mortenson, L. E.; Chen, T. S.; Holm, R. H. *J. Am. Chem. Soc.* **1977**, 99, 584.

(9) Mayerle, J. J.; Denmark, B. V.; DePamphilis, B. V.; Ibers, J. A.; Holm, R.H. *J. Am. Chem. Soc.* **1975**, 97, 1032

(10) Tuzimura, K.; Konno, T.; Meguro, H.; Hatano, M.; Murakami, T.; Kashiwabara, K.; Saito, K.; Davison, A.; Suzuki, T. *Anal. Biochem.* **1977**, 81, 167.

(11) Hendrickson, W. A.; Konnert, J. H. in "Computing in Crystallography", Diamond, R., Ramaseshan, S.,

Venkatesan, K., Eds.; Indian Academy of Sciences: Bangalore, India, 1980; pp. 13.01 - 13.23 .

(12) Wong, G. B.; Bobrik, M. A.; Holm, R. H. *Inorg. Chem.* **1978**, 17, 578.

(13) Nagayama, K.; Ozaki, Y.; Kyogoku, Y.; Hase, T.; Matsubara, H. *J. Biochem.* **1983**, 94, 893 .

(14) Que, L., Jr.; Anglin, J. R.; Bobrik, M. A.; Davison, A.; Holm, R. H. *J. Am. Chem. Soc.* **1974**, 96, 6042 .

(15) Ueno, S.; Ueyama, N.; Nakamura, A.; Tsukihara, T. *Inorg. Chem.* **1986**, 25, 1000.

(16) Que, L. Jr.; Anglin, J. R.; Bobrik, M.A.; Davison, A.; Holm, R.H. *J. Am. Chem. Soc.* **1974**, 96, 6042.

(17) Ueyama, N.; Terakawa, T.; Nakata, M.; Nakamura, A. *J. Am. Chem. Soc.* **1983**, 105, 7098.

(18) Ueyama, N.; Kajiwara, A.; Terakawa, T.; Nakamura, A. *Inorg. Chem.* **1985**, 24, 4700.

(19) McCleverty, J. A.; Atherton, N. M.; Connelly, N. G.; Winscom, C. J. *J. Chem. Soc. (A)* **1969**, 2242.

(20) Ueyama, N.; Nakata, M.; Nakamura, A. *Bull. Chem. Soc. Jpn.* **1981**, 54, 1727.

(21) a) Cambray, J.; Lane, R. W.; Wedd, A. G.; Johnson, R. W.; Holm, R. H. *Inorg. Chem.* **1977**, 16, 2565.
b) Gillum, W.O.; Mortenson, L.E.; Chen, J.-S.; Holm, R.H. *J. Am. Chem. Soc.* **1977**, 99, 584.

(22) Averill, B. A.; Bale, J. R.; Orme-Johnson, W. H. *J. Am. Chem. Soc.* **1987**, 100, 3034.

(23) Salmeen, I.; Palmer, G. *Arch. Biochem. Biophys.* **1972**, 150, 767.

(24) Hagen, K. S.; Watson, A. D.; Holm, R. H. *J. Am. Chem. Soc.* **1983**, 105, 3905.

(25) Tsukihara, T.; Fukuyama, K.; Tahara, H.; Katsube, Y.;Matsuura, Y. ; Tanaka, N. ; Kakudo, M. ; Wada, K. ; Matsubara, H. *J. Biochem.*, **1978**, 84, 1645 .

(26) Nakata, M.; Ueyama, N.; Fuji, M.; Nakamura, A.; Wada, K.; Matsubara, H. *Biochim. Biophys. Acta* **1984**, 788, 306.

(27) Nakata, M.; Ueyama, N.; Terakawa, T.; Nakamura, A. *Bull. Chem. Soc. Jpn.* **1983**, 56, 3647.

(28) Stephens, P. J.; Thomson, A. J.; Dunn, J. B. R.; Keiderling, T. A.; Rawlings, J.; Rao, K. K.; Hall, D. O. *Biochemistry* **1978**, 17, 4770.

(29) Bonomi, F.; Kurtz, P. M., Jr. *Biochemistry* **1982**, 21, 6838.

(30) Tagawa, K.; Arnon, D. I. *Biochem. Biophys. Acta* **1968**, 153, 602.

(31) Kassner, R. J.; Yang, W. *J. Am. Chem. Soc.* **1977**, 99, 4351.

(32) Hill, C. L.; Renaud, J.; Holm, R. H.; Mortenson, L. E. *J. Am. Chem. Soc.* **1977**, 99, 2549.

(33) Nakata, M.; Ueyama, N.; Terakawa, T.; Nakamura, A. *Bull. Chem. Soc. Jpn.* **1983**, 56, 3647.

(34) Venkatachalam, C. M. *Biopolymers* 1968, 6, 1425.

(35) Fukuyama, K.; Hase, T.; Matsumoto, S.; Tsukihara, T.; Katsube, Y.; Tanaka, N.; Kakudo, M.; Wada, K.; Matsubara, H. *Nature* **1980**, 286, 552.

(36) Fritz, J.; Anderson, R.; Fee, J.; Palmer, G.; Sands, R. H.; Tsibris, J. C. M.; Gunsalus, I. C.; Orme-Johnson, W.

H.; Beinert, H. *Biochim. Biophys. Acta* **1971**, 253, 110

(37) Beardwood, P.; Gibson, J. F.; *J. Chem. Soc. Dalton Trans.* **1983**, 737.

(38) Handford,P. T.; Lee, W. K. "Inorganic Biochemistry" ; Hill, H.A.O., Ed.; Royal Society of Chemistry: London , 1979; Vol. 2, pp 84-96.

(39) Bertrand, P.; Gayda, J. P. *Biochim. Biophys. Acta* **1979**, 579, 107.

Chapter 4.

Specific Chelation to Fe(III) Ion of Hexapeptide (Cys-A-B-C-D-Cys) Containing the Invariant Fragment of Plant-Type [2Fe-2S] Ferredoxin

4-1. Introduction.

Native plant-type ferredoxin has a redox potential at -0.64 V vs. SCE in aqueous solution,[1] and simple model complex, $[Fe_2S_2(S_2\text{-}o\text{-xyl})_2]^{2-}$ (S_2-*o*-xyl = α,α'-xylylenedithiolate), has at -1.49 V vs. SCE in N,N-dimethylformamide.[2] Such a large difference in the redox potentials has been proposed to be ascribed to the interaction between $[Fe_2S_2(S\text{-Cys})_4]^{2+}$ core and polar groups of the adjacent amino acid residues, such as NH---S hydrogen bonding.[3] This has been supported by our finding of the same redox potential of one of isomers in the oligopeptide model complex with a 20-peptide (Ac-Pro-Tyr-Ser-Cys-Arg-Ala-Gly-Ala-Cys-Ser-Thr-Cys-Ala-Gly-Pro-Leu-Leu-Thr-Cys-Val-NH_2)[3] which was designed by the conformational analysis for a domain around $[Fe_2S_2]^{2+}$ core of *S. platensis* ferredoxin.[4] However, it is still unknown what portion of the invariant sequence, Cys-A-B-C-D-Cys-X-Y-Cys, contributes to the positive shift of the redox potential. Thus, the short oligopeptide containing a partial invariant fragment around the $[Fe_2S_2]^{2+}$ core is necessary for understanding of the positive shift of the

redox potential.

First, we have synthesized $[Fe_2S_2(Z\text{-}cys\text{-}X\text{-}Y\text{-}cys\text{-}OMe)_2]^{2-}$ (X-Y = Ala-Ala, Val-Val)[5] which has a specific chelation of Cys-Ala-Ala-Cys to one Fe^{III} ion of $[Fe_2S_2]^{2+}$.[6] However, a native ferredoxin fragment, Cys-Ser-Thr-Cys, similar to the Cys-Ala-Ala-Cys fragment has been known to bridge between two Fe^{III} ions of $[Fe_2S_2]^{2+}$.[4] The Cys-X-Y-Cys fragment virtually has no bridging capability to two Fe^{III} ions, but a preferable chelation ability to one Fe^{III} ion. The chelation of a Cys-A-B-C-D-Cys fragment to one Fe^{III} ion has been found in *S. platensis* ferredoxin by the X-ray analysis.[4] Such a chelating ability of hexapeptide, Z-Cys-A-B-C-D-Cys-OMe, is quite important in terms of the conformational preference of the sequence A-B-C-D..

Most of plant-type ferredoxin has some invariant amino acid residues as underlined in the $\underline{Cys}^1\text{-}\underline{Arg}^2\text{-}Ala^3\text{-}\underline{Gly}^4\text{-}Ala^5\text{-}\underline{Cys}^6$ fragment. Ala^3 and Ala^5 are substituted with Ser residue in some plants.[7] In the case of bacterial [2Fe-2S] ferredoxins, Arg^2 is replaced with Gly^2 residue.[8]

In order to study the chelating ability of a hexapeptide, Cys-A-B-Gly-D-Cys, we synthesized two [2Fe-2S] model complexes containing Cys-Gly-Ala-Gly-Ala-Cys and Cys-Ala-Ala-Gly-Ala-Cys. The effect of the chelation on the positive shift of redox potential of the 2Fe-2S complex was investigated.

4-2. Experimental.

All manipulations were carried out under argon atmosphere. N,N-Dimethylformamide (DMF), methanol, diethyl ether, 1,2-dimethoxyethane (DME), acetonitrile, propylene carbonate, Me_2SO-d_6, and acetonitrile-d_3 were purified by distillation before use. 3,4-Toluenedithiol (tdt-H_2) was of commercial grade. $[Hg_2Cl_2$(Z-cys-Gly-Ala-Gly-Ala-cys-OMe)$_2]$ and $[Hg_2Cl_2$(Z-cys-Ala-Ala-Gly-Ala-cys-OMe)$_2]$ were prepared by the same procedure as reported previously.[9]

Synthesis of Cys-deprotected peptides

one gram (9.4 mmol) of $[Hg_2Cl_2$(Z-cys-Gly-Ala-Gly-Ala-cys-OMe)$_2]$ was dispersed in 100ml of DMF/methanol (7/3, v/v). Hydrogen sulfide gas was bubbled through the solution. Black mercury sulfide precipitated with vigorous stirring. The precipitate was removed with filtration. The filtrate was concentrated under reduced pressure and the white residue was washed with fresh ether and dried over in vacuo. The white powder was kept under argon atmosphere.

Z-Cys-Ala-Ala-Gly-Ala-Cys-OMe was synthesized by the same procedure described above.

Synthesis of $[NEt_4]_2[Fe_2S_2$(Z-cys-Gly-Ala-Gly-Ala-cys-OMe)$_2]$ (1)

The complex was synthesized by the same ligand exchange reaction reported in the previous paper.[5] Z-Cys-Gly-Ala-

Gly-Ala-Cys-OMe (16.9 mg, 2.82×10^{-2} mmol) was dissolved in 2ml of DMF solution of $[NEt_4]_2[Fe_2S_2(S\text{-}t\text{-}Bu)_4]$ (10.15 mg, 1.4×10^{-2} mmol) at room temperature. The solution was concentrated under reduced pressure to remove *t*-BuSH. The residue was washed with degassed DME and dried in vacuo. The analysis of $[Fe_2S_2]^{2+}$ content was performed using a core extrusion method with benzenethiol (10 equiv.) in DMF.[10]

Synthesis of $[NEt_4]_2[Fe_2S_2$(Z-cys-Ala-Ala-Gly-Ala-cys-OMe)$_2]$ (2)

2 was synthesized by the same procedure as described in the synthesis of complex **1**.

Ligand exchange reaction

The ligand exchange reaction for determination of chelating structure of the model complexes was carried out by the same procedure as described previously.[11] A DMF solution of tdt-H_2 (3×10^{-4} mmol) was added to a DMF solution of [2Fe-2S] complexes at ambient temperature. The differential absorption spectrum is obtained by subtracting the starting spectrum from the spectrum after addition of tdt-H_2. Hydrogen sulfide was detected by the same procedure as reported previously.[12]

Physical measurements

Absorption spectra were measured on a Jasco UVIDEC-5A spectrophotometer. CD spectra were recorded on a Jasco J-

40 spectropolarimeter. ^{1}H-NMR spectra were taken on a Jeol 400 MHz GX spectrometer at 23 °C. Cyclic voltammetries were measured with a Yanaco P8-CV equipped with a function generator Yanaco model FG-1218. [N(*n*-Bu)$_4$][ClO$_4$] was used for the supporting electrolyte. The cyclic voltamograms were recorded in DMF, acetonitrile, or propylene carbonate at room temperature and a saturated calomel electrode (SCE) as the reference.

4-3. Results

4-3-1. Electronic spectra of the [2Fe-2S] peptide model complexes.

Figure 1 shows the visible absorption spectra of $[NEt_4]_2[Fe_2S_2(Z\text{-cys-Gly-Ala-Gly-Ala-cys-OMe})_2]$ (**1**) and $[NEt_4]_2[Fe_2S_2(Z\text{-cys-Ala-Ala-Gly-Ala-cys-OMe})_2]$ (**2**) in DMF ,acetonitrile, and propylene carbonate at room temperature. Table 1 lists the absorption maxima and their molar coefficient ratios (A_1/A_2) between characteristic two maxima at 410 ~ 450 nm in various solvents. A DMF solution of **1** exhibits the two maxima at 418 nm and 450 nm (A_1/A_2 = 1.13) which are due to $S^*,S\rightarrow Fe$ ligand-metal charge transfer absorptions.[11] In acetonitrile, the A_1/A_2 ratio changed to 1.06 and a new shoulder was observed at 570 nm. In propylene carbonate, the A_1/A_2 becomes 0.99 and the absorption maxima at 570 nm clearly appeared. A [2Fe-2S] protein from Azotobacter 2Fe-2S ferredoxin giving such a smaller A_1/A_2 value has been reported.[12] The specific absorption maximum around 550 nm has been found for the [2Fe-2S] proteins of Putida monooxidase,[13] "red protein" from *Clostridium pasteurianum* W5,[14] Azotobacter [2Fe-2S] ferredoxin,[12] liver mitocondoria [2Fe-2S] ferredoxin,[15] and Pyrazone dioxygenase.[16]

On the contrary, no significant change was observed among the spectra of **2** in DMF, acetonitrile and propylene carbonate. Constant A_1/A_2 values were obtained in the three solvents. A slight solvent effect has been reported for $[NEt_4]_2[Fe_2S_2(S_2\text{-}o\text{-xyl})_2]$ in DMF and

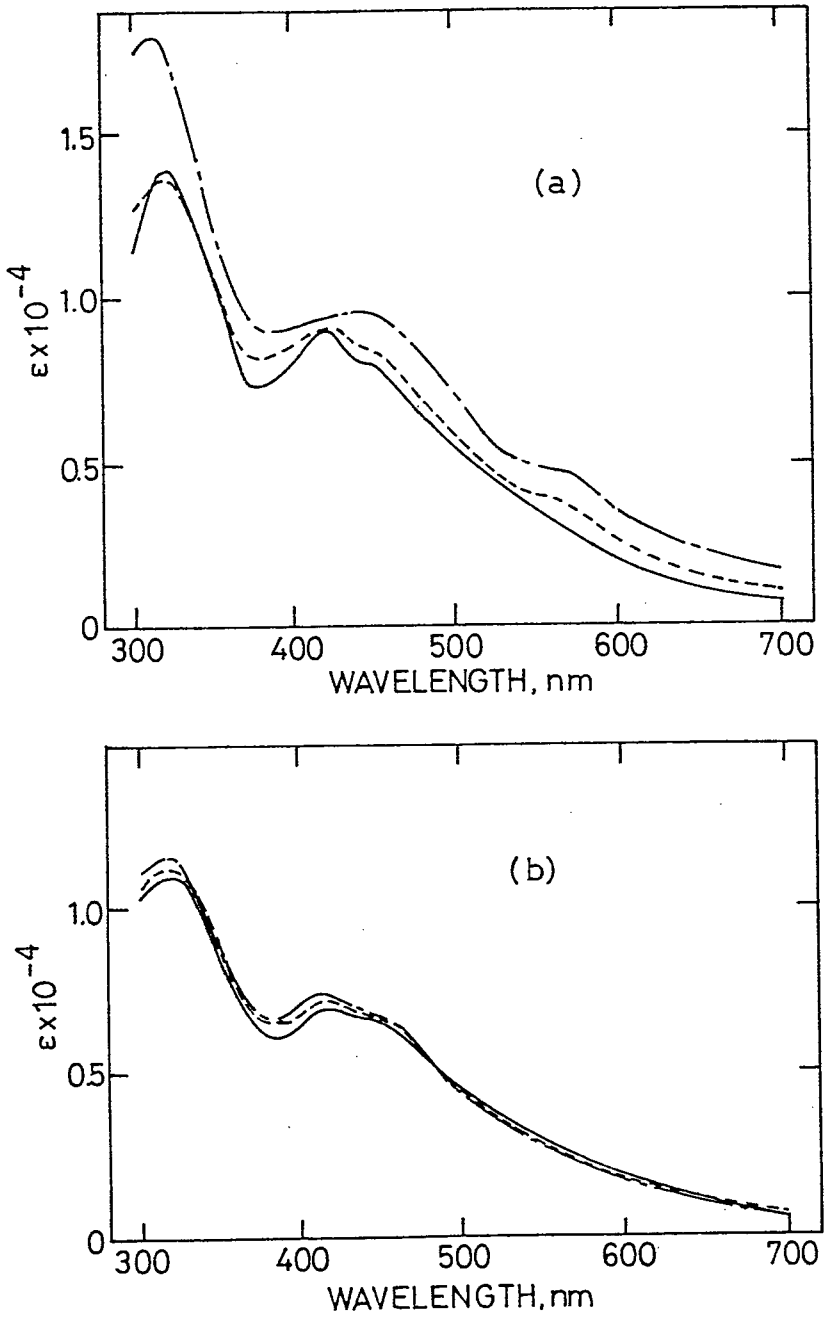

Figure 1. Absorption spectra of a) $[Fe_2S_2(Z\text{-cys-Gly-Ala-Gly-Ala-cys-OMe})_2]^{2-}$ (**1**) and b) $[Fe_2S_2(Z\text{-cys-Ala-Ala-Gly-Ala-cys-OMe})_2]^{2-}$ (**2**) in various solvents : (——); DMF, (—·—); propylene carbonate, (– – –); acetonitrile.

Table 1. Absorption Maxima of 400 ~ 600 Region and Molar Absorption Coefficient Ratio of 2Fe-2S Complexes.

Complexes (solvent)	A_1/nm ($\varepsilon\times10^{-3}$)	A_2/nm ($\varepsilon\times10^{-3}$)	A_3/nm ($\varepsilon\times10^{-3}$)	A_1/A_2
$[Fe_2S_2(Z\text{-cys-Gly-Ala-Gly-Ala-cys-OMe})_2]^{2-}$ (**1**)				
DMF	420(9.0)	440(8.0)	———	1.13
propylene carbonate	420(9.4)	442(9.5)	575(4.5)	0.99
CH_3CN	420(9.0)	440(8.5)	570(4.0)	1.06
$[Fe_2S_2(Z\text{-cys-Ala-Ala-Gly-Ala-cys-OMe})_2]^{2-}$ (**2**)				
DMF	418(7.0)	450(6.5)	———	1.08
propylene carbonate	416(7.4)	450(6.7)	———	1.10
CH_3CN	418(7.1)	450(6.6)	———	1.08
$[Fe_2S_2(S_2\text{-}o\text{-xyl})_2]^{2-}$ a)				
DMF	414(11.0)	455(9.2)	590(4.8)	1.20
CH_2Cl_2	415(9.3)	450(8.2)	590(3.6)	1.13
Azotobacter I b)	418(4.75)	460(4.86)	550(2.8)	0.97
Spinach Ferredoxin c)	420(4.84)	465(4.4)	———	1.10
$[Fe_2S_2(20\text{-peptide})]^{2-}$	424(6.0)	460(5.0)	———	1.20

a) ref. 18. b) ref. 13. c) ref. 1.

dichloromethane.[17]

Thus, the difference in absorption spectra of **1** in propylene carbonate probably comes from the conformational reason of the peptide chain, especially Gly^2 residue substituted by Ala^2 residue.

CD spectra.

Figure 2 shows the CD spectra of **1** in DMF, acetonitrile and propylene carbonate at ambient temperature. Table 2 lists the CD extrema of **1** and **2** in various solvents. The CD patterns of **1** indicate the same solvent dependence as the data of the visible absorption spectra. An extremum at 470 nm ($\Delta\varepsilon$,+3.3) in DMF shifts to 464 nm ($\Delta\varepsilon$,+2.5) in propylene carbonate and to 466 nm ($\Delta\varepsilon$,+5.0) in acetonitrile. A hollow band at 412 nm ($\Delta\varepsilon$,-3.3) in DMF, becomes a broad band in propylene carbonate or acetonitrile as shown in Fig. 2. No solvent dependence was observed for the CD measurements of **2** in the three solvents as the result of the absorption spectral. Similar CD spectral patterns were obtained for DMF solutions of **1** and **2** and suggest the presence of a stiff conformational structure, especially, for the Cys-Ala-Ala-Gly-Ala-Cys chelation. Solvent-dependency of a conformational change in [4Fe-4S] ferredoxin model complex has been found in the case of $[Fe_4S_4(Z\text{-cys-Gly-Ala-OMe})_4]^{2-}$ which having a non-chelating peptide ligand.[18]

The molar ellipticity of the extrema of **1** and **2** is equal to half of the value of $[Fe_2S_2(Z\text{-cys-Ala-Ala-cys-}$

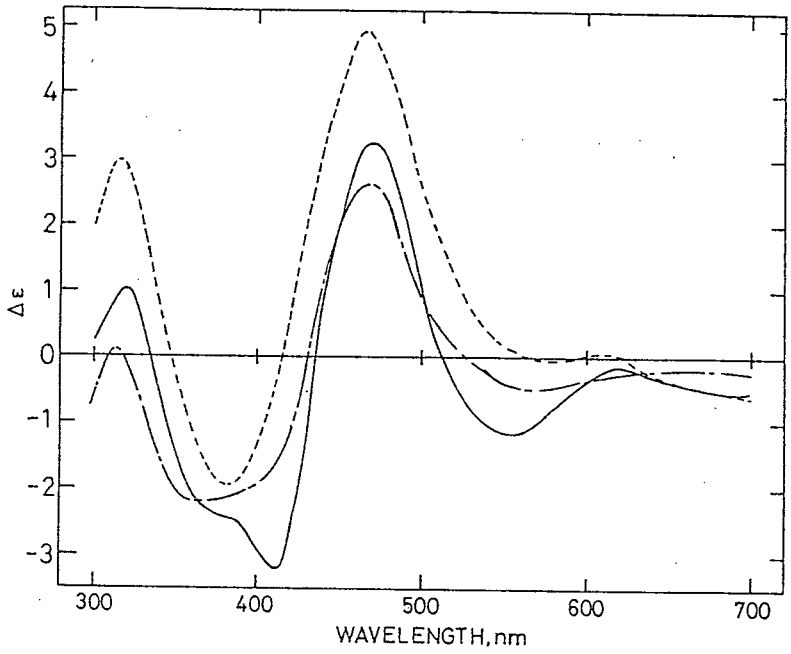

Figure 2. CD spectra of $[Fe_2S_2(Z\text{-cys-Gly-Ala-Gly-Ala-cys-OMe})_2]^{2-}$ in (——); DMF, (—·—); propylene carbonate, (– – –); acetonitrile.

Table 2. CD Spectral Data of 2Fe-2S Complexes.

complexes (solvent)	CD extrema λ/nm ($\Delta\varepsilon$/mol^{-1}cm^{-1})		
$[Fe_2S_2(Z\text{-cys-Gly-Ala-Gly-Ala-cys-OMe})_2]^{2-}$ (**1**)			
DMF	310(+1.0)		380(sh;-2.5)
	412(-3.3)	470(+3.3)	556(-1.3)
propylene carbonate	316(+0.1)	350(-2.3)	390(sh;-2.0)
		464(+2.51)	560(-0.1)
CH_3CN	315(-3.1)		384(-2.95)
		466(+5.0)	580(-0.1)
$[Fe_2S_2(Z\text{-cys-Ala-Ala-Gly-Ala-cys-OMe})_2]^{2-}$ (**2**)			
DMF	314(+1.0)	360(sh-2.5)	395(-3.1)
		466(+2.9)	
propylene carbonate	315(+1.8)	360(sh;-1.4)	390(-2.1)
		466(+2.7)	
CH_3CN	314(+1.9)	360(sh;-2.0)	392(-2.6)
		466(+3.2)	560(-1.2)
$[Fe_2S_2(Z\text{-Ala-cys-OMe})_4]^{2-}$			
DMF	312(+0.91)	377(-1.19)	
		450(-0.86)	

$OMe)_2]^{2-}$ which has been reported to have a rigid chelation to one Fe^{III} ion with the Cys-Ala-Ala-Cys fragment. The molar ellipticity of **1** and **2** is about three times as large as that of the non-chelating peptide complex, $[NEt_4]_2[Fe_2S_2(Z\text{-Ala-cys-OMe})_4]$. The results suggest either the chelation of the hexapeptide to one Fe^{III} ion or the bridging between two Fe^{III} ions of $[Fe_2S_2]^{2+}$ core.

Determination of chelating structure using 3,4-toluenedithiol.

Chapter 3. described the determination of a chelating structure of Cys-X-Y-Cys to $[Fe_2S_2]^{2+}$ core using the ligand exchange reaction with dithiols as shown in the following equations.[6]

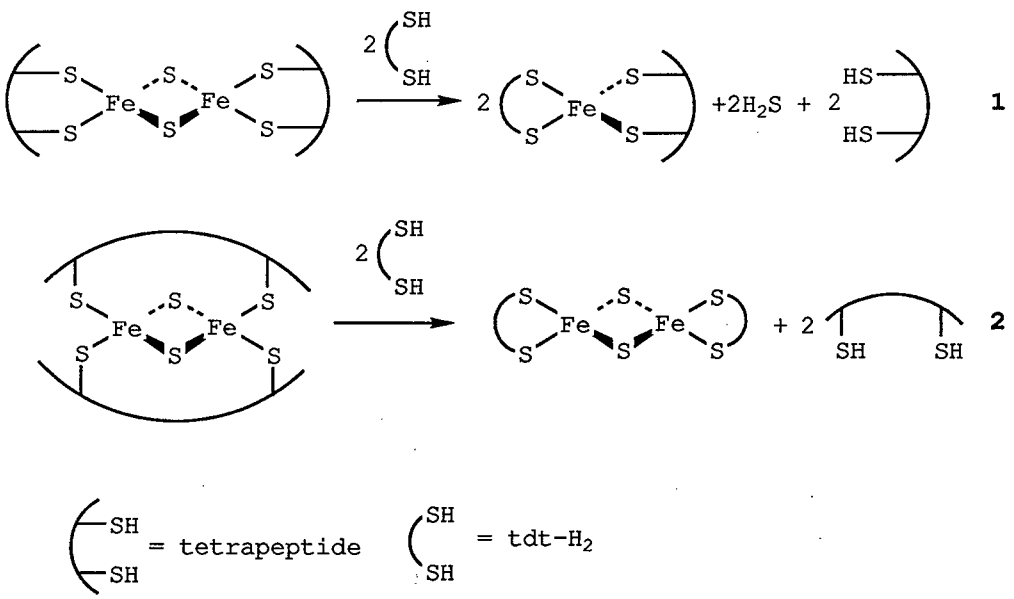

Figure 3-a and 3-b show the absorption spectral change of **1** and **2** with the addition of one equiv. of tdt-H_2. The difference spectrum between **1** and the mixture of **1** and tdt-H_2 exhibits three absorption maxima at 320 nm (15500), 380 nm (17000) and 495 nm (10600), while for **2** at 313 nm (14800),374 nm (16300),and 492 nm (10500). These maxima correspond to those of monomeric $[Fe^{III}(SR)_4]^-$ complex.[19] The hydrogen sulfide generated in this ligand exchange reaction was detected by isolation of silver sulfide. The inorganic sulfide was derived from $[Fe_2S_2]^{2+}$ core as shown in eq.(1).

^{1}H-NMR spectra.

Figures 4-a and 4-b show the partial ^{1}H-NMR spectra of **1** and **2** in the region of the contact-shifted Cys CH_2 signals. The Me_2SO-d_6 solution and the acetonitrile-d_3 solution of **1** exhibit a broad signal (line width, 1400Hz) at 32.9 ppm and two separate signals at 31.0 ppm and 34.4 ppm, respectively. In the case of $[NEt_4]_2[Fe_2S_2$(Z-cys-Ala-Ala-cys-OMe)$_2$] having a relatively smaller macrocyclic ring, two separate Cys CH_2 signals have been observed at 22.9 ppm and 30.7 ppm with a line-width of 800 Hz.[5] Therefore, the broad signal of **1** and **2** in Me_2SO-d_6 consists of two overlapping signals of the two Cys CH_2 groups of the Cys-A-Ala-Gly-Ala-Cys fragment. Observation of two separated Cys CH_2 signals for **1** in acetonitrile-d_3 indicates a solvent-dependent change of the Fermi contact shift from Fe^{III} through S atom.

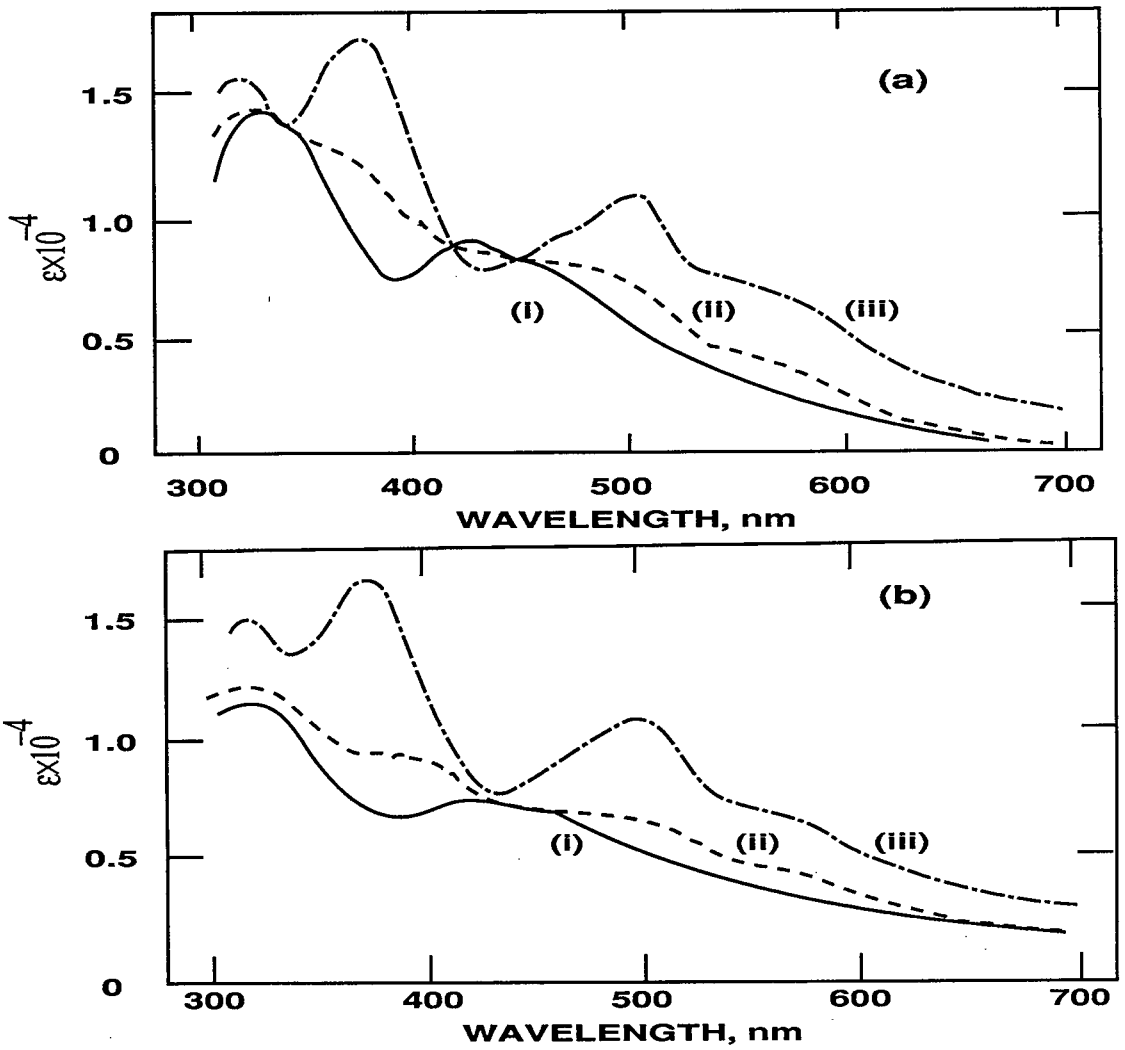

Figure 3. Absorption spectra of a-i) $[Fe_2S_2(Z\text{-cys-Gly-Ala-Gly-Ala-cys-OMe})_2]^{2-}$, a-ii) solution(i) plus one molar equiv. of tdt-H_2, a-iii) the difference spectrum between a-i and a-ii, b-i) $[Fe_2S_2(Z\text{-cys-Ala-Ala-Gly-Ala-cys-OMe})_2]^{2-}$, b-ii) solution(i) plus one molar equiv. of tdt-H_2, and b-iii) the difference spectrum between b-i and b-ii.

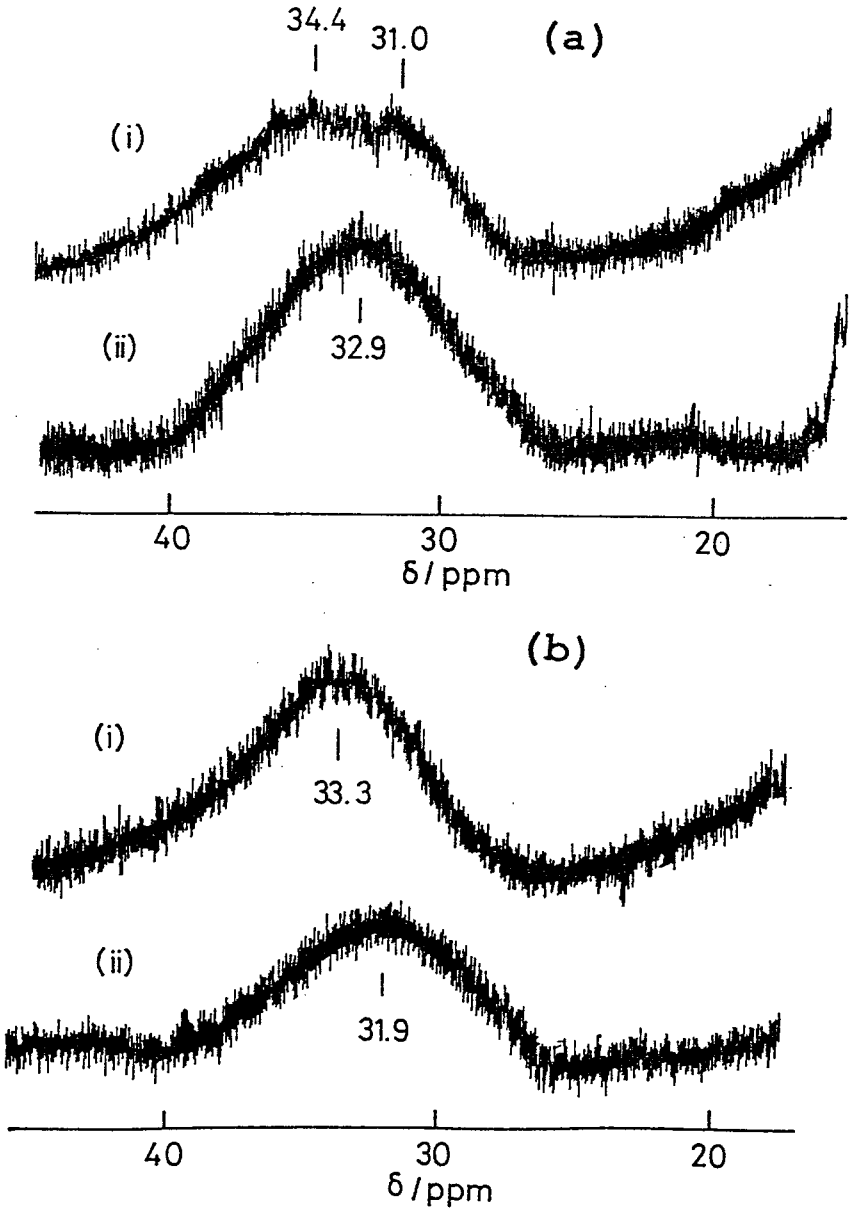

Figure 4. a) ^{1}H-NMR spectra (Cys CβH$_2$ region) of $[Fe_2S_2(Z\text{-cys-Gly-Ala-Gly-Ala-cys-OMe})_2]^{2-}$ in i) acetonitrile-d_3 and ii) in Me_2SO-d_6 and b) ^{1}H-NMR spectra of $[Fe_2S_2(Z\text{-cys-Ala-Ala-Gly-Ala-cys-OMe})_2]^{2-}$ in i) acetonitrile-d_3 and ii) in Me_2SO-d_6 at room temperature.

Temperature dependence of the Cys CH_2 signals of **1** and **2** was measured in DMF-d_7 shown in Fig. 5. Isotropic shift ($\Delta H/Ho$) of the Cys CH_2 signals changes linearly against with temperature with a diamagnetic behavior which is ascribed antiferromagnetic interaction between two iron ions in $[Fe_2S_2]$.

Electrochemical properties.

The macro-cyclic ring chelation effect of Cys-Ala-Ala-Gly-Ala-Cys fragment was examined in terms of the redox potential of the $[Fe_2S_2]$ complex. Table 3 lists the redox potentials, $E_{1/2}$, of **1** and **2** in various solvents at room temperature. **1** and **2** exhibit the same redox potential at -0.95 V (vs SCE) in DMF. A remarkable solvent dependence of redox potential of **1** was observed, e.g. at -0.80 V in propylene carbonate and at -0.76 V in acetonitrile. However, **2** has the redox potential at -1.10 V in propylene carbonate and -0.94 V in acetonitrile. The trend of the positive shift for **1** corresponds to the conclusion obtained from the absorption, CD, and ^{1}H-NMR spectral changes in various solvent. The changes are due to formation of the NH---S hydrogen bonds supported by non-polar solvent.

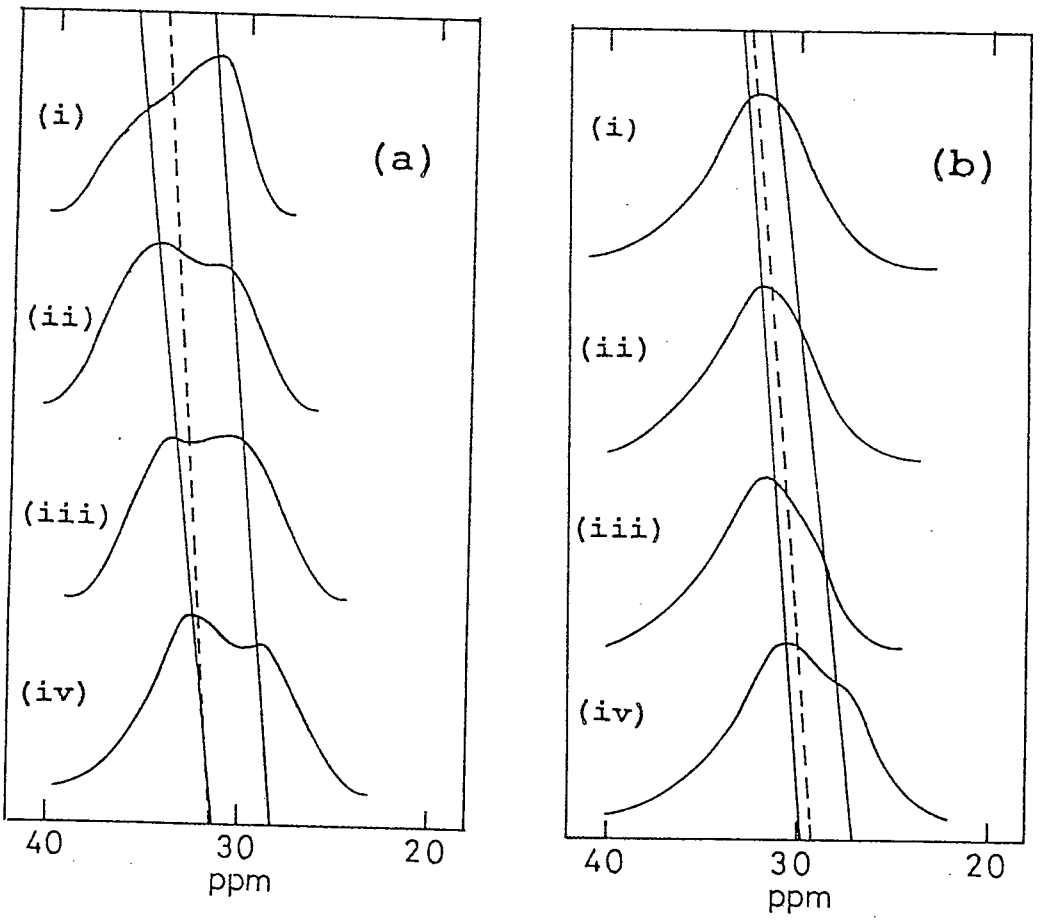

Figure 5. ^{1}H-NMR spectra (Cys CβH$_2$ region) of a) [Fe$_2$S$_2$(Z-cys-Gly-Ala-Gly-Ala-cys-OMe)$_2$]$^{2-}$ and b) [Fe$_2$S$_2$(Z-cys-Ala-Ala-Gly-Ala-cys-OMe)$_2$]$^{2-}$ in acetonitrile-d_3 at i) 40°C, ii) 20°C, iii) 0°C, iv) -20°C.

Table 3 Electrochemical Data of 2Fe-2S Complexes

Complexes (Solvents)	$E_{1/2}$, V(vs. SCE)	i_{pc}/i_{pa}
$[Fe_2S_2(Z\text{-cys-Gly-Ala-Gly-Ala-cys-OMe})_2]^{2-}$ **(1)**		
DMF	-0.95	0.67
propylene carbonate	-0.80	0.86
CH_3CN	-0.76	0.80
$[Fe_2S_2(Z\text{-cys-Ala-Ala-Gly-Ala-cys-OMe})_2]^{2-}$ **(2)**		
DMF	-0.94	0.80
propylene carbonate	-1.10	0.50
CH_3CN	-0.94	0.80

4-4. Discussion.

Structure of [2Fe-2S] complexes of a hexapeptide Z-Cys-A-Ala-Gly-Ala-Cys-OMe

The addition of 3,4-toluenedithiol to **1** or **2** resulted in formation of mononuclear $[Fe(SR)_4]^-$ type complex accompanied with evolution of hydrogen sulfide. Therefore, the bidentate hexapeptide ligand chelates to one Fe^{III} ion of $[Fe_2S_2]^{2+}$ core. The relatively strong chelation withstands against the replacement with tdt-H_2 and the inorganic sulfur bridge of $[Fe_2S_2]^{2+}$ is cleaved by the tdt-H_2 as the in equation (1).

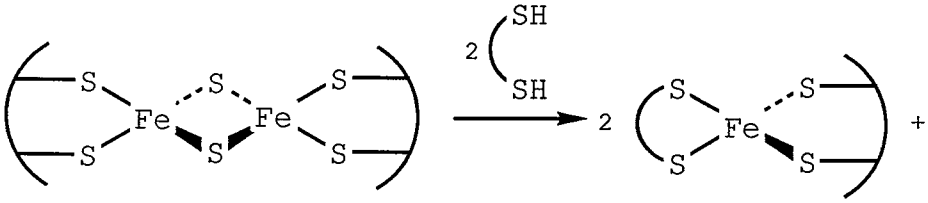

1

The chelating structure described above for **1** and **2** was supported by the CD results. Almost the same large molar ellipticity of **1** or **2** in DMF, compared with the small one for $[NEt_4]_2[Fe_2S_2(Z\text{-Ala-cys-OMe})_4]$ in DMF, indicates the chelation to one Fe^{III} ion. The solvent-dependence of the CD spectra of **1** is ascribed to a slight, conformational change of the hexapeptide fragment in a macrocyclic ring.

The solvent effect of **1** was detected by the change of ligand-metal charge transfer absorption (i.e. sulfur to iron). A slight solvent effect has been reported for $[Fe_2S_2(S_2\text{-}o\text{-xyl})_2]^{2-}$ by Mayer et al.[2] They have speculated

S→Fe ligand-metal charge transfer shift to be dependent on the solvent dielectric constant. Bonomi and Kurtz have reported the absorption spectral change between native and denatured ferredoxins.[20] This change also depends on the difference in environment around $[Fe_2S_2(S\text{-}cys)_4]^{2-}$ core upon denaturation of the protein.

The change of the ligand metal charge transfer absorption in various solvent seems to be dependent on the substitution of an amino acid residue (e.g. Gly-substitution of an amino acid residue ($Gly^2 \rightarrow Ala^2$) next to the Cys^1 residue). The previous studies of the peptide [4Fe-4S] model complex have revealed that a Cys-Gly-Ala fragment has a conformational advantage for the formation of NH---S hydrogen bond between Cys S and Ala NH. Such a conformation has been found in *P.aerogenes* ferredoxin by Adman et al.[21] Therefore, substitution of Gly^2 residue with Ala^2 residue was now found sterically unfavorable to form the NH---S hydrogen bond.

X-ray analysis of *S. platensis* ferredoxin has proposed the presence of NH---S hydrogen bonds between Cys^1 S and Ala^3 NH or Ala^5 NH and between S^* (bridged inorganic sulfur atom) and Gly^4 NH. The NH---S hydrogen bond should be more stabilized by weaker solvation. Such a NH---S hydrogen bond may contribute to the positive shift of $[Fe_2S_2(S\text{-}cys)_4]^{2-/3-}$ redox potential, e.g. from -0.95 V in DMF to -0.76 V in acetonitrile. The difference in the redox potentials between **1** and **2** in acetonitrile is estimated to be 180 mV which corresponds to the change of the ligand-

metal charge transfer absorption induced by the NH---S hydrogen bonding.

Two explanations are possible for the separation of two Cys CH_2 ^1H NMR signals of **1** at 31.0 ppm and 34.4 ppm in acetonitrile. One is a change of π-bonding character of Fe-S bond by the rotation of S^*-Fe-S-C torsion angle. The difference between bond characters of the two Cys thiolato-Fe bonds is revealed by the contact shift through the Fe-S bond. The rotation of the Fe-S torsion angle will be induced by the conformational restriction accompanied with the NH---S hydrogen bond formation. Actually, such a conformational restriction has been found for the Cys-Ala-Ala-Cys chelating fragment of $[Fe_2S_2(Z\text{-cys-Ala-Ala-cys-OMe})_2]^{2-}$ which exhibits two separate Cys CH_2 signals at 22.9 ppm and 30.7 ppm in Me_2SO-d_6. The alternative explanation is that a Fermi-type contact shift is diminished by the NH---S hydrogen bond formation, since the formation of the hydrogen bond decreases electron density of Fe-S bond.

Conclusion

Synthetic model peptide fragments, Cys-A-Ala-Gly-Ala-Cys (A = Gly, Ala), were found to preferably chelate to one Fe^{III} ion of $[Fe_2S_2]^{2+}$ core as the model of invariant sequence, Cys-Arg-Thr-Gly-Ser-Cys in *S. platensis* ferredoxin. When A is a Gly residue, formation of a stronger NH---S hydrogen bond in propylene carbonate occurs and results in the positive shift of redox potential of

$[Fe_2S_2(SR)_4]^{2-/3-}$. On the other hand, when A is an Ala residue, the chelation provides a disadvantageous conformation for the formation of the NH---S hydrogen bond.

References

(1) Tagawa, K.; Arnon, D. I. *Biochem. Biophys. Acta* **1968**, 153, 602.

(2) Mayerle, J.J.; Frankel, R.B.; Holm, R.H.; Ibers, J.A.;Phillips, W.D.; Weiher, J.F. *Proc. Nat. Acad. Sci. U.S.A.* **1973**, 70, 2429.

(3) Tsukihara, T.; Kobayashi, M.; Nakamura, M.; Katsube, Y.; Fukuyama, K.; Hase, T.; Wada, K.; Matsubara, H. *BioSystems* **1982**, 15, 243.

(4) Fukuyama, K.; Hase, T.; Matsumoto, S.; Tsukihara, T.; Katsube, Y.; Tanaka, N.; Kakudo, M.; Wada, K.; Matsubara, H. *Nature* **1980**, 286, 552.

(5) Ueno, S.; Ueyama, N.; Nakamura, A.; Tsukihara, T. *Inorg. Chem.* **1986**, 25, 1000.

(6) Ueyama, N.; Ueno, S.; Nakamura, A. *Bull. Chem. Soc. Jpn.* **1987**, 60, 283.

(7) Dayhoff, M. O."Atlas of Protein Sequence and Structure", National Biochemical Foundation, Washungtom D. C. Vol. 5, Suppl. 2.

(8) Noodleman, L.; Baerends, E. J. *J. Chem.Am. Soc.* **1984**, 106, 2316.

(9) Ueno, S.; Ueyama, N.; Nakamura, A. *Pept. Chem.* **1985**, 33.

(10) Gillum, W.O.; Mortenson, L.E.; Chen, T.S.; Holm, R.H. *J. Am. Chem. Soc.* **1977**, 99, 584.

(11) Stethna, Y. I.; DerVartanian, D.V.Beinert, H. *Biochem. Biophys. Res. Commun.* **1968**, 31, 862.

(12) Bernhardt, F.; Heymann, E.; Traylor, P.S. *Eur. J. Biochem.* **1978**, 92, 209.

(13) Cardenas, J.; Mortenson, Y.; Yoch, D. C. *Biochem. Biophys. Acta* **1976**, 434, 244.

(14) Pedersen, J. I.; Oftebro, H.; Vänngård, T. *Biochem. Biophys. Res. Commun.* **1977**, 76, 666.

(15) Sauber, K.; Fröhner, C.; Rosenberg, G.; Eberspächer, J.; Lihgens, F. *Eur. J. Biochem.* **1978**, 92, 209.

(16) Mayerle, J.J.; Denmark, B.V.; DePamphilis, B.V.; Ibers, J.A.; Holm, R.H. *J. Am. Chem. Soc.* **1975**, 97, 1032

(17) Ueyama, N.; Terakawa, T.; Nakata, M.; Nakamura, A. *J. Am. Chem. Soc.* **1983**, 105, 7098.

(18) Do, Y.; Simhon, E.D.; Holm, R.H. *Inorg. Chem.* **1983**, 22, 3809.

(19) Bonomi, F.; Kurtz, P. M., Jr. *Biochemistry* **1982**, 21, 6838.

(20) Adman, E. T.; Sieker, L. C.; Jensen, L. H.; Bruschi, M.; LeGall, J. *J. Mol. Biol.* **1976**, 107, 179.

Chapter 5.

Chelation Structures of Cys-A-B-C-D-Cys-X-Y-Cys Tridentate Peptide Complexes of $[Fe_2S_2]^{2+}$ Core.

5-1. Introduction.

Plant-type ferredoxin containing one $[Fe_2S_2]^{2+}$ core and four Cys thiolate ligands has s redox potential at -0.64 V (vs. SCE).[1] A typical model complex $[Fe_2S_2(S_2\text{-}o\text{-xyl})_2]^{2-}$ (S_2-*o*-xyl = α,α'-xylylenedithiolate), has been reported to exhibit a redox potential at -1.49 V (vs. SCE).[2] We have synthesized a [2Fe-2S] model complex of 20-peptide containing all amino acid residues within from $[Fe_2S_2]^{2+}$ core in *S. platensis* ferredoxin.[3] The peptide model complex could realize the similar redox potential in N,N-dimethylformamide to that of native plant-type ferredoxin. However, reasons for the positive shift of the redox potential are still ambiguous because there are many factors perturbing $[Fe_2S_2(SR)_4]^{2-}$ core in the 20-peptide model complex.

Recently we have reported that the synthesis and characterization of $[Fe_2S_2(Z\text{-cys-X-Y-cys-OMe})_2]^{2-}$ (X-Y = Ala-Ala, Val-Val) or $[Fe_2S_2(Z\text{-cys-A-Ala-Gly-Ala-cys-OMe})_2]^{2-}$ (A = Gly, Ala).[4,5] The Cys^1-A^2-Ala^3-Gly^4-Ala^5-Cys^6 fragment chelated to one Fe^{III} ion in native plant-type ferredoxin.[6] On the other hand, the invariant Cys-X-Y-Cys fragment of plant-type ferredoxin bridges between two Fe^{III} ions of $[Fe_2S_2]^{2+}$ core.[7] The possible chelating structures of these

peptide fragments are shown in Scheme 1. The preference of an invariant fragment (Cys-A-B-C-D-Cys-X-Y-Cys) in plant-type ferredoxin for the two chelating structures, I and II must depend on the identity of peptide residues, A ~ D and X,Y. As an example the structures of Z-Cys-Gly-Ala-Gly-Ala-Cys-Ala-Ala-Cys-OMe tridentate peptide complexes are described below.

In the ligand exchange reaction with $[Fe_2S_2(S\text{-}t\text{-}Bu)_4]^{2-}$ and the nonapeptide, one of the four *t*-BuS ligands remains as *t*-BuS$^-$ which can be substituted with Z-Val-Cys-Val-OMe. In *S. platensis* ferredoxin, a Thr-Cys-Val fragment coordinates to the Fe_2S_2 core. The tripeptide, Z-Val-Cys-Val-OMe was creates since no interaction between the Thr residue and $[Fe_2S_2(S\text{-cys})_4]^{2-}$ cluster has been reported in the X-ray analysis of *S. platensis* ferredoxin.[6] Furthermore, the Thr-Cys-Val fragment builds a hydrophobic environment around the $[Fe_2S_2]^{2+}$ core. The Val-Cys-Val fragment will provide more hydrophobic circumstances.

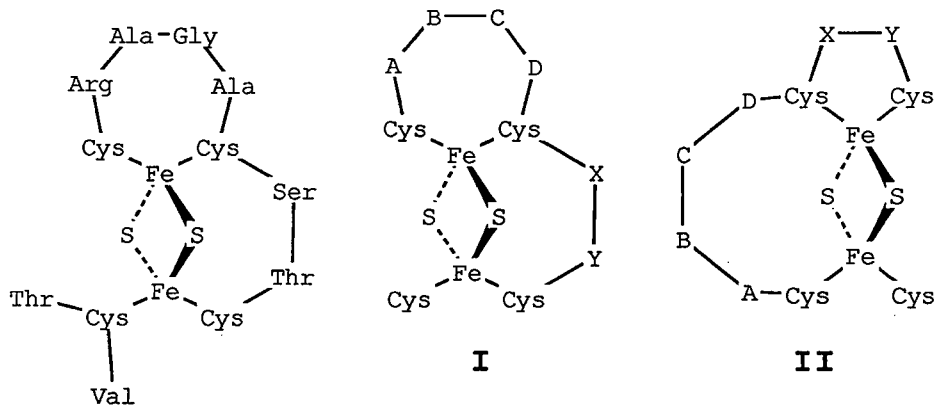

Scheme 1. Schematic structure of *S. Platensis* and Possible Structure of the Nonapeptide 2Fe-2S Complexes (I and II).

5-2. Experimental.

Materials.

Glycine, L-alanine, L-cysteine hydrochloride, benzyloxycarbonyl chloride (Z-Cl), TFA, 4.8 N anhydrous hydrogen chloride in dioxane, N,N'-dicyclohexylcarbodiimide (DCC), N-hydroxybenzotriazole (HOBt), 2-*t*-butyloxycarbonyloxyimino-2-phenyl-acetonitrile (Boc-ON) and 1-ethyl-3-(3-diethylaminopropyl)carbodiimide (WSCI) were obtained from Protein Research Foundation, Osaka. All solvents were purified by distillation before use. All other reagents were of commercial grade.

Peptide Synthesis.

Benzyloxycarbonyl derivatives of L-alanine was prepared by the same procedures as cited in the literature.[8] t-Butoxycarbonyl derivative of L-alanine and glycine were prepared by the according to the literature method using Boc-ON.[9] HCl·H-Cys(Acm)-OH was prepared by the modified reaction as discrived in a literature.[10] HCl·H-Cys(Acm)-OMe was also prepared under the analogous reaction scheme as discrived in a literature.[11] Z-Cys(Acm)-Gly-Ala-Gly-OPac was prepared by the same procedure as reported previously.[12]

Boc-Ala-Cys(Acm)-OMe.

Boc-Ala-OH (10.4 g 55 mmol), HOBt (3 g 23 mmol), triethylamine (7 ml,50 mmol) and HCl·H-Cys(Acm)-OMe (15 g,50 mmol) was dissolved in 300 ml of THF. DCC (11.35 g, 55 mol) in CH_2Cl_2 (30 ml) was slowly added to the stirring solution

at 0°C and after the reaction the solution was concentrated. The residue was dissolved in AcOEt and filtered. The filtrate was washed with H_2O, 1 N HCl aq., H_2O, 5 % $NaHCO_3$ aq., and H_2O, and dried over Na_2SO_4. It was concentrated under vacuo followed by recrystallization from AcOEt/ether to give the title compound (11.1 g, 58.3 %).
Anal. Found: C,47.70; H,7.21; N,11.10. Calcd. for $C_{15}H_{27}N_3O_6S$: C,47.73; H,7.21; N,11.13.

Boc-Ala-Ala-Cys(Acm)-OMe.

Boc-Ala-Cys(Acm)-OMe (10.3 g, 27.3 mmol) was dissolved in 150 ml of 3.5 N HCl/AcOEt. After 30 min, 400 ml of dry ether was added to the reaction mixture and the precipitate was collected by filtration. The precipitate was washed with ether, and dried over NaOH pellets in vacuo. To a solution of the precipitate (deblocked peptide) in DMF (200 ml) was added HOBt (4.06 g, 30 mmol) and Boc-Ala-OH (5.7 g, 30 mmol). WSCI (5.5 ml, 30 mmol) was added to the solution with stirring at -20 °C. After the reaction, the solution was concentrated under reduced pressure. The residue was dissolved in $CHCl_3$. The extract was washed with H_2O, 1 N HCl aq., H_2O, 5 % $NaHCO_3$ aq., and H_2O, and dried over Na_2SO_4. It was concentrated under vacuo by two precipitation from AcOEt/ether to give the titled compound (8 g, 80.5 %).
Anal. Found: C,48.20;H,7.15;N,12.50. Calcd. for $C_{18}H_{32}N_4O_7S$: C,48.20; H,7.19; N,12.49

Boc-Cys(Acm)-Ala-Ala-Cys(Acm)-OMe.

The titled peptide was synthesized by the same method as described for the synthesis of Boc-Ala-Ala-Cys(Acm)-OMe.
Yield 7 g, 84 %
Anal. Found: C,46.30;H,6.70;N,9.61. Calcd. for $C_{24}H_{42}N_6O_9S_2$: C,46.29; H,6.71; N,9.65

Boc-Ala-Cys(Acm)-Ala-Ala-Cys(Acm)-OMe.

The titled peptide was synthesized by the WSCI method which was described for the synthesis of Boc-Ala-Ala-Cys(Acm)-OMe. Yield 5 g, 78 %.
Anal. Found: C,46.70;H,6.85;N,14.10. Calcd. for $C_{27}H_{47}N_7O_{10}S_2$: C,46.74; H,6.83; N,14.13

Z-Cys(Acm)-Gly-Ala-Gly-OH.

A solution of Z-Cys(Acm)-Gly-Ala-Gly-OPac (1.9 g, 3 mmol) in AcOH (400 ml) containing Zn powder (4 g, 80 mmol) was stirred for 2.5 h at 40 °C. After the reaction, the reaction mixture was filtered. The filtrate was concentrated and added ether to give the title compound.

Z-Cys(Acm)-Gly-Ala-Gly-Ala-Cys(Acm)-Ala-Ala-Cys(Acm)-OMe

Boc-Ala-Cys(Acm)-Ala-Ala-Cys(Acm)-OMe (2 g, 3mmol) was dissolved in 10 ml of TFA at 0 °C. The reaction mixture was concentrated to about a half volume under reduced pressure, 3.5 N HCl/AcOEt (4 ml, 10 mmol) was added to the solution. All solvents were evaporated in vacuo. The residue was washed with ether, dried over NaOH pellets in vacuo. The residue was washed with ether, dried over NaOH pellets in

vacuo. The residue was dissolved in DMF (100 ml) together with HOBt (0.4 g, 3.3 mmol) and Z-Cys(Acm)-Gly-Ala-Gly-OH (3 mmol). WSCI (0.55 ml, 3.3 mmol) was added to the stirring solution at -20 °C. After the reaction, the solution was concentrated under reduced pressure. The crude product was triturated with H_2O, 1/3 N HCl aq., H_2O, 5 % $NaHCO_3$ aq. and H_2O, and followed by precipitation from MeOH/ether to give the title compound (2 g,69.8 %).

Anal. Found: C,48.00; H,6.20; N,15.30. Calcd. for $C_{44}H_{68}N_{12}O_{15}S_3$: C,47.99; H,6.22;N,15.26.

Synthesis of Hg(II) complexes

Hg_3Cl_3(Z-cys-Gly-Ala-Gly-Ala-cys-Ala-Ala-cys-OMe)

To a solution of Z-Cys(Acm)-Gly-Ala-Gly-Ala-Cys(Acm)-Ala-Ala-Cys(Acm)-OMe (1.5 g,1.57 mmol) in 100 ml of DMF was added 4 g (8.0 mmol) of $HgCl_2$ and 1 ml of water during stirring at room temperature. After 10 h, 100 ml of NaCl saturated water was added to the solution. The white precipitate obtained was collected with filtration and washed twice with of methanol. The white powder was dried over P_2O_5 in vacuo.

Anal. Found: C,26.32; H,3.25; N,7.91. Calcd. for $C_{35}H_{50}Cl_3Hg_3N_9O_{12}S_3$: C,26.39; H,3.16;N,7.85.

Synthesis of Cys-deprotecting peptides.

All Cys-deprotecting peptides were manipulated under Ar atmosphere.

Z-Cys-Gly-Ala-Gly-Ala-Cys-Ala-Ala-Cys-OMe

Hg_3Cl_3(Z-cys-Gly-Ala-Gly-Ala-cys-Ala-Ala-cys-OMe) 1g (0.63mmol) was dispersed in 100ml of DMF/MeOH (9:1 v/v) and H_2S gas was bubbled through the stirring mixture. After 40 minute, the white Hg complex was completely dissolved and black HgS was precipitated. HgS was filtered off and the filtrate was concentrated under reduced pressure. The white residue was washed with ether and dried in vacuo.

Synthesis of $[NEt_4]_2[Fe_2S_2$(Z-cys-Gly-Ala-Gly-Ala-cys-Ala-Ala-cys-OMe)(S-*t*-Bu)] (1)

1 was synthesized by the ligand exchange reaction of $[NEt_4]_2[Fe_2S_2(S\text{-}t\text{-}Bu)_4]$ (20mg, 2.78×10^{-5}mol) with Z-Cys-Gly-Ala-Gly-Ala-Cys-Ala-Ala-Cys-OMe (26.2mg, 3.0×10^{-5}mol) in DMF (2ml). After the reaction mixture was stirred for 5 min, the solution was concentrated under reduced pressure. The dark brown residue was washed with degassed DME and dried in vacuo. The purity was checked by the core extrusion reaction using benzenethiol (10 equivs) in DMF (A_{458}/A_{550}=1.09). The ratio of absorbance at 458nm to that at 550nm of pure $[Fe_2S_2(SPh)_4]$ was 1.12.[13]

Synthesis of $[NEt_4]_2[Fe_2S_2$(Z-cys-Gly-Ala-Gly-Ala-cys-Ala-Ala-cys-OMe)(Z-Val-cys-Val-OMe)] (2)

2 was synthesized by the ligand exchange reaction of complex **1** (10 mg, 7.21×10^{-6} mol)with Z-Val-Cys-Val-OMe (3.4

mg, 7.29×10^{-6} mol) in 2 ml of DMF. After mixed for 5 min, the solution was concentrated under reduced pressure. The residue was dissolved in 10 ml of acetonitrile. The excess peptide was collected by filtration. The solution was concentrated again under reduced pressure. Brown powder was obtained. Content of $[Fe_2S_2]^{2+}$ core in **2** was determined using 10 equiv. of benzenethiol in DMF (A_{458}/A_{550} = 1.10) as described above.

Physical measurement

Absorption spectra were measured on a JASCO UVIDEC-5A spectrophotometer in visible region. CD spectra were recorded on a JASCO J-40 spectropolarimeter using an 1mm path cell. 400 MHz ^{1}H-NMR spectra were recorded at 23 °C. Cyclic voltammetries were performed with a Yanaco-P8-CV equipped with a function generator Yanaco model FG-1218. [N(n-Bu)$_4$][ClO_4] was used as a supporting electrolyte. The voltamograms were recorded at room temperature, and a saturated calomel electrode (SCE) was used as the reference.

5-3. Results

Synthesis of [2Fe-2S] peptide complexes.

$[NEt_4]_2[Fe_2S_2$(Z-cys-Gly-Ala-Gly-Ala-cys-Ala-Ala-cys-OMe)(S-*t*-Bu)] (**1**) and $[NEt_4]_2[Fe_2S_2$(Z-cys-Gly-Ala-Gly-Ala-cys-Ala-Ala-cys-OMe)(Z-Val-cys-Val-OMe)] (**2**) were synthesized by the ligand exchange reaction as employed for the synthesis of $[NEt_4]_2[Fe_2S_2$(Z-cys-X-Y-cys-OMe)$_2$] in the previous chapters. This method has an advantage for synthesis of [2Fe-2S] peptide complex under mild conditions. The reaction proceeds as shown in the following schemes. *t*-BuS$^-$ ligand of **1** was detected by ^{1}H-NMR spectrum giving *t*-Bu signals at 4.72 ppm which are contact-shifted. Absence of *t*-BuS$^-$ proton signals for **2** indicates the complete exchange of *t*-BuS$^-$ ligand with Z-Val-Cys-Val-OMe.

$[NEt_4]_2[Fe_2S_2(S\text{-}t\text{-}Bu)_4]$ + nonapeptide

$$\xrightarrow[-3\ t\text{-BuSH}]{} [NEt_4]_2[Fe_2S_2(\text{nonapeptide})(S\text{-}t\text{-}Bu)]\ \mathbf{1}$$

$[NEt_4]_2[Fe_2S_2$(nonapeptide)(S-*t*-Bu)] + Z-Val-Cys-Val

$$\xrightarrow[-t\text{-BuSH}]{} [NEt_4]_2[Fe_2S_2(\text{nonapeptide})(\text{Z-Val-cys-Val-OMe})]\ \mathbf{2}$$

Electronic spectra of [2Fe-2S] peptide complexes.

Figure 1 shows the absorption spectra of **1** and **2** in DMF. **2** exhibits two absorption maxima at 419 and 459 nm which are characteristic for [2Fe-2S] plant-type ferredoxins and simple

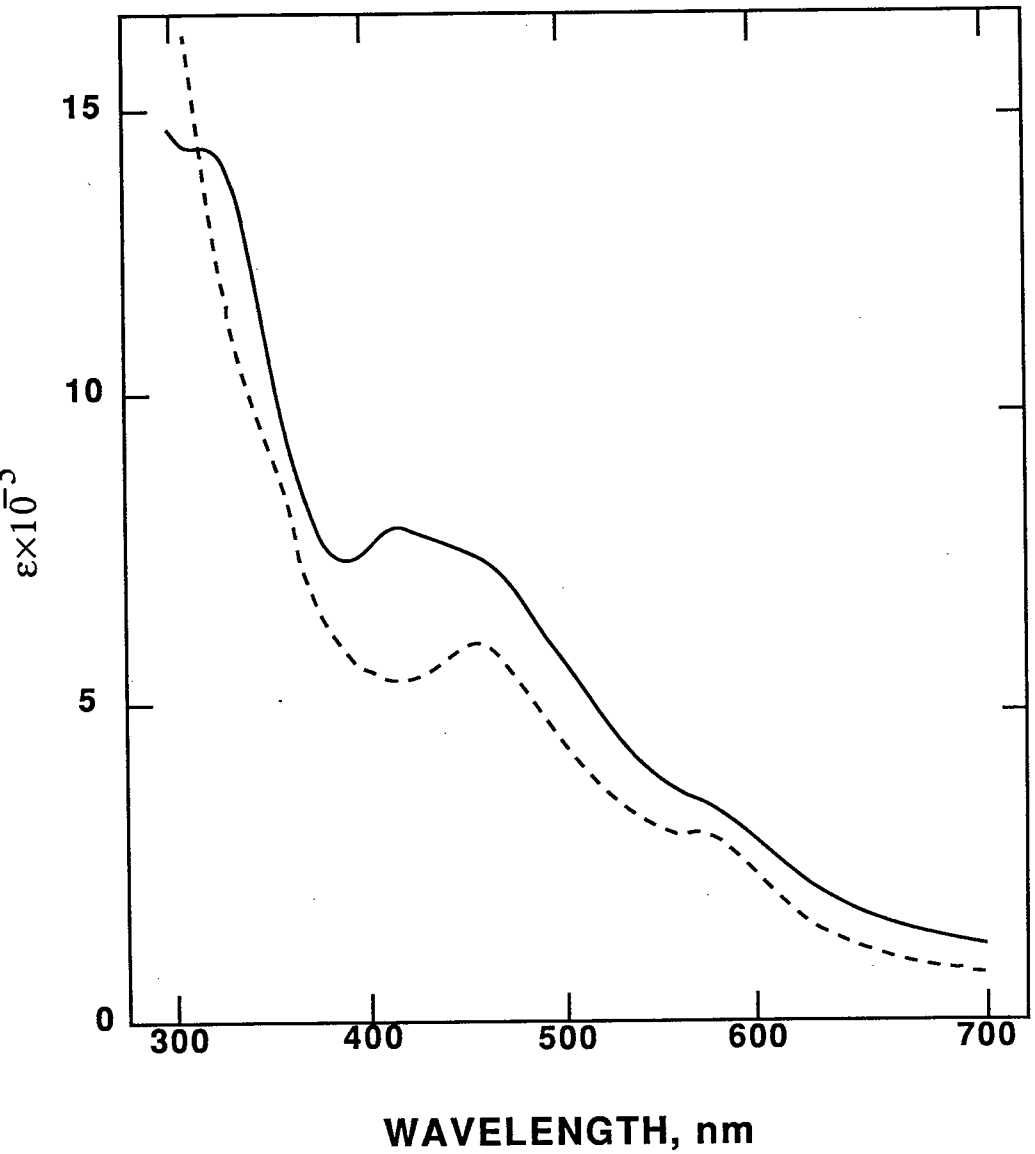

Figure 1 Absorption spectra of (---) $[Fe_2S_2(Z\text{-cys-Gly-Ala-Gly-Ala-cys-Ala-Ala-cys-OMe})(S\text{-}t\text{-Bu})]^{2-}$ and (——) $[Fe_2S_2(Z\text{-cys-Gly-Ala-Gly-Ala-cys-Ala-Ala-cys-OMe})(Z\text{-Val-cys-Val-OMe})]^{2-}$ in DMF.

model complexes. On the contrary, **1** shows only one maximum at 460 nm in the 400 - 500 nm region and a clear maximum at 573 nm. Such an absorption spectrum is due to change of S^*,S $\rightarrow$Fe ligand-metal charge transfer. The change is induced by the different environment around $[Fe_2S_2(S\text{-cys})_4]^{2-}$core.[14] Observation of two strong maxima at 458 nm and 550 nm in the 400 - 600 nm region has been reported for the [2Fe-2S] cluster of *Tritrichomonas foetus* protein.[15]

Table 1 lists the absorption maxima of **1** and **2** in DMF compared with those of $[Fe_2S_2(Z\text{-cys-Ala-Ala-cys-OMe})_2]^{2-}$ (**3**) in DMF and $[Fe_2S_2(Z\text{-cys-Gly-Ala-Gly-Ala-cys-OMe})_2]^{2-}$ (**4**) in propylene carbonate. **3** shows the typical [2Fe-2S] absorption maxima at 417 nm and 450 nm, while **4** exhibits a relatively weaker absorption maximum at 420 nm and a relatively strong maximum at 442 nm in propylene carbonate.[5] This trend corresponds to that of **1** in DMF.

CD spectra.

Figure 2 shows the CD spectra of **1** and **2** in DMF. Both complexes exhibit the same CD profile, although the molar ellipticity of each extremum of **2** has three times of that of **1**. The results indicate that the substitution of *t*-BuS^- ligand with Z-Val-Cys-Val-OMe induces the restricted conformational mobility of the peptide chain with the bulky ligand.

^{1}H-NMR spectra

Figure 3 shows the 400 MHz ^{1}H-NMR spectra of Me_2SO-d_6

Table 1. Absorption Spectra of [2Fe-2S] Oligopeptide Complexes in DMF.

Complexes	Absorption maxima λ/nm (ε×10^{-3}/M^{-1}cm^{-1})		
[Fe_2S_2(Z-cys-Gly-Ala-Gly-Ala-cys-Ala-Ala-cys-OMe)(S-*t*-Bu)]$^{2-}$ **(1)**	348(sh;10.0)		459.8(6.2)
[Fe_2S_2(Z-cys-Gly-Ala-Gly-Ala-cys-Ala-Ala-cys-OMe)(Z-Val-cys-Val-OMe)]$^{2-}$ **(2)**	318(14.3)	418.8(8.1)	458.8(7.7)
[Fe_2S_2(Z-cys-Ala-Ala-cys-OMe)$_2$]$^{2-}$ **(3)**	327(14.3)	417(10.0)	450(sh;8.9)
[Fe_2S_2(Z-cys-Gly-Ala-Gly-Ala-cys-OMe)$_2$]$^{2-}$ **(4)** a)		420(sh;9.4)	442(9.5)

a) in propylene carbonate.

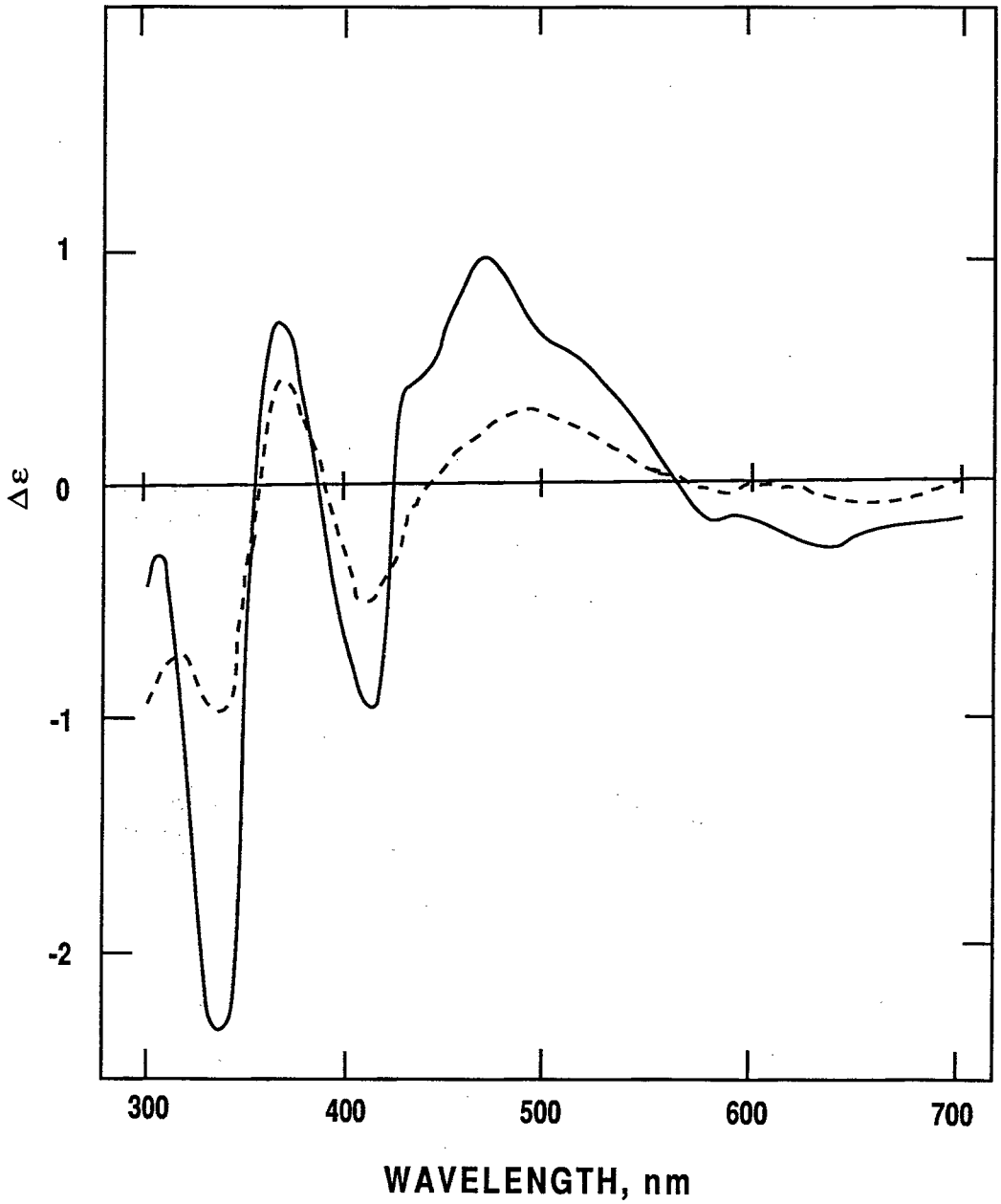

Figure 2 CD spectra of (---) $[Fe_2S_2$(Z-cys-Gly-Ala-Gly-Ala-cys-Ala-Ala-cys-OMe)(S-*t*-Bu)$]^{2-}$ and (——) $[Fe_2S_2$(Z-cys-Gly-Ala-Gly-Ala-cys-Ala-Ala-cys-OMe)(Z-Val-cys-Val-OMe)$]^{2-}$ in DMF.

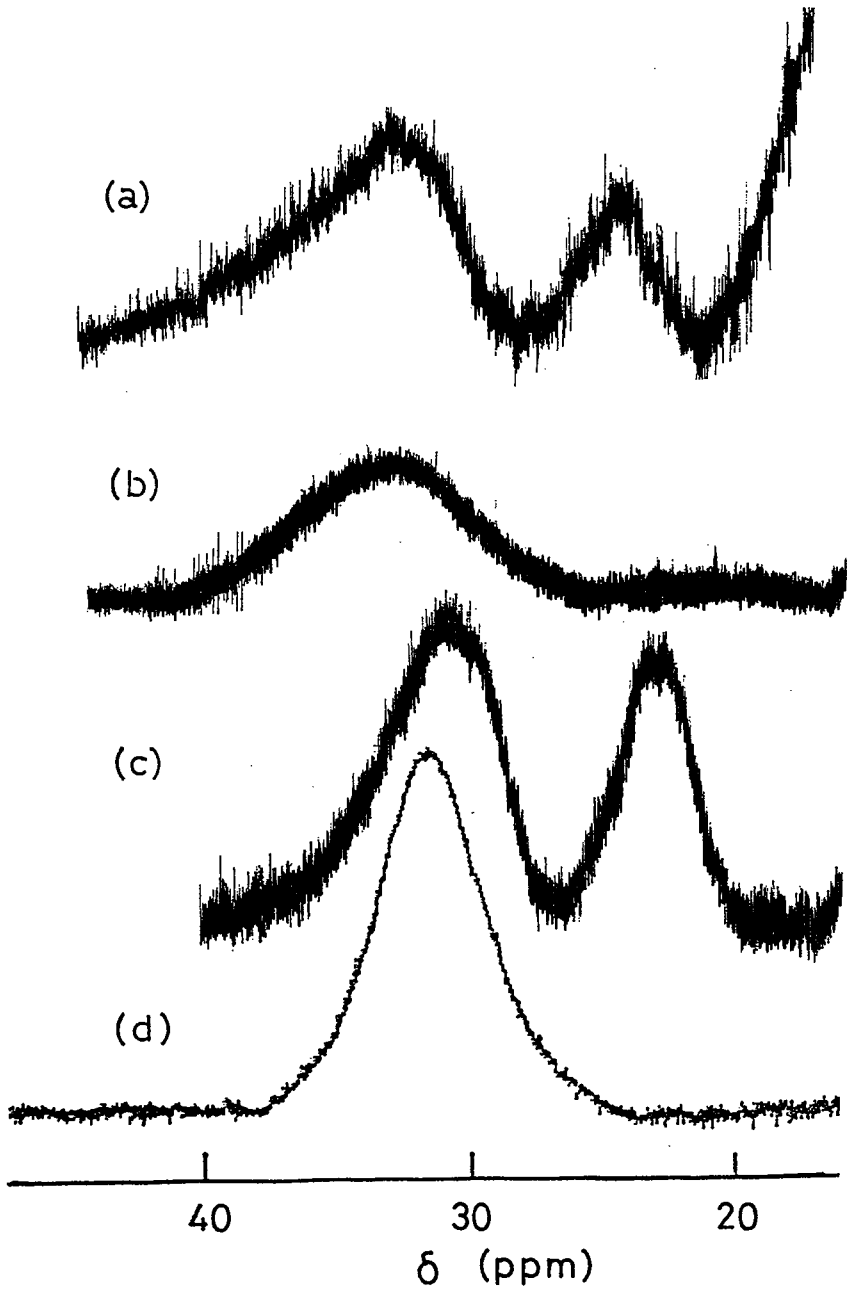

Figure 3 ^{1}H-NMR spectra in the Cys CβH$_2$ region of (a) [NEt$_4$]$_2$[Fe$_2$S$_2$(Z-cys-Gly-Ala-Gly-Ala-cys-Ala-Ala-cys-OMe)(S-*t*-Bu)] (**1**), (b) [NEt$_4$]$_2$[Fe$_2$S$_2$(Z-cys-Gly-Ala-Gly-Ala-cys-OMe)$_2$] (**3**), (c) [NEt$_4$]$_2$[Fe$_2$S$_2$(Z-cys-Ala-Ala-cys-OMe)$_2$] (**4**), and (d) [NEt$_4$]$_2$[Fe$_2$S$_2$(Z-cys-Gly-Val-OMe)$_4$] in Me$_2$SO-d_6 .

solution of **1** in the Cys CH_2 region (20~40 ppm) compared with those of **3**, **4** and a non-chelating peptide complex, $[NEt_4]_2[Fe_2S_2(Z\text{-cys-Gly-Val-OMe})_4]$. Two separate peaks at 25ppm (line width, 800Hz) and 35ppm (line width, 1400Hz) were observed with an integrated ratio of 6:7 due to two isomers postulated in Scheme 1. The signal at 25ppm corresponds to one of two separate signals of **3** at 23 ppm. Thus, the Cys-Ala-Ala-Cys part of the nonapeptide ligand chelates to one Fe^{III} ion of $[Fe_2S_2]^{2+}$core. However, the peak integral at 25 ppm is smaller than that expected for the structure I as shown in Scheme 1. In addition, observation of only one broad peak will be expected when **1** adopts the structure I as reported for native plant-type ferredoxin by Nagayama et al.[16] The presence of two isomers, structure I and II, is thus established. We roughly estimated the ratio by integration of ^{1}H-NMR signals. The ratio of I/II is thus approximately 5.7:4.3. Complex **2** also exhibits two separate signals at 25 ppm and 35 ppm with (1:9) ratio. **2** consists of the two isomers with a ratio 6:4 (I:II) which is similar to the ratio (5.7/4.3) of **1**. Therefore, no rearrangement in the tridentate ligand occurs upon substitution of *t*-BuS^- ligand with Z-Val-Cys-Val-OMe.

Electrochemical properties of 1 and 2.

The redox potentials of $[Fe_2S_2(S\text{-cys})_4]^{2-/3-}$ in DMF or acetonitrile were determined using cyclic voltammetries. Table 3 lists the redox potentials at -1.06 V and -0.94 V vs. SCE for **1** and **2**, respectively. The value of i_{pc}/i_{pa} = 0.4

Table 2. Electrochemical Data of $[Fe_2S_2$(Z-cys-Gly-Ala-Gly-Ala-cys-Ala-Ala-cys-OMe)(S-*t*-Bu)$]^{2-}$ and $[Fe_2S_2$(Z-cys-Gly-Ala-Gly-Ala-cys-Ala-Ala-cys-OMe)(Z-Val-cys-Val-OMe)$]^{2-}$ in DMF.

Complex	$(E_{pc}+E_{pa})/2$,V vs SCE (E_{pc}, E_{pa} ,V vs SCE)	i_{pc}/i_{pa}
$[Fe_2S_2$(Z-cys-Gly-Ala-Gly-Ala-cys-Ala-Ala-cys-OMe)(S-*t*-Bu)$]^{2-}$ (**1**)	-1.06 (-0.96,-1.15)	0.4
$[Fe_2S_2$(Z-cys-Gly-Ala-Gly-Ala-cys-Ala-Ala-cys-OMe)(Z-Val-cys-Val-OMe)$]^{2-}$ (**2**)	-0.94 (-0.87,-1.01)	0.9

for **1** is smaller than that of **2** (i_{pc}/i_{pa} = 0.9), indicates that the reduced form (3- state) of **1** is less stable than **2**. The bulky ligand, Z-Val-Cys-Val-OMe, is effective to stabilized the 3- state.

Figure 4 shows the solvent-dependence of differential pulse polarograms of **2** in DMF or acetonitrile. Two redox couples at -0.82V and -0.93V (vs.SCE) were observed in acetonitrile, although only one redox couple at -0.95V (vs. SCE) was found in DMF. Two isomers (I and II) exist in **2** as determined by the ^{1}H-NMR spectroscopy. These isomers exhibit the same redox potentials in DMF but different ones in acetonitrile. The consumed current ratio, $I_{-0.82}/I_{-0.93}$, upon reduction is 5.5/4.5. Thus, the ratio obtained from the consumed current is close to that obtained by the ^{1}H-NMR spectral measurement.

One isomer (redox couple at -0.82 V in acetonitrile) seems to have structure I found in native plant-type ferredoxin. Although $[Fe_2S_2(Z\text{-cys-Ala-Ala-cys-OMe})_2]^{2-}$ exhibits no solvent dependence of the redox potential as described in the previous chapter, $[Fe_2S_2(Z\text{-cys-Gly-Ala-Gly-Ala-cys-OMe})_2]^{2-}$ having a ligand chelating to one Fe^{III} ion exhibits a remarkable solvent dependence (180 mV difference between DMF and acetonitrile). Thus, the solvent dependence (90 mV) of the redox potential of **2** between DMF and acetonitrile is due to chelation to one Fe^{III} ion of $[Fe_2S_2]^{2+}$ core by the Cys-Gly-Ala-Gly-Ala-Cys fragment of the nonapeptide ligand as shown in structure I.

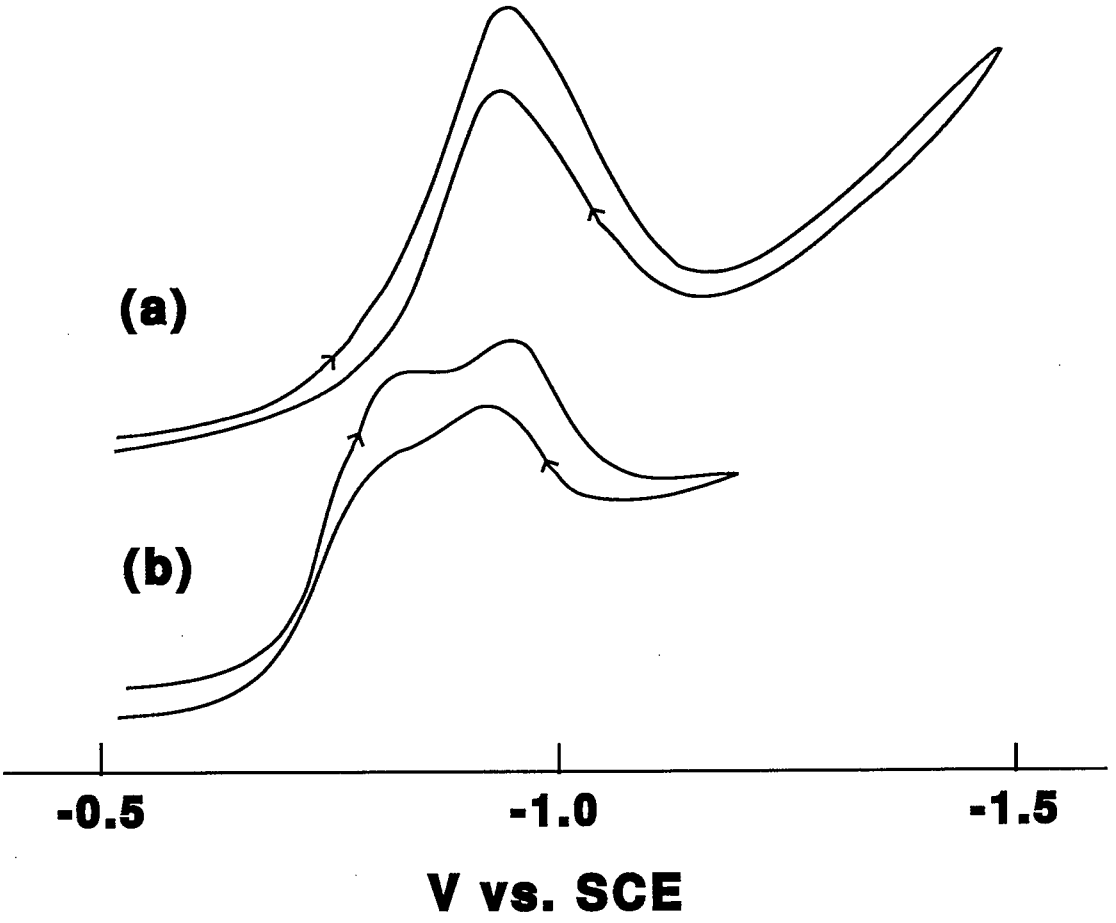

Figure 4 Differential pulse polarograms of $[Fe_2S_2(Z\text{-cys-Gly-Ala-Gly-Ala-cys-Ala-Ala-cys-OMe})(Z\text{-Val-cys-Val-OMe})]^{2-}$ in a) DMF and b) acetonitrile.

5-4. Discussion.

Non-selective chelation by the tridentate nonapeptide to $[Fe_2S_2]^{2+}$ core.

1 and **2** synthesized by the ligand exchange method in DMF contain two isomers such as structures I and II shown in Fig.4. The ratios (60~55/45~40 in I/II) are determined by the ^{1}H-NMR spectra and the differential pulse polarogram. The results indicate that the Cys-Gly-Ala-Gly-Ala-Cys-Ala-Ala-Cys ligand has almost no selectivity for chelation to $[Fe_2S_2]^{2+}$ core since both of the Cys-Ala-Ala-Cys and the Cys-Gly-Ala-Gly-Ala-Cys fragments have chelating tendency to one Fe^{III} ion of $[Fe_2S_2]^{2+}$ core.

In native plant-type ferredoxin, reconstitution from apoferredoxin using inorganic sulfide and iron(III) ion has been reported.[17] Pagani et al. have reconstituted spinach ferredoxin with [2Fe-2S] cluster using rhodanase.[18] Takahashi et al. have recently reported a solution of iron-sulfur synthetase which can incorporate the $[Fe_2S_2]^{2+}$ to apoferredoxin.[19] These reconstitutions provide a specific arrangement of $[Fe_2S_2]^{2+}$ core in the apoprotein. For the correct orientation of $[Fe_2S_2]^{2+}$ core in the peptide chain, two crucial factors are considered. Firstly, conformational restriction of the tridentate nonapeptide determines the orientation of $[Fe_2S_2]^{2+}$ core. Such restriction will be induced by NH---S hydrogen bond which are supported in non-solvated mediator. Secondly, a steric hindrance around the Cys (49) residue besides the tridentate ligand may be cited. Large contribution of the residual ligand (*t*-BuS and Z-Val-

Cys-Val-OMe) to the conformational restriction was recognized by the CD and electrochemical results. Substitution of *t*-BuS$^-$ with Z-Val-Cys-Val-OMe increases the molar ellipticity of the CD spectral extrema up to three times. The positive shift (100 mV) of the redox potential in complex **2** may be interpreted as follows. The bulky ligand, Z-Val-Cys-Val-OMe, facilitates the conformational restriction around $[Fe_2S_2(S\text{-}cys)_4]^{2-}$ core and realizes shielding of NH---S hydrogen bond from solvent DMF.

The introduction of a bulky ligand also contributes to the stabilization of a reduced state, $[Fe_2S_2(S\text{-}cys)_4]^{3-}$. Such a redox stabilization may be ascribed to formation of NH---S hydrogen bond in the reduced state.

Conclusion.

Nonapeptide, Z-Cys-Gly-Ala-Gly-Ala-Cys-Ala-Ala-Cys-OMe which is an analogous sequence of the invariant fragment in plant-type ferredoxin, has chelating ability to $[Fe_2S_2]^{2+}$ core as a tridentate ligand. Non-selective binding by the nonapeptide to the cluster provides two isomers. One of them has a relatively positive-shifted redox potential in non-solvated media.

An analogous complex, $[NEt_4]_2[Fe_2S_2$(Z-cys-Gly-Ala-Gly-Ala-cys-Ala-Ala-cys-OMe)(Z-Val-cys-Val-OMe)], having all amino acid residues around the $[Fe_2S_2]^{2+}$core of plant-type ferredoxin was synthesized. The complex provides the relatively stable reduced state. The NH---S hydrogen bond in this complex is sufficient by shielded from direct solvation

by DMF. Therefore, this may be the best model so far prepared for plant-type ferredoxin.

References.

(1) Masaki, R.; Yoshikawa, S.; Matsubara, H. *Biochem. Biophys. Acta* **1982**, 700, 101.

(2) Mayerle, J. J.; Frankel, R. B.; Holm, R. H.; Ibers, J. A.;Phillips, W. D.; Weiher, J. F. *Proc. Nat. Acad. Sci. U.S.A.* **1973**, 70, 2429.

(3) Chapter 2.

(4) Ueno, S.; Ueyama, N.; Nakamura, A.; Tsukihara, T. *Inorg. Chem.* **1986**, 25, 1000.

(5) Ueyama, N.; Ueno, S.; Nakamura, A. *Bull. Chem. Soc. Jpn.* **1987**, 60, 283.

(6) Chapter 4.

(7) Fukuyama, K.; Hase, T.; Matsumoto, S.; Tsukihara, T.; Katsube, Y.; Tanaka, N.; Kakudo, M.; Wada, K.; Matsubara, H. *Nature* **1980**, 286, 552.

(8) Bergmann, M.; Zervas, L. *Chem. Ber.* **1932**, 65, 1192.

(9) Itoho, M.; Hagiwara, D.; Kamiya, T. *Tetrahedron Lett.* **1975**, 4393.

(10) Veber, D. F.; Milkowski, J. D.; Denkewalter, R. R.; Hirschmann, K. *Tetrahedron Lett.* **1968**, 3057.

(11) Brenner, M.; Huber, W. *Helv. Chim. Acta* **1953**, 36, 1109.

(12) Ueno, S.; Ueyama, N.; Nakamura, A. *Pept. Chem.* **1985**, 33.

(13) Gillum, W. O.; Mortenson, L E.; Chen, T. S.; Holm, R. H. *J. Am. Chem. Soc.* **1977**, 99, 584.

(14) Noodleman, L.; Baerends, E. J. *J. Chem.Am. Soc.* **1984**, 106, 2316.

(15) Marczak, R.; Gorrell, T. E.; Müller, M. *J. Biol. Chem.* **1983**, 258, 12427.

(16) Nagayama, K.; Ozaki, Y.; Kyogoku, Y.; Hase, T.; Matsubara, H. *J. Biochem.* **1983**, 94, 893 .

(17) Fee, J. A.; Palmer, G. *Biochem. Biophys. Acta* **1971**, 254, 175.

(18) Pagani, S.; Bonomi, F.; Cerletti, P. *Eur. J. Biochem.* **1984**, 142, 361.

(19) Takahashi, Y.; Mitsui, A.; Hase, T.; Matsubara, H. *Proc. Natl. Acad. Sci. USA* **1986**, 83, 2434.

Chapter 6.

The Synthesis, Molecular Structure, and Spectro- and Electrochemical Properties of Bulky Thiolate/2Fe-2S Complexes.

6-1. Introduction

Tetrapeptide complexes of Fe_2S_2 core, $[Fe_2S_2(Z\text{-cys-X-Y-cys-OMe})_2]^{2-}$ (X-Y = Ala-Ala, Ala-Pro, Pro-Leu, Z = benzyloxylcarbonyl)[1], in which the Z-Cys-X-Y-Cys-OMe ligands chelate to single Fe^{III} center, were found to exhibit the positive shift of the redox potential.[2] The chelation effect facilitates the formation of NH---S hydrogen bonds which induces the positive shift. Besides the hydrogen bonding, a restricted rotation of $S^*\text{-Fe-S}_\gamma\text{-C}\beta$ torsion angles from the stable position to the eclipsed position by the chelating Cys-X-Y-Cys segment must be considered. The two distinct contact-shifted ^{1}H-NMR signals of the cys CH_2 protons in $[Fe_2S_2(Z\text{-cys-Ala-Ala-cys-OMe})_2]^{2-}$ were observed at 30.7 and 22.9 ppm even in $Me_2SO\text{-}d_6$ which may disrupt the NH---S hydrogen bonds. In native plant-type ferredoxins, a large tridentate chelating sequence, Cys-A-B-C-D-Cys-X-Y-Cys, induces a definite Fe-S-C orientation. A quite similar orientation in its model complexes has been demonstrated also on the basis of the observed near-infrared CD peaks at 6000 and 7400 cm^{-1} arising from d-d transitions.[3] For the

model complex, $[Fe(Z\text{-}cys\text{-}Pro\text{-}Leu\text{-}cys\text{-}OMe)_2]^{1-}$, appearance of the characteristic MCD band at 28800 cm^{-1}, due to the ligand-to-metal charge transfer transition, was taken as an evidence of the splitting of the Fe(III) d orbitals induced by the chelation effect of Cys-X-Y-Cys.[4]

Recently, various iron complexes of bulky thiolate ligands have been synthesized, for example, $[Fe(2,3,5,6\text{-tetramethylbenzenethiolato})_4]^{1-}$,[5] and $[Fe_4S_4(2,4,6\text{-trialkylbenzene thiolato})_4]^{2-}$,[6-8] in an attempt to stabilize the Fe^{III} states.

In this Chapter, we describe the synthesis, molecular structure, and spectro- and electrochemical properties of the anion, $[Fe_2S_2(2,4,6\text{-trimethylbenzenethiolato})_4]^{2-}$. Effects of the torsion angle on the Fe-S(C) bond character were examined by the extended Hückel MO calculations on a simplified model complex, $[Fe_2S_2(SH)_4]^{2-}$.

6-2. Experimental Section

Materials and Methods.

All operations were carried out under an argon atmosphere. Solvents were distilled also under an argon atmosphere before use. Methanol, acetonitrile, 1,2-dimethoxyethane (DME), diethyl ether, and acetonitrile-d_3 were purified according to the literature methods.[9] The distillation of N,N'-dimethylformamide (DMF) under reduced pressure was repeated several times before use as a solvent for the electrochemical measurement. Mesitylenesulfonyl chloride was prepared by the reported method.[10] $[NEt_4]_2[Fe_2S_2Cl_4]$ was prepared according to the literature method.[16]

Bis(2,4,6-trimethylphenyl)disulfide.

In a three-necked flask (100 ml) with a condenser and a dropping funnel, was placed a suspension of lithium hydride (16.1 g, 0.424 mol) in diethyl ether (300 ml). A solution of mesitylenesulfonyl chloride (44.2 g, 0.203 mol) in diethyl ether (200 ml) was added to the suspension with vigorous stirring at 5 °C. After the evolution of hydrogen subsided, the reaction mixture was allowed to stand at room temperature for 1 h and then refluxed for 6 h. After treatment with water and 1 N-sulfuric acid, the ether layer was separated and was concentrated. The residue was dissolved in ethanol and oxidized by iodine (15 g) to give a pale yellow precipitate. The precipitate was collected by filtration, washed with ethanol and recrystallized from

ethanol/acetonitrile (15.1 g, 48 % yield).Anal. Calcd for $C_{18}H_{22}S_2$: C, 71.47; H, 7.33; S, 21.27. Found: C, 71.08; H, 7.37; S, 20.98. ^1H NMR ($CDCl_3$): 2.18 (s, *o*-CH_3), 2.21 (s, *p*-CH_3), 6.83 ppm (s, *m*-H).

Sodium 2,4,6-trimethylbenzenethiolate. Na(tmbt).

Sodium metal (0.53 g, 23 mmol) was added to a solution of bis(2,4,6-trimethylphenyl)disulfide (3.5 g, 11.4 mmol) in DME (50 ml) at 0 °C. The solution was allowed to stand at room temperature overnight after heating at 40°C for 1 h. The product precipitated as white needles, collected by filtration, washed with n-hexane, and dried over sodium hydroxide in vacuo. The product was obtained as colorless needles (4.3 g). ^1H NMR (C_6D_6): 2.81 (s, *o*-CH_3), 2.93 (s, *p*-CH_3), 7.00 (s, *m*-H).

$[NEt_4]_2[Fe_2S_2(tmbt)_4]$

An acetonitrile solution (50 ml) of 1.1 g (3.3 mmol) of Na(tmbt) was added to a solution of $[NEt_4]_2[Fe_2S_2Cl_4]$ in acetonitrile (100 ml). The reaction mixture was stirred for 1 h and filtered, and the filtrate was concentrated in vacuo. The crude product was recrystallized by dissolution in acetonitrile (50 ml) and slow cooling to 0°C. Air-sensitive black needles were obtained, yield 67%. Anal. Calcd for $C_{52}H_{84}N_2S_6Fe_2$; C, 59.98; H, 8.13; N, 2.69. Found; C, 59.44; H, 8.03; N, 2.76.

X-ray Diffraction Measurements. Collection of Data.

The crystals of $[NEt_4]_2[Fe_2S_2(tmbt)_4]$ sealed in glass

capillaries under argon were mounted on a Rigaku AFC-C-4 automated four-circle diffractometer for data collection and processing at room temperature using graphite-monochromatized Mo K-α radiation. Cell dimension was obtained from 20 reflections ($10° < 2\theta < 20°$) and refined with other 25 reflections ($2\theta < 20°$). Three standard reflections were chosen and monitored with every 100 reflections. The positions of Fe and S atoms were determined by the direct method (MULTAN 80). Subsequent Fourier synthesis based on the phases of Fe and S atoms determined the positions of the remaining nonhydrogen atoms. The final refinement was carried out using full-matrix least-squares techniques. The refined isotropic thermal parameters resulted in convergence to at R = 0.0667. Crystal data concerning crystal characteristics and X-ray diffraction measurements are listed in Table 1.

Physical measurements

Absorption spectra were recorded on a JASCO UVIDEC-5A spectrophotometer with a 1-mm cell. Sample solution was 8×10^{-4} mol·dm^{-3}. The ^{1}H-NMR spectra were obtained on a JEOL FX-90Q or a JEOL FX-200 spectrometer at 23 °C. Cyclic voltammetry was performed on a YANACO P8-CV equipped with a YANACO Model FG-1218 function generator. The voltammograms were obtained at room temperature with a three- electrode system consisting of a glassy-carbon working electrode, a platinum-wire auxiliary electrode, and a saturated calomel electrode (SCE) as the reference. [N(*n*-Bu)$_4$][ClO$_4$] was employed as a supporting electrolyte.

Table 1. Crystallographic Data for $[NEt_4]_2[Fe_2S_2(tmbt)_4]$.

Formula	$C_{52}H_{82}N_2S_6Fe_2$
Mw	1041.31
Crystal	monclinic
Space group	$P2_1/c$
a/Å	15.241
b/Å	16.174
c/Å	16.768
β/°	135.840
V/Å^3	2879.6
Z	2
D_C/g cm^{-3}	1.20
Radiation	Mo-Kα
Unique data	1393
Number of parameters	280
R	0.067
Data collection	$2\theta < 40°$

The measurements were carried out at several scanning rates (50 - 200 mV s^{-1}). The value of $E_{1/2}$ was estimated from (Epc + Epa)/2.

Extended Hückel MO calculation

In the extended Hückel calculations, the D_{2h} symmetry was assumed for the Fe_2S_4 portion with a tetrahedral geometry of the two Fe(III) ions as found in the structure of $[Fe_2S_2(S\text{-}p\text{-}tol)_4]^{2-}$.[2] The following geometrical parameters were used for the calculations. Bond distances: Fe- S*, 2.201 Å; Fe-S(H), 2.305 Å; S-H, 1.34 Å. Bond angles: Fe-S*- Fe, 75.39° ; S*-Fe-S, 110.27° ; Fe-S-H, 109.5°. The extended Hückel parameters for Fe were taken from an earlier work,[12] and those for S and H are the standard ones. In Table 2, parameters were summarized.

Table 2. Extended Hückel Parameters.

Orbitals		H_{ii}(eV)	ζ_1	ζ_2	C_1[a]	C_2
Fe	4s	-8.39	1.9			
	4p	-4.74	1.9			
	3d	-11.46	5.35	1.8	0.5366	0.6678
S	3s	-20.00	1.817			
	3p	-13.30	1.817			
H	1s	-13.6	1.3			

a) Exponents and coefficients used in double zeta expansion of Fe d orbitals.

6-3. Results and Discussion

Synthesis.

The bulky thiolato complex, $[Fe_2S_2(tmbt)_4]^{2-}$ was prepared by the reaction (eq.1) between $[NEt_4]_2[Fe_2S_2Cl_4]$ and Na(tmbt) under strictly anaerobic conditions in acetonitrile.

$$[NEt_4]_2[Fe_2S_2Cl_4] + 4\ Na(tmbt) \longrightarrow [NEt_4]_2[Fe_2S_2(tmbt)_4] + 4\ NaCl \quad \text{--- (1)}$$

The air-sensitive complex was isolated by filtration of sodium chloride, and purified by crystallization from acetonitrile at 0 °C. The black needle shaped $[NEt_4]_2[Fe_2S_2(tmbt)_4]$ was soluble in acetonitrile, DMF, and DMSO.

Crystallographic Studies.

Description of the structure of $[NEt_4]_2[Fe_2S_2(tmbt)_4]$.

This complex crystallizes in space group C2 - P21/c of monoclinic system with two formula units per unit cell. Crystal data are collected in Table 1. The structure of the anion is shown in Figure 1. Selected interatomic distances and angles are collected in Table 3. The complex contains a normal $[Fe_2S_2]^{2+}$ core having a planar structure as that of $[Fe_2S_2(S\text{-}p\text{-}tol)_4]^{2-}$.[2] The core Fe-S* distances divide into two sets of two short (2.195 Å) and two long (2.204 Å) bonds with the indicated ranges and mean values. This arrangement provides two sets of the related bond lengths and angles,

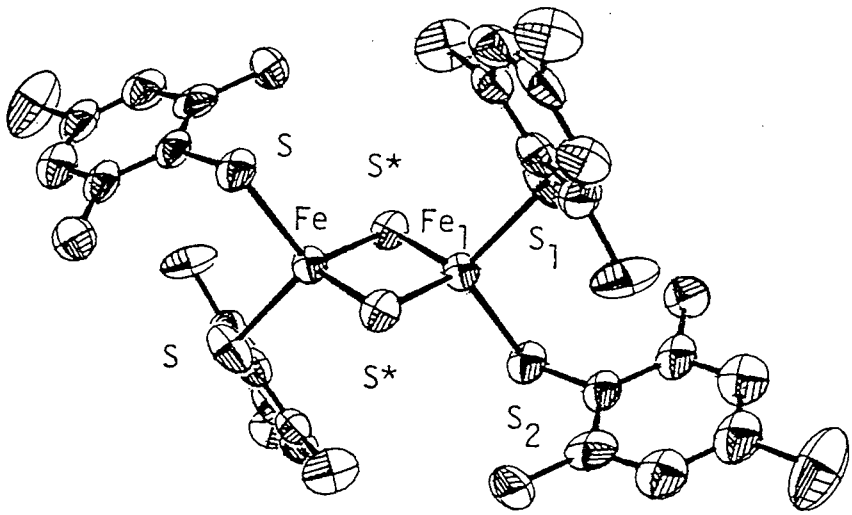

Figure 1 Crystal Structure of $[Fe_2S_2(tmbt)_4]^{2-}$ showing 50% probability ellipsoid.

Table 3. Selected Interatomic Distances (Å) and Angles (°) of $[Fe_2S_2(tmbt)_4]^{2-}$ compared with those of the related [2Fe-2S] complexes.

Parameters		tmbt	S_2-*o*-xyl[a]	S-*p*-tol[a]
Fe-S*	Fe(1)-S*(1)	2.195(7)	2.185(2)	2.200(1)
	Fe(1)-S*(2)	2.204(7)	2.232(1)	2.202(1)
Fe-S	Fe(1)-S(3)	2.299(8)	2.306(1)	2.312(1)
	Fe(1)-S(4)	2.318(7)	2.303(1)	2.312(1)
Fe-Fe	Fe(1)-Fe(2)	2.698(5)	2.698(1)	2.691(1)
S-S	S*(1)-S*(2)	3.475(8)	3.498(3)	3.483(3)
	S(3)--S(4)	3.733(10)	3.690(2)	3.816(1)
S-C	S(3)-C	1.791(27)	1.835(4)	1.758(4)
	S(4)-C	1.764(22)	1.847(4)	1.760(4)
S*-Fe-S*	S*(1)-Fe(1)-S*(2)	104.35(25)	104.73(5)	104.61(4)
S*-Fe-S	S*(1)-Fe(1)-S(3)	112.90(28)	112.33(5)	114.48(4)
	S*(2)-Fe(1)-S(4)	104.16(25)	110.66(5)	115.81(4)
S-Fe-S	S(3)-Fe(1)-S(4)	107.85(22)	106.4	11.2
Fe-S-Fe	Fe(1)-S*(1)-Fe(2)	75.65(22)	75.27(5)	75.39(4)
Fe-S-C	Fe(1)-S(3)-C	112.35(91)	99.8(1)	110.8(1)
	Fe(1)-S(4)-C	104.95(75)	98.1(1)	110.4(1)
S*-Fe(1)-S(3)-C		1.98	56.2	51.97
S*-Fe(1)-S(4)-C		50.60	-62.4	54.00

a) These data are from ref. 13.

i.e. S-C, Fe-S, and Fe-S-C. The Fe---Fe distance (2.698(5) Å) resembles to that (2.698(1) Å) of $[Fe_2S_2(S_2\text{-}o\text{-}xyl)_2]^{2-}$.[2] The terminal Fe- S(C) bond (2.318(7)Å) is slightly longer than another terminal Fe-S(C) bond (2.299(8)Å). The longer Fe-S(C) bond is close to the Fe-S(C) bond (2.312(1)Å) in $[Fe_2S_2(S\text{-}p\text{-}tol)_4]^{2-}$, and the shorter Fe-S(C) bond is similar to the Fe-S(C) bonds in $[Fe_2S_2(S_2\text{-}o\text{-}xyl)_2]^{2-}$.

The steric hindrance of methyl groups on the phenyl ring gives two kinds of Fe-S(C) bonds as listed in Table 3. The sulfur pπ orbitals are incapable of overlapping with the π system of two of the four phenyl rings because the Fe-S-C planes are perpendicular to their phenyl plane, although all Fe-S-C groups and phenyl rings are coplanar for $[Fe_2S_2(S\text{-}p\text{-}tol)_4]^{2-}$. The two phenyl rings in $[Fe_2S_2(tmbt)_4]^{2-}$ bend toward $Fe_2S_2^{2+}$. In the case of $[Fe_4S_4(tmbt)_4]^{2-}$, all of the four Fe-S torsion angles are rotated into the eclipsed position from the staggered position and the eclipsed Fe-S form becomes longer than the staggered one.[7] However, the eclipsed Fe-S bond does not necessarily mean less-interaction between Fe d and S p orbitals as discussed below.

Electronic Spectra.

Spectral data for $[NEt_4]_2[Fe_2S_2(tmbt)_4]$ are listed in Table 4, and compared to those of $[Fe_2S_2(S\text{-}Ph)_4]^{2-}$ and $[Fe_2S_2(S\text{-}p\text{-}tol)_4]^{2-}$ reported by Mayer et al.[13] and Beardwood and Gibson.[4] $[Fe_2S_2(tmbt)_4]^{2-}$ exhibits a well-resolved absorption maximum at 434 nm (ε: 17600). This

Tabel 4. Electronic Spectra of $[Fe_2S_2(SR)_4]^{2-}$ Complexes in DMF.

Complexes	Absorption maxima (λ)/nm (ε)	
$[Fe_2S_2(tmbt)_4]^{2-}$	346 (1690)	434 (17600)
$[Fe_2S_2(SPh)_4]^{2-}$,a	330 (19500)	490 (11200)
$[Fe_2S_2(S\text{-}p\text{-}tol)_4]^{2-}$,a	336 (18600)	502 (11200)
$[Fe_2S_2(bpdt)_2]^{2-}$,b,c	335 (21800)	375 (sh)
	425 (19100)	460 (sh)
	518 (9100)	550 (8400)

a) These data from ref.13. b) bpdt = 2,2'-biphenyldithiolate. c) from ref. 8.

absorption maximum is blue-shifted compared with those of other substituted-benzenethiolato 2Fe-2S complexes. The addition of 8 equivs of benzenethiol to a DMF solution of the complex resulted in observation of a broad maximum at 490 nm (ε:11000) with a shoulder (540 nm) as shown in Fig. 2. The spectral data coincided those for $[Fe_2S_2(S\text{-}Ph)_4]^{2-}$ reported.[13] The blue-shifted absorption maximum (434 nm) is distinct from the ligand-to-metal charge transfer (LMCT) absorption maxima (482 - 502 nm) for the complexes having a *p*-substituted benzenethiolate ligand. Holm and coworkers have pointed out that the LMCT band of $[Fe_2S_2(S\text{-}p\text{-}X\text{-}Ar)_4]^{2-}$ red-shifts in the order of X = Cl < H < CH_3 due to the increasing inductive effect of the X group.[13] The blue shift of the LMCT absorption maximum of $[Fe_2S_2(tmbt)_4]^{2-}$ is ascribed to the steric inhibition of π-interaction between sulfur and phenyl ring. This trend has also been observed in the case of highly distorted biphenyldithiolate [2Fe-2S] complex, $[Fe_2S_2(2,2'\text{-biphenyldithiolate})_2]^{2-}$ and an analogous [4Fe-4S] complex, $[Fe_4S_4(tmbt)_4]^{2-}$ in DMF.[6] The CPK model of $[Fe_2S_2(2,2'\text{-biphenyldithiolate})_2]^{2-}$ indicated that all of the four phenyl ring plane were perpendicular to Fe-S-C planes.[9]

^{1}H NMR Spectra

The chemical shifts of *o*- or *p*-substituted benzenethiolato Fe_2S_2 complexes are compared in Table 5 in terms of the isotropic shifts defined by Reynolds et al.[11] The isotropic shifts of $[Fe_2S_2(tmbt)_4]^{2-}$ were found to be -

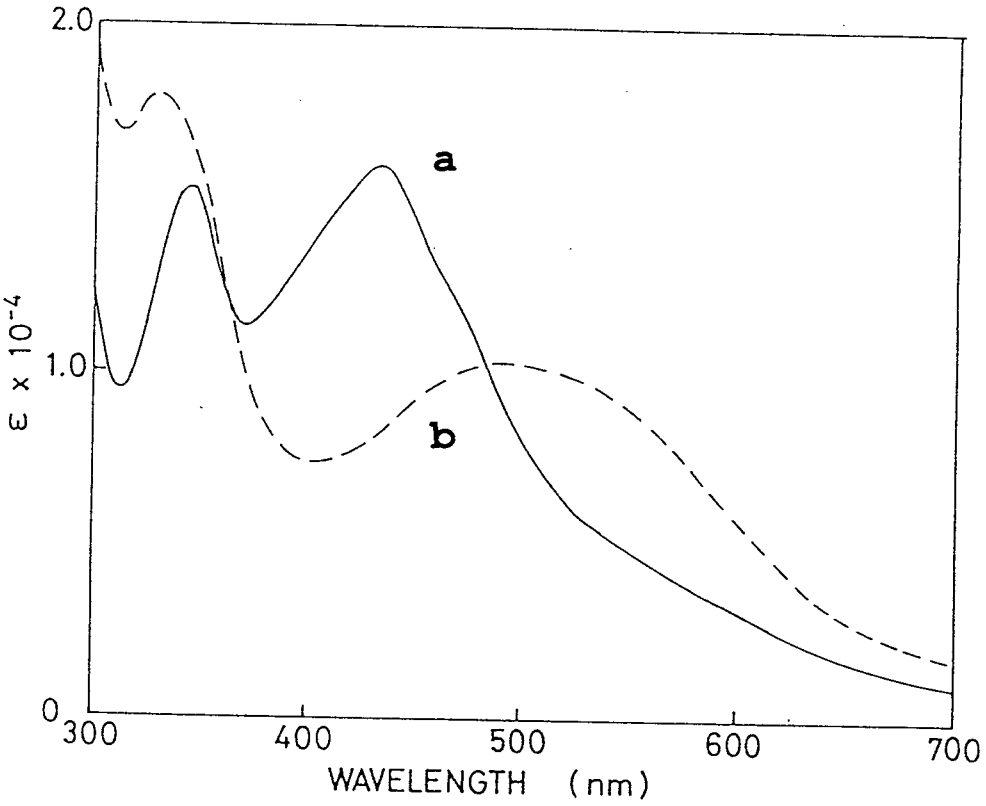

Figure 2. Absorption spectra of (a) $[NEt_4]_2[Fe_2S_2(tmbt)_4]$ (5×10^{-4} mol dm^{-3}) in DMF and (b) after core extrusion by thiophenol (4×10^{-3} mol dm^{-3}) from the solution-(a).

Table 5. The Contact Shifts in ^{1}H-NMR Spectra of $[NEt_4]_2[Fe_2S_2(tmbt)_4]$ in Acetonitrile-d_3.

Complexes	Chemical Shifts (ppm)	$(\Delta H/H_o)_{iso}$[a]
$[Fe_2S_2(tmbt)_4]^{2-}$	5.80 (*o*-CH_3)	-3.47
	9.73 (*m*-H)	-3.06
	6.36 (*p*-CH_3)	-4.24
$[Fe_2S_2(SPh)_4]^{2-}$,a	4.90 (*o*-H)	-2.30
	9.31 (*m*-H)	-2.11
	3.38 (*p*-H)	+3.82
$[Fe_2S_2(S\text{-}p\text{-}tol)_4]^{2-}$,a	4.6 (*o*-H)	+2.42
	9.2 (*m*-H)	-2.10
	6.0 (*p*-CH_3)	-3.74

a) Relative isotropic shifts were estimated as $(\Delta H/H_o)_{iso}$ as defined in ref. 11.

3.47, -3.06, and -4.24 for *o*-CH_3, *m*-H, and *p*-CH_3, respectively. The large isotropic shifts are expected by weaker antiferromagnetic interaction between two Fe(III) ions of $Fe_2S_2^{2+}$, when compared to those of $[Fe_4S_4(tmbt)_4]^{2-}$ (-1.15 ~ -1.45). The isotropic shifts of *m*-H and *p*-CH_3 in $[Fe_4S_4(tmbt)_4]^{2-}$ were found to be larger than those of $[Fe_4S_4(S\text{-}o\text{-}tol)_4]^{2-}$. The larger contact shift through Fe-S-C to *p* or *m*-C*H* is quite unusual because of prevention of steric inhibition of π-interaction between sulfur and phenyl ring.

Electrochemical Property

Table 6 shows the redox potentials of $[Fe_2S_2(tmbt)_4]^{2-}$ measured using cyclic voltammetry. These data are compared with those of $[Fe_2S_2(S\text{-}Ph)_4]^{2-}$ and $[Fe_2S_2(S\text{-}p\text{-}tol)_4]^{2-}$. $[Fe_2S_2(tmbt)_4]^{2-}$ exhibits a 3-/2- redox couple at -0.87 V vs. SCE in DMF which is irreversible (i_{pa}/i_{pc}=0.75). The irreversible redox couple is accompanied by a new reversible redox couple at -1.40V vs. SCE. The instablity of the electrochemically reduced species, $[Fe_2S_2(tmbt)_4]^{3-}$, leads to formation of $[Fe_4S_4(tmbt)_4]^{2-}$ by decomposition. Such a reaction has been known for the chemical reduction of some [2Fe-2S] complexes.[6]

The redox potentials of $[Fe_2S_2(S\text{-}Ph)_4]^{2-}$, $[Fe_2S_2(S\text{-}p\text{-}tol)_4]^{2-}$, and $[Fe_2S_2(S\text{-}C_6H_4\text{-}p\text{-}NMe_2)^4]^{2-}$ are at -1.09V, -0.97 V, or -0.83 V vs. SCE, respectively in DMF. Mayerle et al.[13] found a correlation between the redox potential and the Hammett σ_p constants of the substituent of

Table 6. Electrochemical Data of $[Fe_2S_2(tmbt)_4]^{2-}$ compared with Other [2Fe-2S] Complexes in DMF.

Complexes	Solvent	$E_{1/2}$ (V vs.SCE)	i_{pa}/i_{pc}
$[Fe_2S_2(tmbt)_4]^{2-}$	DMF	-0.87	0.75
	DME	-1.15	0.50
$[Fe_2S_2(SPh)_4]^{2-}$,a	DMF	-1.09	
$[Fe_2S_2(S\text{-}p\text{-}tol)_4]^{2-}$,a	DMF	-1.15	

a) These values were cited from ref. 3.

benzenethiolate ligands. The electron withdrawing effect of the phenyl group contributes to the positive shift of the redox potentials. In the case of the tmbt complex, the electron-donating methyl substituents are expected to shift the redox potential to the negative side. However, $[Fe_2S_2(tmbt)_4]^{2-}$ shows a positive shift as shown in Table 6. The crystal structure of $[Fe_2S_2(tmbt)_4]^{2-}$ indicates that the Fe-S-C plane is perpendicular to the phenyl plane and that sulfur pπ orbital does not conjugate with the phenyl π-system. Thus, the electron donating effect of the methyl groups at *o*-and *p*-positions is almost completely offset.

Evaluation of Torsion Angle Dependence of Fe-S Bond Character by MO Calculation.

The MO calculations were performed on $[Fe_2S_2(SH)_4]^{2-}$ with variation of two of the four Fe-S torsion angles in the same direction as the crystal structure of $[Fe_2S_2(tmbt)_4]^{2-}$ with two skewed Fe-S torsion angles in C_{2v} symmetry. The two sets of 5 electrons in each Fe center configurated the lowest orbitals in turn and a diamagnetic Fe_2S_2 center was assumed for the calculations. Figure 3 shows the schematic drawing of the structure of a model complex ion $[Fe_2S_2(SH)_4]^{2-}$ for the calculation. This geometry is taken from the symmetrical structure (D_{2h}) of $[Fe_2S_2(S\text{-}p\text{-}tol)_4]^{2-}$ which has an eclipsed Fe-S(C) torsion angle ($\psi \simeq 0°$) as illustrated in Fig. 4. The Fe-S(C) torsion angle is defined as the position of the C atom in S-Fe-S-C bonds with the smallest steric hindrance (Fig. 4). Two of the Fe-S torsion

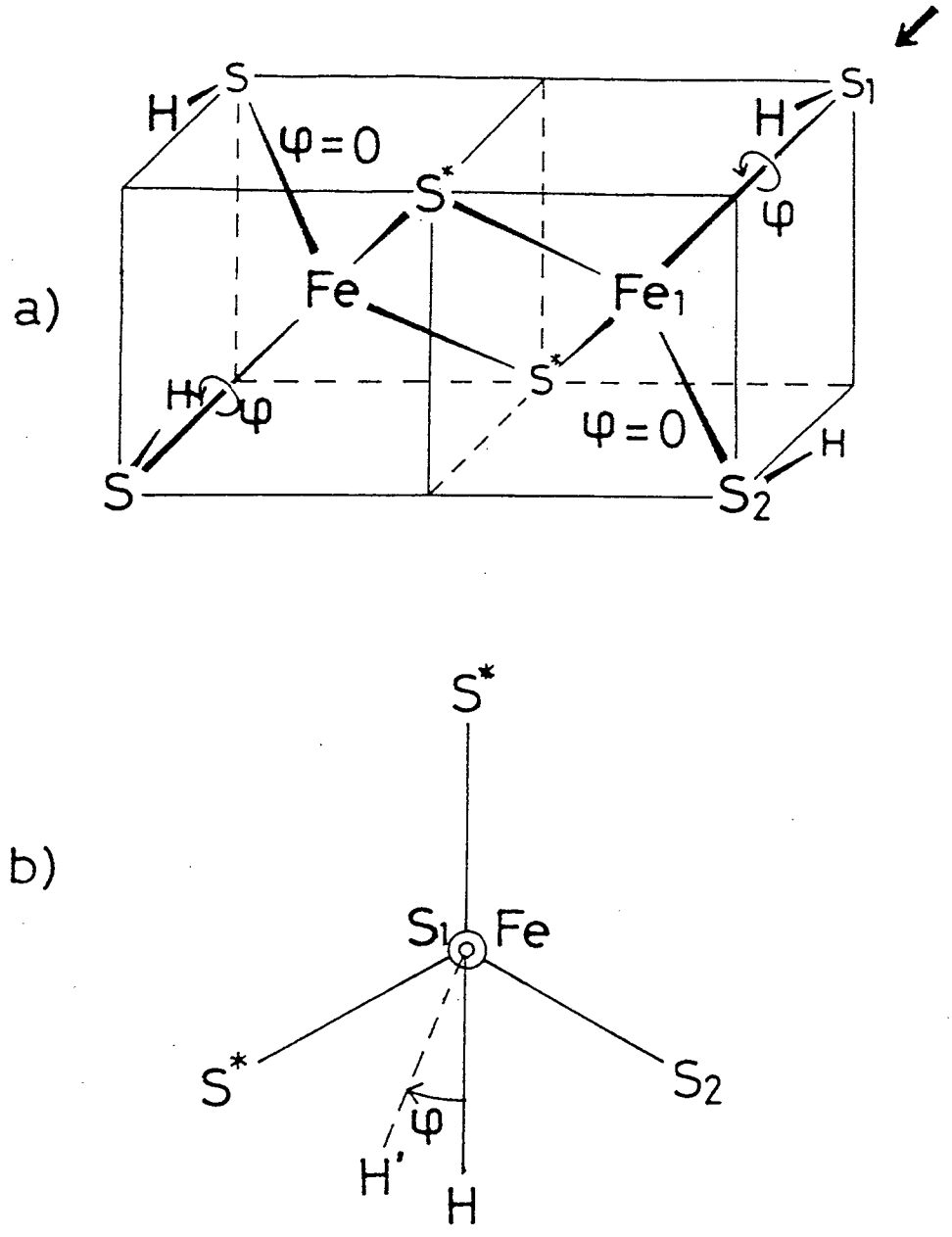

Figure 3.(a) Illustration of $[Fe_2S_2(SH)_4]^{2-}$ in D_{2h} symmetry.
(b) Definition of Fe-S(H) torsion angles (Ψ).

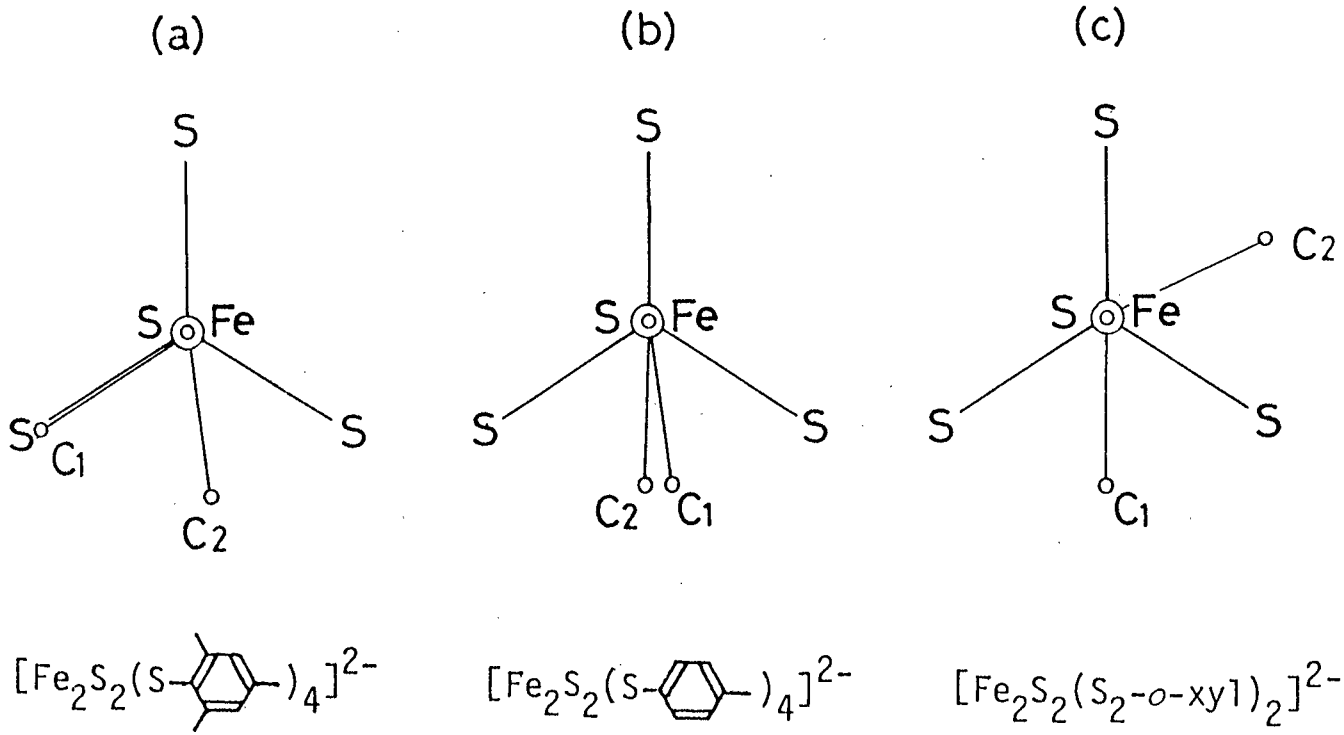

Figure 4. Illustration of the skewed S*-Fe-S-C torsion angle for (a) $[Fe_2S_2(tmbt)_4]^{2-}$, (b) $[Fe_2S_2(S\text{-}p\text{-}tol)_4]^{2-}$, and (c) $[Fe_2S_2(S_2\text{-}o\text{-}xyl)_2]^{2-}$.

angles of $[Fe_2S_2(SH)_4]^{2-}$ were rotated to the direction as shown in Fig. 4a. The Fe-S torsion angle dependence of the overlap population for two sets of the Fe-S bonds (two Fe(1)-S(1) and two Fe(1)-S(2)) is shown in Fig.5. The overlap population of Fe(1)-S(1) bond with various torsion angles was calculated to have a maximum at $\psi=60°$, while the overlap population of Fe(1)-S(2) bond with $\psi=0°$ is lowered. The results are consistent to the crystal structure parameters for $[Fe_2S_2(tmbt)_4]^{2-}$ in that the Fe-S(C) length (2.318Å) with a eclipsed torsion angle ($\psi=60°$) is larger than the length of another set of Fe-S ($\psi=0°$, 2.299Å).

The π-bonding character of Fe(1)-S(1) seems to cause the unusual contact shift of *p*-CH_3 on 2,4,6-trimethylbenzenethiolate group. However, there is no interaction between S(C) $p\pi$ and π-system of phenyl ring. The skewed Fe-S bond also contributes to the observed contact shift. The average of the contact shifts through four Fe-S bonds (two Fe(1)-S(1) and two Fe(1)-S(2)) was found to be relatively large (Table 4). This may be rationalized by the overlap populations of Fe(1)-S(1) and Fe(1)-S(2) bonds which increase at $\psi > 0°$ when compared with those having the staggered torsion angles ($\psi = 0°$).

The variation of energy levels of Fe d orbitals in $[Fe_2S_2(SH)_4]^{2-}$ was estimated with the rotation of the Fe-S(C) torsion angle. When the complex is assumed to have a diamagnetic electron configuration, the energy level of the lowest unoccupied orbital decreases with an increase of the Fe-S torsion angle. Thus, the decrease of the orbital

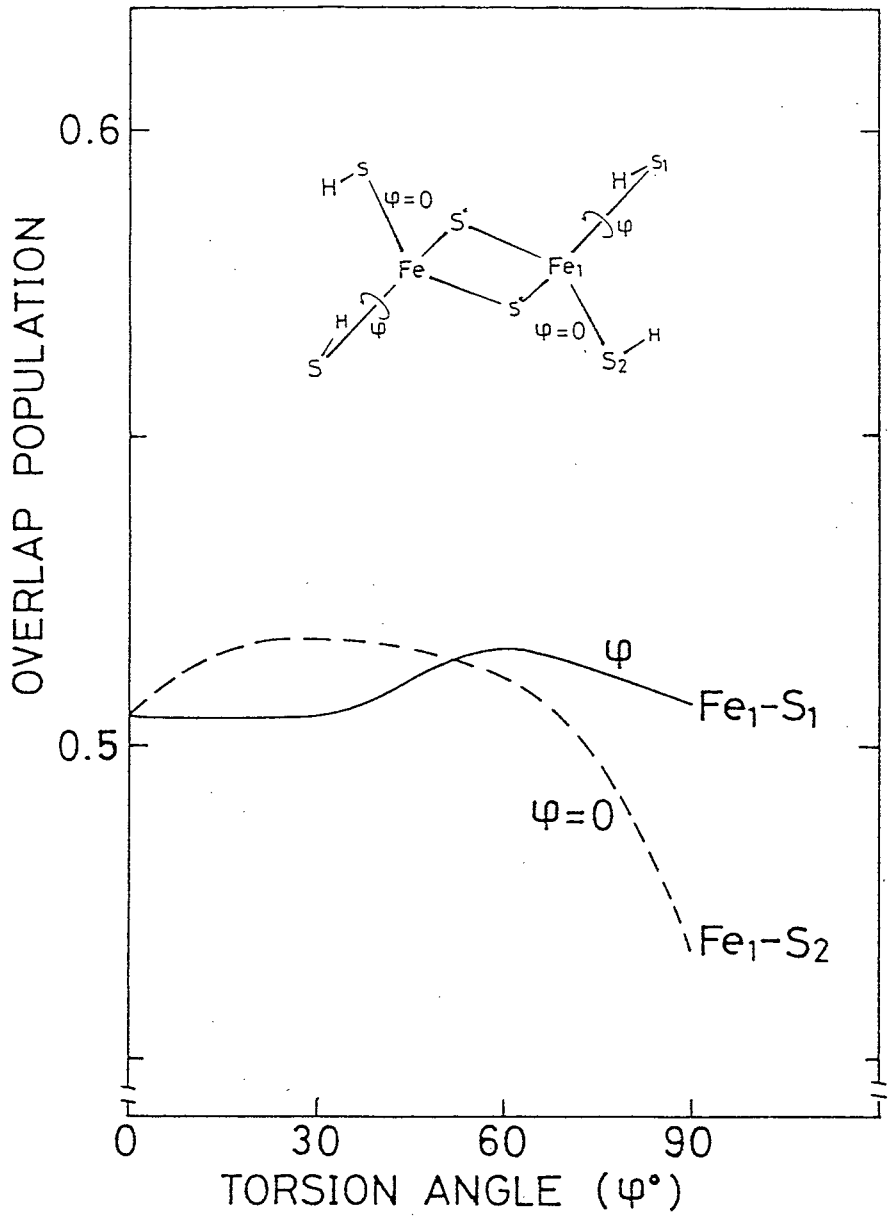

Figure 5. Variation of the Fe-S(H) overlap population with the change of two of the four Fe-S(H) torsion angles.

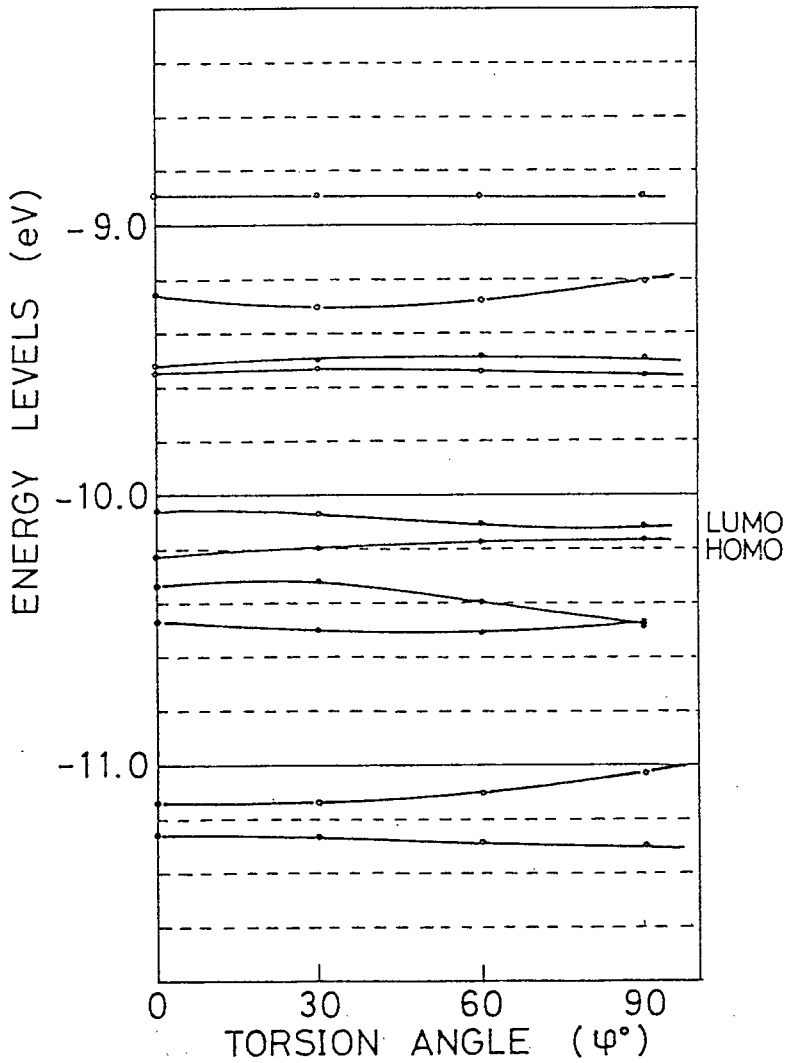

Figure 6. Variation of the energy levels of Fe d orbitals with the change of two of the four Fe-S(H) torsion angles.

energy causes the positive shift of the reduction potential.

The increase in π-interaction of the Fe-S bonds in $[Fe_2S_2(SR)_4]^{2-}$ should contribute to a negative shift of the redox potentials (3-/2-). Figure 7 shows the net charges of Fe(III), S*, and S(H) atoms in $[Fe_2S_2(SH)_4]^{2-}$. Fe(III) has a maximum net charge at ψ= 60°, which is correlated with the positive shift of the redox potentials. This is also supported by lowering the energy level orbital at ψ= 60°. The lower redox potential (-0.87 V vs. SCE) of $[Fe_2S_2(tmbt)_4]^{2-}$ in DMF is explicable by the increase of dative π-bonding at the staggered Fe-S bonds. Furthermore, the instability of the 3- state is presumably due to the more positive net charge of Fe(II) ion. Such an instability of the Fe(II) state by the eclipsed Fe-S(C) bonds was found for $[Fe_4S_4(tmbt)_4]^{2-}$, which has four restrictedly rotated Fe-S(C) torsion angles (two ψ= 30° and two ψ= -30°). Actually, the 3- /2- redox couple of the 4Fe-4S complex in DMF is less stable than those of usual alkyl- and arylthiolate 4Fe-4S model complexes.

$[Fe_2S_2(S_2\text{-}o\text{-}xyl)_2]^{2-}$ has been reported to exhibit a C_2 structure with the Fe-S(C) torsion angles (ψ= +2.4° and ψ= +243.8°) and the four almost equal Fe-S(C) bond lengths (two 2.303 and two 2.306 Å), but two sets of the different Fe-S* bond lengths (2.185 and 2.232Å). When the two torsion angles (ψ= 0° and ψ= +240°, staggered) are employed for the calculation, the two Fe-S overlap populations are equal with each other as well as the parent geometry with two ψ= 0° (Fig. 5). The results are in accord with the observed equal

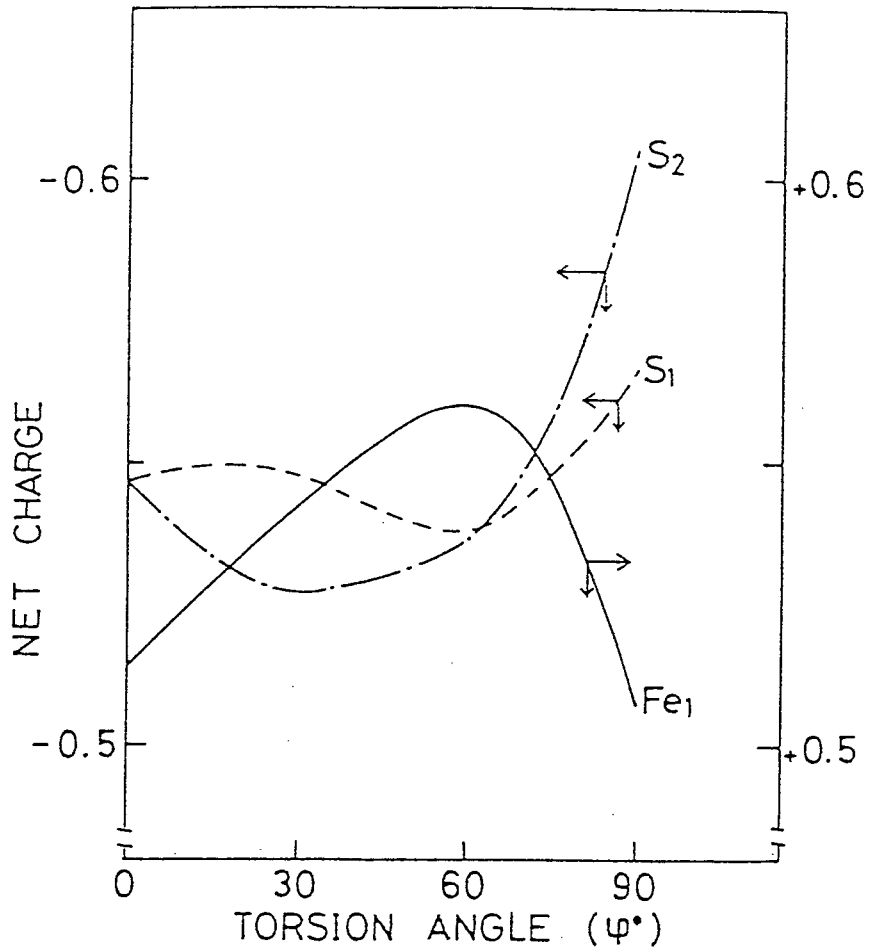

Figure 7. Variation of the net charges on Fe(III), S*, and S(H) with the change of two of the four Fe-S(H) torsion angles.

Fe-S(C) lengths by the X-ray analysis. Fe-S bonds have a single bond character with two small Fe-S-C angles (98.1° and 98.8°). Then the two distinguishable overlap populations were observed for Fe-S* bonds which are also consistent with the structural parameters reported by Mayerle et al.[13] The *o*-xyl-S_2 ligand has the conformationally restricted chelate ring and provides a relatively stable structure with the staggered Fe-S(C) torsion angles as shown in Fig.4.

The structure of Fe_2S_2 part as revealed by the X-ray structure of *Spirulina platensis* ferredoxin is similar to the parent D_{2h} geometry used for the calculation. Only one Fe-S torsion angle (Cys(49)) is rotated from the staggered position and the others (Cys(42) and Cys(47)) are normal.[12] We calculated the Fe-S overlap population with variation of one (Fe(1)-S(2)) of the four Fe-S torsion angles. The small overlap population was found for two Fe-S* bonds in each Fe of $Fe_2S_2^{2+}$ion and the staggered Fe-S(C) bond, whereas the overlap population was higher for the eclipsed Fe-S bond. From these calculations, it is likely in native plant-Type ferredoxin that the torsion of the Cys(49) residue induced weakening the Fe-S bond as compared from Cys(47) or Cys(42) were reported to form NH---S hydrogen bond with the side chains of Cys-A-B-C-D-Cys-X-Y-Cys sequence.[14] The NH---S hydrogen bonds decrease the Fe-S overlap because of the absence of lone pair at sulfur. In summary, the restrictedly orientated Fe-S(C) bond of one of the Two Fe(III) ions, which gives a positive shift of the one-

electron redox potential of Fe_2S_2 core. The inequivalence in environments of the two Fe(III) ions is probably associated with the directed electron flow in biological electron-transfer chains.

References

(1) Ueyama, N.; Ueno, S.; Nakata, M.; Nakamura, A., *Bull. Chem. Soc. Jpn.* **1984**, 57, 984 .

(2) Ueno, S.; Ueyama, N.; Nakamura, A.; Tsukihara, T., *Inorg.Chem.* **1986**, 25, 1000.

(3) Eaton, W. A.; Lovenberg, W., "Iron-Sulfur Proteins", vol II,Ed. Lovenberg, W., Academic Press, New York, p.131 (1973).

(4) Nakata, M.; Ueyama, N.; Nakamura, A., *Bull. Chem. Soc. Jpn.* **1983**, 56, 3647 .

(5) Millar, M.; Lee, J. F.; Koch, S. A.; Fikar, R., *Inorg. Chem.* **1982**, 21, 4106.

(6) Ueyama, N.; Terakawa, T.; Sugawara, T.; Fuji, M.; Nakamura, A. *Chem. Lett.* **1984**, 1287.

(7) Ueyama, N.; Sugawara, T.; Fuji, M.; Nakamura, A.; Yasuoka, N., *Chem. Lett.* **1985**, 175.

(8) Beardwood, P.; Gibson, J. F. *J. Chem. Soc. Dalton Trans.* **1983**, 737.

(9) O'Sullivan, T.; Millar, M. M., *J. Am. Chem. Soc.* **1985**, 107, 4096.

(10).Mann, C. K., *Electroanal. Chem.* **1963**, 3.

(11) Wong, G. B.; Bobrik, M. A.; Holm, R. H., *Inorg. Chem.* **1978**, 17, 578.

(12) Reynolds, J. G.; Holm, R. H., *Inorg. Chem.* **1980**, 19, 3257.

(13) Mayerle, J. J.; Denmark, S. E.; Depamphilis, B. V.; Ibers, J.A.; Holm, R. H., *J. Am. Chem. Soc.* **1975**, 97,

1032.

(14) Tsukihara, T., private communication.

List of Publicatios

1. "A novel method for determining the chelation ability of the cysteine-containing peptides with 3,4-toluenedithiol. Application to [2Fe-2S]-ferredoxin model systems."
   Ueyama, N.; Ueno, S.; Nakamura, A. *Bull. Chem. Soc. Jpn.* **1987**, 60, 283.
2. "Synthesis, spectro- and electrochemical properties of the 2Fe-2S ferredoxin model complexes containing nonapeptide."
   Ueno, S.; Ueyama, N.; Nakamura, A. *Pept. Chem.* **1986**, 269.
3. "Synthesis of tetrapeptide 2Fe-2S complexes of Cys-X-Y-Cys segments by a ligand-exchange reaction. Peptide models of 2Fe ferredoxin characterized by electrochemistry and spectroscopy."
   Ueno, S.; Ueyama, N.; Nakamura, A.; Tukihara, T. *Inorg. Chem.* **1986**, 25, 1000.
4. "Synthesis of the 2Fe2S ferredoxin model complexes containing oligopeptides and their electrochemical properties"
   Ueno, S.; Ueyama, N.; Nakamura, A. *Pept. Chem.* **1985**, 33.

5. "Synthetic analog of the active site of plant type ferredoxin"
   Ueno, S.; Ueyama, N.; Nakamura, A.; Wada, K. Matsubara, H.; Kumagai, S.; Sakakibara, S.; Tsukihara, T. Pept.

Chem. 1984, 133.

6. "Syntheses of 2Fe-2S ferredoxin model complexes of Cys-containing oligopeptides by reaction with dithiodiiron(2+) ion or by sulfide incorporation" Ueyama, N.; Ueno, S.; Nakata, M.; Nakamura, A. *Bull. Chem. Soc. Jpn.* **1984**, 57, 984.

Other Related Paper.

1. "Redox potentials of oligopeptide/$Fe_4S_4^{2+}$ complexes. Remarkable positive shift of the redox potential with (benzyloxycarbonyl)-L-Cys-Gly-L-Ala-L-Cys-OMe as helating ligands"
   Ueyama, N.; Kajiwara, A.; Terakawa, T.; Ueno, S.; Nakamura, A. *Inorg. Chem.* **1985**, 24(26), 4700-4.